

SLOPE STABILITY ANALYSIS AND DESIGN IN ELBİSTAN-ÇÖLLÖLÖR
OPEN CAST MINE

A THESIS SUBMITTED TO THE GRADUATE SCHOOL OF NATURAL AND
APPLIED SCIENCES
OF
MIDDLE EAST TECHNICAL UNIVERSITY

BY

İBRAHİM FERİD ÖGE

IN PARTIAL FULFILLMENT OF THE REQUIREMENTS
FOR
THE DEGREE OF MASTER OF SCIENCE
IN
MINING ENGINEERING

SEPTEMBER 2008

Approval of the thesis:

**SLOPE STABILITY ANALYSIS AND DESIGN IN ELBISTAN-
ÇÖLLÖLAR OPEN CAST MINE**

submitted by **İBRAHİM FERİD ÖGE** in partial fulfillment of the requirements
for the degree of **Master of Science in Mining Engineering Department,**
Middle East Technical University by;

Prof. Dr. Canan Özgen
Dean, Graduate School of **Natural and Applied Sciences**

Prof Dr. Celal Karpuz
Head of Department, **Mining Engineering**

Prof Dr. Celal Karpuz
Supervisor, **Mining Engineering Dept., METU**

Examining Committee Members:

Prof. Dr. Seyfi Kulaksız
Mining Engineering Dept., Hacettepe University

Prof. Dr. Celal Karpuz
Mining Engineering Dept., METU

Assoc. Prof. Dr. Levent Tutluoğlu
Mining Engineering Dept., METU

Assoc. Prof. Dr. Sadık Bakır
Civil Engineering Dept., METU

Assist. Prof. Dr. Mehmet Ali Hindistan
Mining Engineering Dept., Hacettepe University

Date:

05/09/2008

I hereby declare that all information in this document has been obtained and presented in accordance with academic rules and ethical conduct. I also declare that, as required by these rules and conduct, I have fully cited and referenced all material and results that are not original to this work.

Name, Last name : İbrahim Ferid Öge

Signature :

ABSTRACT

SLOPE STABILITY ANALYSIS AND DESIGN IN ELBİSTAN- ÇÖLLÖLAR OPEN CAST MINE

Öge, İbrahim Ferid

M.Sc., Department of Mining Engineering

Supervisor: Prof. Dr. Celal Karpuz

September 2008, 136 pages

Slope stability is an important aspect of geotechnical engineering. Input parameters for the analysis are the governing factors and they must be determined accurately and precisely. Field investigations, laboratory testing and back analyses are vital instruments for the input parameters.

This study presents the results of slope stability analysis for the soil slopes at Elbistan-Çöllolar lignite mine. After executing the drilling programme, samples taken from the drilling work, delivered to soil mechanics laboratory for testing. The basic input parameters, namely cohesion and friction angle determined at soil mechanics laboratory were compared to the parameters obtained from back analysis of a large scale slope failure. Input parameters for the analysis are determined by this way.

After determining the input parameters, slope stability analyses were carried out both for the permanent and temporary slopes in Afşin-Elbistan lignite basin, Çöllolar sector. The effect of ground water on the stability of slopes was investigated in detail and maximum safe slope angles were determined for different water levels. For limit equilibrium analysis, Rocscience SLIDE software,

for finite difference analysis in 3-D, Itasca FLAC3D was used. In the limit equilibrium analyses both circular and composite failures were considered. Shear strength reduction method is used for the finite difference method. The results between limit equilibrium and 3-D finite difference methods were compared. When the failure surfaces obtained from the finite difference analyses were imposed to limit equilibrium analysis, computations are resulted in lower factor of safety values for limit equilibrium analysis.

Keyword: Slope Stability, Limit Equilibrium Methods, Continuum Analysis, Finite Difference Analysis

ÖZ

ELBİSTAN ÇÖLLÖLAR AÇIK LİNYİT OCAĞI, ŞEV DURAYLILIĞI ANALİZLERİ VE TASARIMI

Öge, İbrahim Ferid

Yüksek lisans, Maden Mühendisliği Bölümü

Tez Yöneticisi: Prof. Dr. Celal Karpuz

Eylül 2008, 136 sayfa

Şev duraylılığı, jeoteknik mühendisliğinde çok önemli bir konudur. Analiz sonuçlarını doğrudan etkileyecek olan girdi parametreleri hassas ve kesin şekilde tespit edilmelidir. Saha çalışmaları, laboratuvar deneyleri ve geriye dönük analizler, girdi değişkenlerinin tespitinde önemli rol oynamaktadır.

Bu çalışma, Elbistan Çöllolar linyit madeninde şev duraylılığı analizlerini sunmaktadır. Jeoteknik sondajlardan alınan örselenmemiş numuneler zemin mekaniği deneylerine tatbik edilmiştir. Temel girdi değişkenleri, kohezyon ve içsel sürtünme açıları laboratuvar deneylerince tespit edilmiş, geriye dönük analiz çalışmaları ile bulunan değerler ile karşılaştırılmıştır. Girdi değerleri bu şekilde tespit edilmiştir.

Tasarım değişkenleri tespit edildikten sonra, şev duraylılık analizi ve tasarımı safhasına geçilmiştir. Analizler, havzada Elbistan Çöllolar linyit madeninde ve geçici şevleri kapsamaktadır. Yerltı suyunun duraylılık üzerindeki etkileri ayrıntılı bir şekilde incelenmiş ve en yüksek güvenli şev açıları değişen yer altı su durumlarına göre tespit edilmiştir. Denge sınırı analizleri için Rocscience SLIDE yazılımı, sonlu farklar analizi için üç boyutta analiz gerçekleştirebilen Itasca FLAC3D yazılımı kullanılmıştır. Analizlerde güvenlik katsayısı hesaplamaları

denge sınırı analiz yöntemleri kullanılarak dairesel ve kompozit kayma durumlarında ve sonlu farklar yöntemi kullanılarak gerçekleştirilmiştir. Makaslama dayanımı azaltma yöntemi, sonlu farklar yöntemi ile analizde kullanılmış, denge sınırı yöntemleri ile karşılaştırma gerçekleştirilmiştir. Sonlu farklar yöntemi ile tespit edilen kayma düzlemleri denge sınırı yöntemlerine uygulanmış, bu analizlerde denge sınırı yöntemi daha düşük güvenlik katsayısı değerleri vermiştir.

Anahtar kelimeler: Şev Duraylılığı, Geriye Dönük Analiz, Sonlu Farklar Yöntemi, Sürekli Ortam Analizi.

To my family,

ACKNOWLEDGEMENTS

I express my most sincere appreciation to my supervisor, Prof. Dr. Celal Karpuz, for her valuable suggestions, guidance, encouragements and insight throughout the study. I would particularly like to thank Assoc.Prof.Dr. Levent Tutluoğlu, who encouraged me during the research and gave his support throughout this study.

I am also indebted to Prof.Dr. Seyfi Kulaksız, Assoc.Prof.Dr. Sadık Bakır, Assist.Prof.Dr. Mehmet Ali Hindistan for accepting to serve in my committee and for their participation. I would also thank to Hacettepe University, Mining Engineering Department for enabling the use of Itasca FLAC3D software for the research.

I would like to thank my friend research assistant Arman Koçal for his help and sharing his valuable knowledge for my research study. I am grateful to my friends for their continuous support and moral boost.

Finally, any thank to my family, who have been supporting me all through my life, would be an understatement.

TABLE OF CONTENTS

ABSTRACT	iv
ÖZ	vi
ACKNOWLEDGEMENTS	ix
LIST OF TABLES	xiii
LIST OF FIGURES.....	xv
CHAPTERS	
1. INTRODUCTION.....	1
1.1 Slope stability in geotechnical engineering.....	1
1.2 Statement of the problem	1
1.3 Objective of thesis.....	2
1.4 Methodology	3
1.5 Organization of thesis.....	4
2. BASICS OF SOIL SLOPE STABILITY	5
2.1 Introduction	5
2.2 Slope failure mechanisms.....	6
2.2.1 Discontinuity failures	7
2.2.2 Continuum failures.....	8
2.3 Limit equilibrium methods for soil slope stability analysis	8
2.3.1 Limit Equilibrium Analysis.....	8
2.3.2 Rotational Shear Failure.....	9
2.3.3 Assumptions for limit equilibrium methods	10
2.3.4 Shape of slip surface and critical failure surface	11
2.3.5 Method selection	12
2.4 Numerical Methods for Soil Slope Stability Analysis	15
2.4.1 Continuum modelling.....	16
2.4.2 Discontinuum modelling.....	16
2.4.3 Itasca FLAC3D	17

2.4.4 Factor of safety in numerical modeling	18
2.5 Shear strength characterization	21
2.5.1 Definition of shear strength.....	21
2.5.2 Total and effective stress analysis.....	22
2.5.3 Long and short term conditions.....	24
2.6 Previous studies.....	27
3. GENERAL INFORMATION ABOUT THE STUDY AREA AND FIELD STUDIES	30
3.1 History of area.....	30
3.2 General description of the working area	31
3.3 Mine planning in the first five years	32
3.4 General geology of the area	34
3.5 Hydrogeology.....	36
3.6 Water Drainage	37
4. ELBİSTAN-ÇÖLLÖLAR SLOPE STABILITY ANALYSES	38
4.1 Introduction	38
4.2 Geotechnical drilling.....	39
4.3 Laboratory testing and results	43
4.4 Back-analysis of Kışlaköy 2006 failure	44
4.4.1 Summary of Back-analysis conducted by MTA	44
4.4.2 Back-analysis of black clay.....	48
4.5 Limit equilibrium back-analysis in 2-D	48
4.5.1 Back-analysis of 1 st stage of the 2006 Kışlaköy failure.....	49
4.5.2 Back-analysis of 2 nd stage of the 2006 Kışlaköy failure.....	50
4.5.3 Back-analysis of 3 rd stage of the 2006 Kışlaköy failure	51
4.6 Finite difference back analysis in 3-D.....	52
4.6.1 Finite difference model	52
4.6.2 Elastic parameters	54
4.6.3 Strength parameters.....	54
4.6.4 Back analysis of black clay	55
4.6.5 Sensitivity analysis of gyttja and lignite	64
4.7 Input parameters for design.....	67

LIST OF TABLES

TABLES

Table 2.1 Comparison of Features of Limit Equilibrium Methods (Anon, 2003)	13
Table 2.2 Brief Comparison of Limit Equilibrium Methods (Duncan and Wright, 2005)	13
Table 4.1 Coordinates of the boreholes in global coordinate system.....	40
Table 4.2 Summary of laboratory experiment results (Karpuz et al., 2007).....	43
Table 4.2 Shear strength parameters decided to be used as design parameters by MTA (Akbulut et al., 2007)	47
Table 4.3 Mohr-Coulomb and tensile strength parameters of the formations	55
Table 4.4 Input design parameters	68
Table 4.5 Factor of safety analysis of permanent slopes with a water level 85 m beneath the surface	71
Table 4.6 Factor of safety analysis of permanent slopes with a water level 50 m beneath the surface	72
Table 4.7 Factor of safety analysis of permanent slopes with a water level on the surface	73
Table 4.8 Thickness of layers in the model.....	80
Table 4.9 Shear strength (Mohr-Coulomb) parameters used in the model.	83
Table 4.10 Factor of safety analysis of bucket wheel excavator working slopes with a water level on the surface.....	101
Table 4.11 Back-analysis and sensitivity analysis results.....	112
Table 4.12 Factor of safety analysis of permanent slopes with respect to three different ground water levels by limit analysis (circular failure).....	113
Table 4.13 Overall slope angles vs. water table depth plot to keep 1.5 factor of safety	113
Table 4.14 Composite failure analysis around fault for cross section #6	114

Table 4.15 Finite Difference Analysis of permanent slopes for different overall slope angles	114
Table 4.16 Finite difference and limit equilibrium methods result comparison (Slip surfaces are the same with FLAC3D failure zones).....	114
Table 4.17 Factor of safety analysis of bucket wheel excavator working slopes with a water level on the surface by limit analysis (circular failure)	114
Table 4.18 Factor of safety vs. water table depth from surface graph for 15° overall slope angle by Limit equilibrium analysis (for circular failure)	115
Table 4.19 Overall slope angle vs. ground water level satisfying 1.30 factor of safety for temporary slopes	115
Table 4.20 Finite Difference analysis, factor of safety calculation by FLAC3D for bucket wheel excavator production slopes.....	115
Table A.1 Laboratory test results of Loam	122
Table A.2 Laboratory test results of Blue Clay.....	123
Table A.3 Laboratory test results of Gyttja.....	124
Table A.4 Laboratory test results of Lignite	125
Table A.5 Laboratory test results of Black clay.....	126
Table A.6 Laboratory test results of Green clay (Footwall clay).....	127

LIST OF FIGURES

FIGURES

Figure 2.1 A typical planar failure with a tension crack	7
Figure 2.2 A typical circular failure	8
Figure 3.4 Formations and their thicknesses in Çöllolar mine	35
Figure 4.1 Locations of geotechnical research boreholes	39
Figure 4.2 Kışlaköy 2006 slope failure.(Akbulut et al., 2007)	45
Figure 4.3 Kışlaköy 2006 slope failure (from Park Teknik personnel)	45
Figure 4.4 Plan view of the 2006 failure (Akbulut et al., 2007)	46
Figure 4.5 Kışlaköy 2006 failure in detail for cross section A-A'	47
Figure 4.6 Slip surface and factor of safety plot of 1st stage of the 2006 failure (cross section A'-A)	49
Figure 4.7 Slip surface and factor of safety plot of 2nd stage of the 2006 failure (cross section A'-A)	50
Figure 4.8 Slip surface and factor of safety plot of 3rd stage of the 2006 failure (cross section A'-A)	51
Figure 4.9 Kışlaköy 2006 slope failure, 3D model in FLAC3D, finite difference grids, dimensions and materials	52
Figure 4.11 Kışlaköy 2006 slope failure 3D model in FLAC3D, history points for recording displacements during cycling for solution	53
Figure 4.12 Horizontal displacements vs. solution step plot using shear strength parameters obtained from laboratory testing at MTA (Akbulut et al., 2007) gyttja and lignite ($c' = 17$ kPa and $\phi' = 38^\circ$) keeping $c' = 8$ kPa for black clay	56
Figure 4.13 Horizontal displacements vs. solution step plot using shear strength parameters obtained from laboratory testing at METU for gyttja and lignite ($c' = 54$ kPa and $\phi' = 32^\circ$) keeping $c' = 8$ kPa for black clay	56

Figure 4.14 Finite difference solution convergence plot using shear strength parameters obtained from laboratory testing at MTA (Akbulut et al., 2007) gyttja and lignite ($c' = 17$ kPa and $\phi' = 38^\circ$) keeping $c' = 8$ kPa for black clay	57
Figure 4.15 Finite difference solution convergence plot using shear strength parameters obtained from laboratory testing at METU for gyttja and lignite ($c' = 54$ kPa and $\phi' = 32^\circ$) keeping $c' = 8$ kPa for black clay	58
Figure 4.16 History plot for $c' = 8$ kPa and $\phi' = 9.5^\circ$ for black clay indicating stability	59
Figure 4.17 History plot for $c' = 8$ kPa and $\phi' = 9^\circ$ for black clay indicating instability	59
Figure 4.18 Horizontal displacement vs. friction angle of black clay with $c' = 5$..	61
Figure 4.19 Horizontal displacement vs. friction angle of black clay.....	61
Figure 4.20 Cohesion vs. internal friction angle for black clay satisfying the condition of factor of safety=1	62
Figure 4.21 Horizontal displacement contours	63
Figure 4.22 Shear strain rate contour	63
Figure 4.23 Horizontal displacements at 100000 # of steps at history point #2 ..	65
Figure 4.24 Horizontal displacement contours. Coloured range indicates failed range	66
Figure 4.25 Shear strain contours are visible in front of the model, black clay and fault zone	66
Figure 4.26 Horizontal displacement vs. solution step # plot.	67
Figure 4.27 Cross-sections taken for analysis	70
Figure 4.29 Section #3, slip circle of lowest factor of safety with a ground water table 50 m beneath the surface	73
Figure 4.30 Section #3, slip circle of lowest factor of safety with a ground water table on the surface	74
Figure 4.31 Factor of safety vs. water table depth from surface graph for 21° overall slope angle for section #3	74
Figure 4.32 Slope with overall slope angle of 17° having a water table having a depth of 50 m from the surface	75

Figure 4.33 Slope with overall slope angle of 14° having a water table on the surface	76
Figure 4.35 Overall slope angle vs. water table depth plot to reach 1.5 factor of safety value	76
Figure 4.35 Inclination of black clay and possible fault is shown on cross section #6	78
Figure 4.36 Slip surface and factor of safety output	78
Figure 4.37 FLAC3D model in 3D, finite difference grids, dimensions and materials of the south-west permanent slopes in Çöllolar open cast mine	80
Figure 4.38 Water table geometry	81
Figure 4.39 History points for recording displacements during stepping (or cycling) for solution	81
Figure 4.40 Horizontal displacement contours	84
Figure 4.41 Shear strain rate contours.....	84
Figure 4.42 History point of #4	85
Figure 4.43 History point of #7	86
Figure 4.44 Horizontal displacement vs. reduction factor plot at 5000 steps of plastic solution cycling.	87
Figure 4.45 Horizontal displacement contour (Reduction factor of 1.20)	88
Figure 4.46 Shear strain rate contour (Reduction factor of 1.20)	88
Figure 4.47 Horizontal displacement vs. solution steps graph (Reduction factor of 1.20)	89
Figure 4.48 Horizontal displacement contour (Reduction factor of 1.10)	89
Figure 4.49 Shear strain rate contour (Reduction factor of 1.10) 90	
Figure 4.50 Horizontal displacement vs. solution steps graph (Reduction factor of 1.10)	90
Figure 4.51 Horizontal displacement contour of last non-equilibrium state	91
Figure 4.52 Shear strain contours of last non-equilibrium state	91
Figure 4.53 Horizontal displacement vs. solution steps graph of last non-equilibrium state at history point #4	92
Figure 4.54 Shear strain contour of the numerical model and slip surface used in limit analysis	93

Figure 4.55 Non-circular failure surface analyzed for the same model properties as implemented in FLAC3D	93
Figure 4.56 Overall slope angle vs. Horizontal displacement graph	94
Figure 4.57 Horizontal displacement contour (overall slope angle 36°)	95
Figure 4.58 Shear strain rate contour (overall slope angle 36°)	95
Figure 4.59 Horizontal displacement vs. solution steps graph (overall slope angle 36°)	96
Figure 4.60 Horizontal displacement contour (overall slope angle 35°)	96
Figure 4.61 Shear strain rate contour (overall slope angle 35°)	97
Figure 4.62 Horizontal displacement vs. solution steps graph (overall slope angle 35°)	97
Figure 4.63 Factor of safety variation with respect to overall slope angle	98
Figure 4.64 Shear strain contour of the numerical model and slip surface applied in the limit analysis	99
Figure 4.65 Non-circular failure surface analyzed for the same model properties as implemented in FLAC3D	100
Figure 4.65 Slip circle and factor of safety is shown	101
with an overall slope angle of 15°	101
Figure 4.66 Section #5, slip circle of lowest factor of safety with a ground water table 50 m beneath the surface	102
Figure 4.67 Section #5, slip circle of lowest factor of safety with a ground water table 85 m beneath the surface	103
Figure 4.68 Factor of safety vs. water table depth from surface graph for 15° overall slope angle	103
Figure 4.69 Temporary slope having 18° overall slope angle with a ground water level at the surface	105
Figure 4.70 Temporary slope having 21° overall slope angle with a ground water level having a 50 m depth from surface	105
Figure 4.71 Temporary slope having 23° overall slope angle with a ground water level having a 85 m depth from surface	106
Figure 4.72 Overall slope angle vs. ground water level satisfying 1.30 factor of safety	106

Figure 4.73 Finite difference grids and material boundaries with dimensions ..	107
Figure 4.74 History points for recording displacements during stepping (or cycling) for solution	108
Figure 4.75 Horizontal displacement vs. solution steps graph	109
Figure 4.76 Horizontal displacement contours	109
Figure 4.77 Shear strain rate of the model	110
Figure 4.78 Horizontal displacement contour	111
Figure 4.79 Shear strain rate contour	111
Figure B.1 Section#1	128
Figure B.2 Section#2	129
Figure B.3 Section#3	129
Figure B.4 Section#4	129
Figure B.5 Section#5	130
Figure B.6 Section#6	130
Figure B.7 Section#7	130
Figure B.8 Section#8	131
Figure C.1 Section#1	132
Figure C.2 Section#2	133
Figure C.3 Section#3	133
Figure C.4 Section#4	133
Figure C.5 Section#5	134
Figure C.6 Section#6	134
Figure C.7 Section#7	134
Figure C.8 Section#8	135
Figure D.1 Section#1	136
Figure D.2 Section#2	137
Figure D.3 Section#3	137
Figure D.4 Section#4	137
Figure D.5 Section#5	138
Figure D.6 Section#6	138
Figure D.7 Section#7	138
Figure D.8 Section#8	139

Figure E.1 Section#1	140
Figure E.2 Section#2	141
Figure E.3 Section#3	141
Figure E.4 Section#4	142
Figure E.5 Section#5	142
Figure E.6 Section#6	142

CHAPTER 1

INTRODUCTION

1.1 Slope stability in geotechnical engineering

Both civil and mining engineering works require extensive profession on rock and soil engineering in order to accomplish a slope stability study. Rock and soil slope stability concepts have different point of view that the rock and soil structures are completely different. Strength properties, deformation principles etc. are all different. Rock slopes are susceptible to discontinuity failures rather than material failures or failure of the intact parts of the slope. In soil formations, failure line finds its own way including weak zones. Heavily fractured or weak rock formations sometimes exhibit common failure mechanisms.

Increasing temporary or permanent excavations in especially mining or civil engineering works forced engineers to understand analytical methods, investigative tools, and stabilization methods to solve slope stability problems. Construction techniques involving specialty must be understood well and realistic modeling is essential for these problems (Abramson et al., 2001).

1.2 Statement of the problem

Turkey has about 9.3 billion tons of lignite reserve and 47% of the overall reserve of lignite is located at Afşin-Elbistan lignite basin (in Kahramanmaraş). Thus the

basin possesses the most important potential in electricity production in Turkey (Koçak et al., 2003).

Kışlaköy open pit mine is the current running mine in the basin. Kışlaköy sector is being mined by EÜAŞ (Electricity Production Co. Inc.). Çöllolar sector is the second large size mine in the basin and will be operated by Park Teknik A.Ş.

For the open pit lignite mines, production scheduling is critical in order to establish proper lignite feed to the power plants. Thus a successful mine planning and equipment selection projects have to be accomplished. Overall slope angle is an essential parameter in mine planning governing the stripping ratio. Also, an overall slope failure may lead man and equipment losses as well as production stall.

Kışlaköy sector faced with an overall slope failure in 2006 and luckily no life loss was occurred. Production was also not delayed. However such a large size failure could lead considerable man and equipment loss blockading the production. This event forced the Çöllolar mine management to conduct an extensive analysis of slope stability in order to prevent a slope failure which can cause life and economical losses.

1.3 Objective of thesis

In Çöllolar sector, geological formations exhibit soil or weak rock properties and the mine will reach a depth of ~145 m.

Hence, the main aim of this thesis was to carry out an extensive slope stability analysis for the high slopes of Çöllolar sector. The slope stability analyses considered the presence of ground water and weak nature of the strata as well as the depth of the mine.

Another objective of the thesis is to make a contribution to the world literature for the slope design in weak rock or soil.

1.4 Methodology

Field study was the start point of the slope stability analysis. Samples were obtained from the geotechnical drilling for laboratory testing of the soil or rock units. Main rock types and soil units were distinguished and hydrogeological conditions were investigated.

Slope stability analyses were conducted by utilizing both 2-D limit equilibrium methods and 3-D finite difference method. Circular failure analyses and composite failure analyses were accomplished by using Rocscience SLIDE version 5.0 software for limit equilibrium analysis. Itasca FLAC3D version 3.1 software enabled 3-D analysis of the slope stability and factor of safety values were determined.

The above methods utilize the Mohr-Coulomb failure criteria and the main input parameters were shear strength parameters, namely cohesion and internal friction angle. Strength parameters were obtained as follows:

- 1- Laboratory testing of samples (in Soil Mechanics Laboratory at Civil Eng. Dept. (Karpuz et al., 2008).
- 2- Back-analysis of Kışlaköy large scale failure occurred in 2006.

Ground dewatering studies were considered in the analyses.

Maximum safe slope angles both for temporary and permanent conditions were determined by implementation of slopes with different overall slope angles.

1.5 Organization of thesis

Chapter 2 provides literature review relevant to the study including mechanisms of failure in rock and soil slopes, limit equilibrium and numerical analysis methods. Limit analysis (for circular failure) and continuum analysis with finite difference method is mentioned. Shear strength characterization and drained and undrained conditions in the analyses are stated.

General information about Çöllolar mine and Afşin-Elbistan basin, history of the mining activities in the field, dewatering studies, rock characterizations are presented in Chapter 3.

Chapter 4 presents the slope stability analyses and discussions of the results. Laboratory test results, back analysis of Kışlaköy 2006 slope failure are all included in the chapter utilizing both SLIDE software based on limit equilibrium and FLAC3D finite difference methods. Finally permanent and temporary slopes stability analyses by 2-D circular failure analysis methods and 3-D finite difference analysis methods have been presented and the importance of shear strength reduction (SSR) method is stressed up.

The results of this study are summarized in Chapter 5. Conclusions of this study and recommendations for future studies are given in this chapter.

CHAPTER 2

BASICS OF SOIL SLOPE STABILITY

2.1 Introduction

In order to apply slope stability principles properly, geology, hydrology and soil and rock properties should be understood well. Site conditions must be applied precisely to the model for analysis. Engineering judgments must be based on assessing the results of analyses considering acceptable risk or safety factors (Abramson et al., 2001).

A number of steps and levels of analyses are required in the process of wall design for open pits, from overall stability of the walls, to evaluation of the design performance and calibration of parameters through back-analysis. These studies require the use of different methods of analysis and software ranging from limit equilibrium methods to more involved numerical analyses such as finite difference methods, which can simulate material behaviour more precise and accurate. Before starting design and analysis, necessary field work must be conducted to provide the required information. Gathering and interpretation of the important data is very important that its quality is usually dependable for the accomplishment of the design (Carvalho, 2002). Some of the more important aspects of this preliminary work are summarized by Carvalho (2002):

- Regional geology, regional faulting and emplacement of the ore are vital factors and usually characterize the different lithological and structural domains in the pit.

- Hydrogeology and understanding of the groundwater flow regime have direct effects on overall stability.
- Structural mapping of the different domains and rock types govern both bench design and overall stability, including both joint sets as well as major features such as dykes, faults, contacts, etc.
- Identification of alteration zones affecting rock strength, within the pit is important. Different alterations within the same rock type should be grouped separately.
- Laboratory testing must be conducted on the different rock types with the results grouped by alteration for each rock type.

Under very weak or heavily fractured rock or soil conditions a strongly defined structural pattern no longer exists and the failure surface is free to find the line of least resistance through the slope. Observations of slope failures in soil suggest that this failure surface generally takes the form of a circle and most stability theories are based upon this observation. The conditions under which circular failure will arise when the individual particles in a soil or rock mass are very small as compared with the size of the slope and when these particles are not interlocked as result of their shape. Hence, crushed rock in a large waste dump will tend to behave as a “soil” and large failures will occur in a circular mode. Highly altered and weathered rocks will also tend to fail in this manner and it is appropriate to design the overburden slopes around an open pit mine on the assumption that failure would be by a circular failure process (Anon, 2003).

2.2 Slope failure mechanisms

In fact, it is challenging to determine the failure mechanism. Due to the absence of field data and failed material covering the slip surface may not allow researcher to understand the failure mechanism completely. Experience and knowledge when combined with the good observation lead to successive predictions on failure mechanisms on failed slopes or slopes to be excavated. It is essential to estimate

probable failure mechanism in order to use proper and adequate method during slope stability analysis. Some common failure mechanisms are considered:

2.2.1 Discontinuity failures

Failure mainly depends on the shear strength of the discontinuities or the strength of discontinuity intersections. The failure surface may be developed as a single discontinuity (planar failure), two discontinuities (wedge failure) or in a combination of several discontinuities intersecting each other (step path and step wedge failures). Tension crack commonly exists at the slope crest. These types of failures exist when the material properties are competent where formations like faults or joints are observed in a large scale, (Figure 2.1). These conditions are commonly valid in rock formations (Sjöberg, 1996).

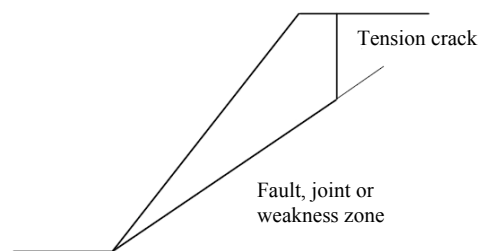


Figure 2.1 A typical planar failure with a tension crack

Failures governed by discontinuities can be analyzed by both conventional methods and numerical methods. Kinematic analysis (stereographic projection) or limit equilibrium analysis (planar or wedge type failure analysis) are commonly conducted. Discontinuum analysis covering discrete element or distinct element methods are two powerful tools in numerical analysis.

2.2.2 Continuum failures

Rotational shear failures exist due to the yielding of the continuous media in the form of circular failure commonly. Rotational shear failure forms in slopes without critically oriented discontinuities or planes of weakness. This is the typical mode of failure in soils and weak, heavily fractured rocks, (Figure 2.2).

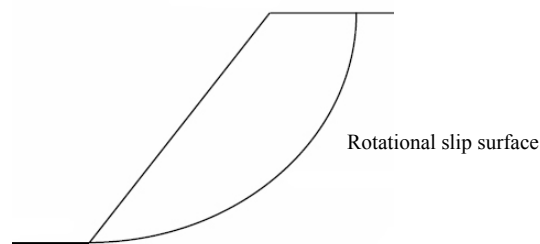


Figure 2.2 A typical circular failure

Limit equilibrium methods assuming a circular failure surface are commonly applied by slicing the slip material. Bishop Simplified (1955) method is a popular conventional analysis method for circular failure analysis. Continuum analysis is adequate for analyzing soil or weak rock formations. Limit equilibrium methods find field of application in analysis of failures having non-circular failure surfaces. Finite element or finite difference methods are the most commonly used numerical analysis methods for analysis of continua.

2.3 Limit equilibrium methods for soil slope stability analysis

2.3.1 Limit Equilibrium Analysis

Conventional slope stability analyses investigate the equilibrium of a mass of soil bounded below by an assumed potential slip surface and above by the surface of the slope. Forces and moments tending to cause instability of the mass are

compared to those tending to resist instability. Most procedures assume a two-dimensional (2-D) cross section for analysis. Successive assumptions are made regarding the potential slip surface until the most critical surface (lowest factor of safety) is found. If the shear resistance of the soil along the slip surface exceeds that necessary to provide equilibrium, the mass is stable. If the shear resistance is insufficient, the mass is unstable. The stability or instability of the mass depends on its weight, the external forces acting on it (such as surcharges or accelerations caused by dynamic loads), the shear strengths and pore water pressures along the slip surface, and the strength of any internal reinforcement crossing potential slip surfaces (Anon, 2003).

2.3.2 Rotational Shear Failure

Under very weak or heavily fractured rock or soil conditions the failure surface tends to find the line of least resistance through the slope. Observations of slope failures in soil exhibit that this failure surface generally takes the form of a circle and most limit equilibrium stability theories are based upon this observation. When the individual particles in a soil or rock mass are very small as compared with the size of the slope, circular failure is expected to be occurred (Hoek and Bray, 1981).

In weak strata, circular failure is the main concern but, inclined weak clay layers or faults can also consist non-circular failure surfaces and lead to a failure.

A typical circular failure analysis can be analyzed for finding factor of safety by utilizing the equation:

$$F = \frac{\sum [(c + \sigma'_n \tan \phi) / \cos \alpha]}{\sum \gamma h \sin \alpha} \quad (2.1)$$

Here h is the height of a slice, γ the volumetric weight of the soil in the slice, R is the radius of the circle and α is illustrated on the Figure 2.3.

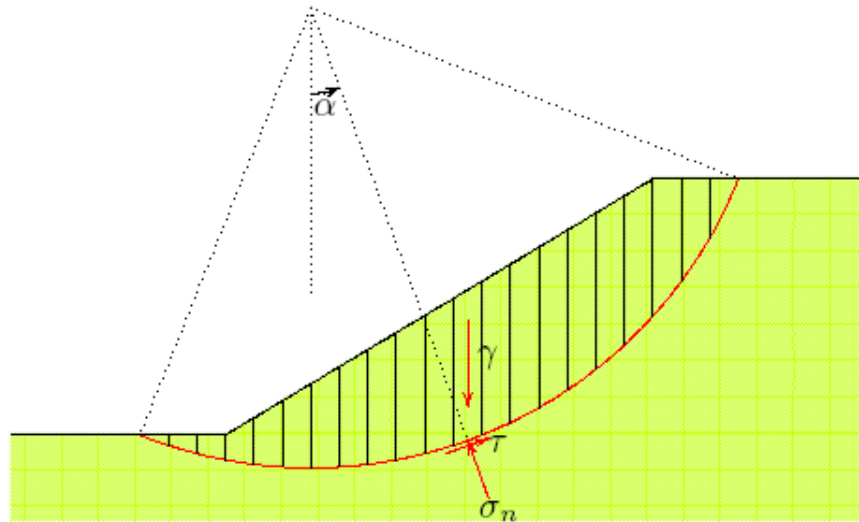


Figure 2.3 A circular slip surface

2.3.3 Assumptions for limit equilibrium methods

Limit equilibrium analysis is a simplification of the more rigorous limit theory in continuum mechanics. The method is used as routine slope stability analysis in soil and rock mechanics. In limit equilibrium analysis, an assumption of the slip-line field is made. The shear strength of the material is generally described by the Mohr-Coulomb yield criterion for simplicity, which sets a linear relation between normal strength and shear strength. A different failure criterion could be applied to several methods of limit equilibrium analysis (Sjöberg, 1996)

Many of the limit equilibrium methods (Ordinary Method of Slices (OMS), Simplified Bishop, Corps of Engineers' Modified Swedish, Spencer) establish static equilibrium by dividing the soil mass above the assumed slip surface into a finite number of vertical slices. The forces are slice weight, horizontal (normal) forces on the sides of the slice, vertical (shear) forces between slices, normal force on the bottom of the slice, shear force on the bottom of the slice. All of these

forces but weight of the slice are unknown and must be calculated in a way that satisfies static equilibrium (Anon, 2003).

2.3.4 Shape of slip surface and critical failure surface

All of the limit equilibrium methods necessitates that a predicted slip surface be designated in order to calculate the factor of safety. Different slip surfaces are tried for calculations in order to obtain the minimum factor of safety. For computation simplicity the slip surface is often assumed to be circular or composed of a few straight lines (Anon, 2003).

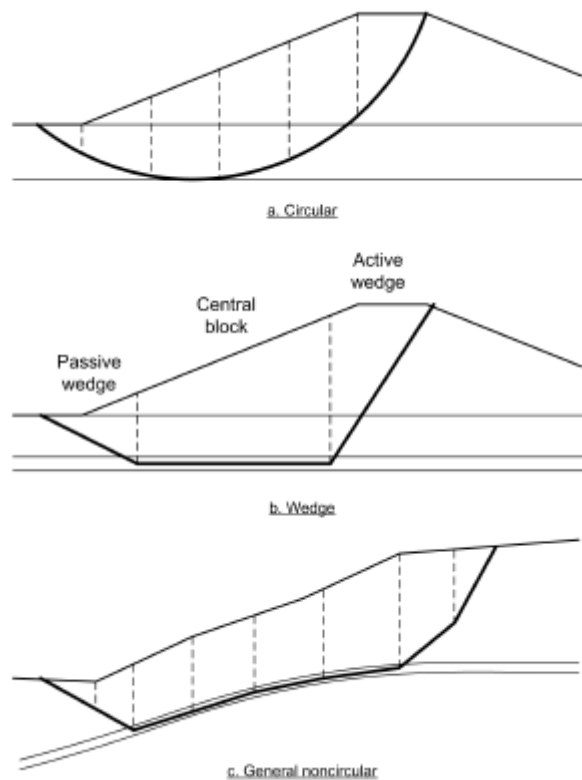


Figure 2.4 Three shapes of slip surfaces (Anon 2003a)

A circular slip surface, like that shown in Figure 2.1a, is often used because it is suitable to sum moments about the center of the circle. Using a circle also simplifies the calculations.

In wedge surface, the failure mechanisms are defined by three straight line segments defining an active wedge, central block, and passive wedge (Figure 2.1b). This type of slip surface may be used for analyzing slopes where the critical potential slip surface comprises a relatively long linear sector through a weak material bounded by stronger material.

In two circular segments with a linear midsection a combination of the two shapes (circular and wedge) discussed above that is used by some computer programs.

The critical slip surface is the surface with the lowest factor of safety. The critical slip surface for a given problem analyzed by a given method is found by a systematic procedure of generating trial slip surfaces until the one with the minimum factor of safety is found (Anon, 2003).

The Rocscience SLIDE software has a critical surface search property, attempting to find a slip surface having an overall minimum factor of safety for both circular and non-circular surfaces. For the circular surfaces, Grid Search, Slope Search, and Auto Refine Search are the methods. For non-circular surfaces, Block Search and Path Search are the methods (Anon 2003b).

2.3.5 Method selection

There are different limit equilibrium methods having superiorities over the other methods, which overcome their limitations. Methods are based on different assumptions or equilibrium conditions to be satisfied.

The various methods are compared in Table 2.1.

Table 2.1 Comparison of Features of Limit Equilibrium Methods (Anon, 2003)

Comparison of Features of Limit Equilibrium Methods						
Feature	Ordinary Method of Slices	Simplified Bishop	Spencer	Modified Swedish	Wedge	Infinite Slope
Accuracy		X	X			X
Plane slip surfaces parallel to slope face						X
Circular slip surfaces	X	X	X	X		
Wedge failure mechanism			X	X	X	
Non-circular slip surfaces – any shape			X	X		
Suitable for hand calculations	X	X		X	X	X

Duncan and Wright (2005) summarized some of limit equilibrium methods with respect to their limitations, assumptions and equilibrium conditions to be satisfied.

Table 2.2 Brief Comparison of Limit Equilibrium Methods (Duncan and Wright, 2005)

Procedure	Use
Infinite Slope	Homogeneous cohesionless slopes and slopes where the stratigraphy restricts the slip surface to shallow depths and parallel to the slope face. Very accurate where applicable.
Logarithmic Spiral	Applicable to homogeneous slopes; accurate. Potentially useful for developing slope stability charts and used some in software for design of reinforced slopes.
Swedish Circle; $\phi = 0$ method	Applicable to slopes where $\phi = 0$ (i.e., undrained analyses of slopes in saturated clays). Relatively thick zones of weaker materials where the slip surface can be approximated by a circle.
Ordinary Method of Slices	Applicable to nonhomogeneous slopes and $c-\phi$ soils where slip surface can be approximated by a circle. Very convenient for hand calculations. Inaccurate for effective stress analyses with high pore water pressures.
Simplified Bishop procedure	Applicable to nonhomogeneous slopes and $c-\phi$ soils where slip surface can be approximated by a circle. More accurate than Ordinary Method of Slices, especially for analyses with high pore water pressures. Calculations feasible by hand or spreadsheet.
Force Equilibrium procedures (Lowe and Karafiath's side force assumption recommended)	Applicable to virtually all slope geometries and soil profiles. The only procedures suitable for hand calculations with noncircular slip surfaces. Less accurate than complete equilibrium procedures and results are sensitive to assumed inclinations for interslice forces.
Spencer's procedure	An accurate procedure applicable to virtually all slope geometries and soil profiles. The simplest complete equilibrium procedure for computing the factor of safety.
Morgenstern and Price's procedure	An accurate procedure applicable to virtually all slope geometries and soil profiles. Rigorous, well-established complete equilibrium procedure.
Chen and Morgenstern's procedure	Essentially an updated Morgenstern and Price procedure. A rigorous and accurate procedure applicable to any shape of slip surface and slope geometry, loads, etc.
Sarma's procedure	An accurate procedure applicable to virtually all slope geometries and soil profiles. A convenient complete equilibrium procedure for computing the seismic coefficient required to produce a given factor of safety. Side force assumptions are difficult to implement for any but simple slopes.

Other than those, two commonly used methods, namely Bishop simplified and Janbu simplified methods are explained in detail.

2.3.5.1 Bishop simplified method of slices (1955)

Bishop Simplified method is a widely used method for analyzing soil slopes. The forces between the slices are taken into account, but it is assumed that the resultant force is horizontal, Figure 2.2. The method assumes that all interslice shear forces are zero. A typical slice of the model is also illustrated in Figure 2.2 which is commonly used in the methods assuming a circular failure surface (Verruijt, 2006).

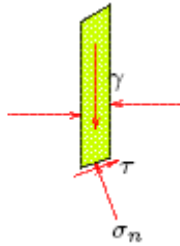


Figure 2.5 A typical slice for Bishop Simplified Method (Verruijt, 2006)

Bishop's method usually results in somewhat smaller values due to the consistency of Bishop's method (vertical equilibrium is satisfied), and it confirms known results for special cases, it is often used in geotechnical engineering. The equation used for calculation of factor of safety is:

$$F = \frac{\sum \frac{c + (\gamma h - p) \tan \phi}{\cos \alpha (1 + \tan \alpha \tan \phi / F)}}{\sum \gamma h \sin \alpha} \quad (2.2)$$

Here p is the pore water pressure and α is the angle of the slip surface of the slice with slip center.

Various other methods have been developed, but the results often differ only slightly from those obtained by Bishop's method. That may explain its popularity (Verruijt, 2006).

2.3.5.2 Janbu simplified method of slices (1968)

Janbu Simplified method uses the method of slices to determine the stability of the slide mass having circular or non-circular failure surface. The simplified procedure assumes interslice shear forces as none. The method satisfies vertical force equilibrium for each slice, as well as overall horizontal force equilibrium for the entire slide mass. Assuming interslice shear forces as zero leads incompleteness of moment equilibrium conditions. However, Janbu presented a correction factor, f_0 , to account for this inadequacy (Abramson et al., 2001).

2.4 Numerical Methods for Soil Slope Stability Analysis

Conventional forms of analysis like limit equilibrium methods are limited to basic and simplified problems. They provide little insight into slope failure mechanisms, with restricted application, basic loading conditions. Many geotechnical slope stability problems involve complexities relating to geometry, material anisotropy, non-linear behaviour, in situ stresses and the presence of several coupled processes (e.g. pore pressures, seismic loading, etc.) (Sjöberg, 1996). It is also important that not like the numerical analysis methods, the conventional limit equilibrium methods that do not consider the material deformation can only be used to describe the strength state of slope material (He MC, et al., 2007).

Numerical methods of analysis used for geotechnical slope stability investigations may simply be divided into two approaches:

- continuum modelling
- discontinuum modelling

2.4.1 Continuum modelling

Continuum modelling is suitable for the analysis of slopes that consist of massive, intact rock, weak rocks, and soil or heavily jointed rock masses while discontinuum modelling is appropriate for slopes controlled by discontinuity behaviour (Sjöberg, 1996).

Continuum approaches used in slope stability analysis include the finite-difference and finite-element methods. In both two methods, problem domain is discretized into a set of sub-domains or elements. In finite-difference method (FDM), solution procedure is based on numerical approximations of the governing equations, which are the differential equations of equilibrium, the strain-displacement relations and the stress-strain equations. In finite-element method (FEM), the procedure may exploit approximations to the connectivity of elements, and continuity of displacements and stresses between elements (Eberhardt, 2003).

3-D continuum codes such as FLAC3D (Itasca 1997) enables the engineer to take on 3-D analyses of rock and soil slopes on a desktop computer. Three-dimensional numerical codes make it possible to explore three-dimensional influences on slope stability, including slope geometry in plan and section, geology, pore water pressures, in situ stress, material properties and seismic loading due to earthquakes (Eberhardt, 2003).

2.4.2 Discontinuum modelling

Discontinuum modelling is an approach mostly applicable in rock formations having multiple joint sets governing the mechanism of failure. Discontinuum methods consider the problem domain as an assemblage of distinct, interacting bodies or blocks that are subjected to external loads and are predicted to exhibit significant motion with time.

This methodology is collectively referred to as the discrete-element method (DEM) (Eberhardt, 2003).

Itasca 3DEC is a powerful tool as a 3D distinct element code, enables user to overcome complex problems including faults, blocky formations or simply discontinuous media (such as jointed rock mass) subjected either static or dynamic loading (Anon, 2007a).

2.4.3 Itasca FLAC3D

Itasca FLAC3D is a three-dimensional explicit finite-difference program for engineering mechanics computation for geomechanics. The program is based on the well-established numerical formulation used by Itasca FLAC for two-dimensional analysis. FLAC3D broadens the analysis competence of FLAC into three dimensions, simulating the behaviour of three-dimensional structures built of soil, rock or other materials that undergo plastic flow when their yield limits are reached. Materials are constructed in a three-dimensional grid represented by polyhedral elements. The behaviour of each element governed by a prescribed linear or nonlinear stress/strain law in response to applied forces or boundary conditions. The material can yield and flow and the grid can deform (in large-strain mode) and move with the material that is represented. FLAC3D can make certain that plastic collapse and flow are modelled very accurately by using the explicit, Lagrangian calculation method and the mixed-discretization zoning technique (Anon, 2006).

The mechanics of the continuous media are derived from general principles (definition of strain, laws of motion), and the use of constitutive equations defining the idealized material. The set of partial differential equations, relating mechanical (stress) and kinematic (strain rate, velocity) variables, resulting mathematical expression, which are to be solved for particular geometries and properties for given specific boundary and initial conditions. Equations of motion are included as

an important subject, although FLAC3D is primarily concerned with the state of stress and deformation of the medium near the state of equilibrium (Anon, 2006).

2.4.4 Factor of safety in numerical modeling

Shear strength reduction method is a powerful and useful tool for different aspects. In limit equilibrium analysis, engineer must select the critical slip surface. In circular failure analysis, computer program is dictated for finding the slip circle having the smallest factor of safety. But, in complex geometries and geological conditions, a non-circular failure surface must be designated by researcher in order to be analyzed by limit equilibrium analysis methods. Finite element or finite difference analysis can present the failure surface as a calculation result. For factor of safety determination, shear strength reduction method is used. Reducing the strength parameters by a factor till collapse, leads to reaching the critical factor (of safety).

Numerical analysis simulates the behaviour of the modelled material and the structure using the linear or nonlinear stress/strain law in response to applied forces or boundary conditions. In contrast to limit equilibrium methods, in finite element (FE) or finite difference (FD) analysis, factor of safety calculation is not conducted directly. Shear Strength Reduction (SSR) method is used for determining collapse and factor of safety (Rocscience, 2004).

The factor of safety of a slope is defined as the “ratio of actual soil shear strength to the minimum shear strength required to prevent failure,” or the factor by which soil shear strength must be reduced to bring a slope to the verge of failure (Duncan, 1996). In the SSR finite element technique elasto-plastic strength is assumed for slope materials. The material shear strengths are progressively reduced until collapse occurs (Rocscience, 2004).

For Mohr-Coulomb material shear strength reduced by a factor (of safety) F can be determined from the equation

$$\frac{\tau}{F} = \frac{c'}{F} + \sigma' \frac{\tan \varphi'}{F} \quad (2.3)$$

This equation can be re-written as

$$\frac{\tau}{F} = c^* + \sigma' \tan \varphi^* \quad (2.4)$$

In this case,

$$c^* = \frac{c'}{F} \quad (2.5)$$

and

$$\varphi^* = \arctan\left(\frac{\tan \varphi'}{F}\right) \quad (2.6)$$

are reduced Mohr-Coulomb shear strength parameters, and these values can be input into an FE model and analyzed. These principles can be applied to finite difference (FD) method and factor of safety calculation can be performed (Rocscience, 2004).

Basic algorithm is:

For Mohr-Coulomb materials, the steps for systematically searching for the critical factor of safety value, F , which brings a previously stable slope to the verge of failure, are as follows (Rocscience, 2004):

Step 1: Develop an FE or FD model of a slope, using the deformation and strength properties established for the slope materials. Compute the model and record the maximum total deformation in the slope.

Step 2: Increase the value of F and calculate factored Mohr-Coulomb material parameters as described above. Enter the new strength properties into the slope model and re-compute. Record the maximum total deformation.

Step 3: Repeat Step 2, using systematic increments of F , until the FE or FD model does not converge to a solution, i.e. continue to reduce material strength until the slope fails. The critical F value just beyond which failure occurs will be the slope factor of safety.

The strength reduction method for determining factor of safety is implemented in FLAC3D through the SOLVE fos command. This command implements an automatic search for factor of safety. The procedure used by FLAC3D during execution of SOLVE fos is as follows.

First, the code finds a “representative number of steps” (denoted by N_r), which characterizes the response time of the system. N_r is found by setting the cohesion to a large value, making a large change to the internal stresses, and finding how many steps are necessary for the system to return to equilibrium. Then, for a given factor of safety, F , N_r steps are executed. If the unbalanced force ratio is less than 10^{-3} , then the system is in equilibrium. If the unbalanced force ratio is greater than 10^{-3} , then another N_r steps are executed, exiting the loop if the force ratio is less than 10^{-3} . The mean value of force ratio, averaged over the current span of N_r steps, is compared with the mean force ratio over the previous N_r steps. If the difference is less than 10%, the system is deemed to be in non-equilibrium, and the loop is exited with the new non-equilibrium, F . If the above-mentioned difference is greater than 10%, blocks of N_r steps are continued until: (1) the difference is less than 10%; or (2) 6 such blocks have been executed; or (3) the force ratio is less than 10^{-3} . The justification for case (1) is that the mean force ratio is converging to a steady value that is greater than that corresponding to equilibrium; the system must be in continuous motion (Anon, 2006).

2.5 Shear strength characterization

Shear strength is the main concern in slope stability analyses. Determination of the shear strength is a sensitive work and understanding the theory is essential in order to conduct analysis successfully.

2.5.1 Definition of shear strength

The limit equilibrium and numerical methods used for evaluating the stability of slopes require an accurate and reliable estimate of the in situ shear strength of the slope materials. However, the shear strength parameters are strongly influenced by many complex conditions, including the in situ state of stress, drainage, loading rates and soil or rock composition (Abramson, 2001).

Shear strengths are usually determined from laboratory tests performed on specimens prepared by compaction in the laboratory or undisturbed samples obtained from exploratory soil borings. The laboratory test data may be supplemented with in situ field tests and correlations between shear strength parameters and other soil properties such as grain size, plasticity, and Standard Penetration Resistance (N) values (Anon, 2003).

Shear strength for all of the slope stability analyses described in general is represented by a Mohr-Coulomb failure envelope that relates shear strength to either total or effective normal stress on the failure plane. In the case of total stresses, the shear strength is expressed as (Anon, 2003):

$$\tau = c + \sigma \tan \phi \quad (2.7)$$

where

c and ϕ = cohesion intercept and friction angle for the failure envelope respectively

σ = total normal stress on the failure plane

For effective stresses the shear strength is expressed as:

$$\tau = c' + (\sigma - u) \tan \phi' \quad (2.8)$$

where

c' and ϕ' = intercept and slope angle for the failure envelope plotted in terms of effective stresses

σ and u = total normal stress and pore water pressure, respectively, on the failure plane

The shear strength parameters, c and ϕ or c' and ϕ' , can be determined from laboratory shear test data. A suitable failure envelope is drawn by plotting the stresses representing failure for each test. In theory the failure envelope is tangent to all of the Mohr's circles of the failure. However, in actual practice there will be deviations among samples tested, and then the failure envelope represents a "best-fit" to the data from several tests. If the failure envelope is derived from direct shear tests, the complete state of stress is not known. The horizontal plane is assumed to be the failure plane, and only the stresses on the horizontal plane are known. The failure envelope is plotted by constructing the series of points representing the values of τ and σ on the horizontal plane from each test (Anon, 2003).

2.5.2 Total and effective stress analysis

The choice of total or effective stress analysis is of importance in the design and analysis of excavations in clay or clayey formations. The shear strength of a soil in terms of the effective shear parameter is given below (Kempfert and Gebreselassie, 2006):

$$\tau = c' + \sigma' \tan \phi' \quad (2.9)$$

where $\sigma' = \sigma - u$, $u = u_0 + \Delta u$, u_0 = steady pore pressure, Δu = excess pore pressure,

and in terms of the total stress shear strength is given by for saturated clay

$$\tau = c_u \text{ (Undrained shear strength)} \quad (2.10)$$

$$\text{Here } \phi = 0^\circ \quad (2.11)$$

Through their complex interactions with water, clays are responsible for a large percentage of problems with slope stability. The strength properties of clays are complex and subject to changes over time through consolidation, swelling, weathering, development of slickensides, and creep. Undrained strengths of clays are important for short-term loading conditions, and drained strengths are important for long-term conditions (Duncan and Wright, 2005).

2.5.2.1 Undrained strength

Undrained strength plays an important role in geotechnical engineering, both as an essential input to calculate the short term stability and bearing capacity, and also as an indicator of soil behaviour to correlation with other engineering properties, such as index parameters. The undrained shear strength of a soil is usually determined in laboratory from unconfined compression test or unconsolidated undrained (UU) triaxial test or consolidated undrained (CU) or laboratory shear vane. In the field it can be readily obtained from field shear vane test, pressuremeter, cone penetrometer, etc. The major factors that influence the undrained strength of normally consolidated soils are the water content (void ratio), the stress history (anisotropy) and time (Kempfert and Gebreselassie, 2006).

2.5.2.2 Drained strength

The drained strength of a soil is represented by the parameters c' and ϕ' and used for long-term analysis. Values of c' and ϕ' which are effective values can be obtained from drained tests or undrained tests with measurements of pore water pressure during shear (Kempfert and Gebreselassie, 2006).

2.5.3 Long and short term conditions

Slope stability analyses may be conducted using either total stresses or effective stresses. The use of total stress as opposed to effective stress analyses and the various ways in which design shear strengths can be selected can produce a wide range of safety factors. Bishop and Bjerrum (1960) set the following basic guidelines on the specification of shear strength for use in limit equilibrium slope stability analyses:

1. *"Effective stress analysis is a generally valid method for analyzing any stability problem and is particularly valuable in revealing trends in stability which would not be apparent from total stress methods. Its application in practice is limited to cases where the pore pressures are measured or can be estimated with reasonable accuracy, such as long-term stability where the pore pressure is controlled either by the static water table or by a steady-state flow pattern."*
2. *"Where a saturated clay is loaded or unloaded at such a rate that there is no significant dissipation of the excess pore pressures set up, the stability can be determined by the $\phi = 0$ analysis, using the undrained strength obtained in the laboratory or from in-situ tests. This is essentially an end of construction method, and in the majority of foundation problems, where the factor of safety increases with time; it provides a sufficient check on stability. For cuts, on the other hand, where the factor of safety generally decreases with time, the long term stability must be calculated by the effective stress method."*
3. *"For saturated soils the values of c' and ϕ' are obtained from drained [triaxial] tests or consolidated undrained tests with pore pressure measurements, carried out on undisturbed samples. The range in stresses at failure should be chosen to correspond to those in the field. Values measured in the laboratory appear to be in satisfactory agreement with field records with two exceptions. In stiff fissured clays the field value of c'*

is lower than the value given by standard laboratory tests; in some very sensitive clays the field value of ϕ' is lower than the laboratory value."

These 1960 guidelines are still generally valid but scientific advancements are going on. These developments are in soil testing in laboratory or in-situ. Especially undrained strengths, since that time now allow us to do more accurate analyses even if at the expense of some difficulty (Anon, 2007b). Experiment techniques have being developed or improved like recompression technique or the SHANSEP technique (Duncan and Wright, 2005).

Due to low permeability, a saturated or partially saturated soil undergoes a change in stress, pore pressure change will develop. By the time, the out-of-balance or excess pore pressure redistribute until an equilibrium state is reached. The final stage is called as long-term condition. Drained loading conditions observed at the stage (Anon, 2007b).

2.5.3.1 Analyses of stability during construction and at the end of construction (Undrained condition)

The most common short-term stability problem is the end-of-construction condition for materials dissipating excess pore pressures slowly when compared with the rate of construction. Sands and gravels which are more permeable soils, the period of pore pressure redistribution is very short and except some special considerations, stability problems typically will fall into the long-term category. Clays, on the other hand, dissipate excess pore pressures slowly. Thus the period of pore pressure redistribution continues for months or years after the completion of construction (Anon, 2007b).

Consolidation analyses can be used to determine for analyzing degree of drainage may develop during the construction period. As a rough guideline, materials having the values of permeability greater than 10^{-4} cm/sec usually accepted as fully drained throughout construction. The values of permeability less than 10^{-7}

cm/sec usually accepted as essentially undrained at the end of construction. For undrained conditions, pore pressures are related to several factors, like the degree of saturation of the soil, the density of the soil, and the loads exerted on it. Results of laboratory tests or various empirical rules enable engineer to estimate the pore pressures for undrained conditions. In fact it is not possible to estimate the pore pressures accurately for undrained conditions. This is the reason that undrained conditions are usually analyzed using total stress procedures rather than effective stress procedures (Anon 2003a).

2.5.3.2 Long-term stability problems (Drained condition)

There are several cases for drained conditions. The pore pressures may be equal to zero and the effective stress strength parameters, c' and ϕ' , should be used. Consolidated-drained (CD) tests should be performed to determine c' and ϕ' . Other case; partially submerged slope may be taken into consideration. In this case, the water table is stabilized and in equilibrium and the pore pressures can easily be determined by taking the depth below phreatic surface and multiplying by the unit weight of water. Effective stress strength parameters should be used as determined by CD or consolidated-undrained (CU) tests with pore pressure measurements. This problem may be solved two ways:

- a. Use total unit weights throughout, apply the boundary water pressure and specify the pore pressures in the slope.
- b. Use buoyant unit weight below the water table and neglect the boundary water pressure and pore pressures.

The common long-term stability problem is the steady state seepage condition. Pore pressures should be determined by drawing a flow net or by field measurement or by finite element analysis. Apply boundary water pressures on upstream and downstream slopes where applicable (Anon, 2007b).

2.6 Previous studies

Soil slope studies have been conducted by a wide range of engineers, scientists for practical and academically purposes.

Shear strength parameters are the most essential part in slope stability analysis. Deciding the design parameters is also a challenging job. Leshchinsky (2001) studied on using of peak or residual strength of soils.

Baker (2006) investigated the relation between safety factors with respect to strength and height of slopes and presented a simple analytical equation among those.

Hack (2002) evaluated the application of rock mass classification use in slope stability.

A practical procedure for back analysis of slope failures was postulated by Sonmez et. al. (1998) for closely jointed rock. Rock mass rating systems were utilized for circular failures.

Sonmez and Ulusay (1999) modified Geological Strength Index (GSI) and its applicability to stability of slopes.

Jiang and Yaagami (2007) determined a new back analysis of shear strength parameters from single slip. The essential point of the proposed method was the unique relationship between the $c'/\tan\phi'$ value and the critical slip surface in homogenous slopes.

Particle flow code in 2D (PFC2D) was used in a numerical analysis of the stability of a heavily jointed rock slope by Wang et. al. (2003).

Location of critical slip circle in slicing methods for circular failure is an essential work. Cheng (2003) presented a procedure in order to locate the critical slip circle by using a computer program finding the lowest value of factor of safety.

In a study conducted by Hammah et al. (2004), finite element analysis was used for factor of safety calculation of slopes by the method of “shear strength reduction”. Limit equilibrium and finite element analysis results were compared and concluded as consistent.

M. Cala et al.(2006) studied on slope stability analysis by using numerical analysis. FLAC and FLAC3D were used. Shear strength reduction method was utilized and 3-D analysis resulted in higher factor of safety values than 2-D solutions. In another study M. Cala et al. (2004) used modified shear strength reduction method for analyzing more complex problems. This method enabled user to determine different factor of safeties of different benches in one model.

Stead et al. (2006) collected developments in the characterization of complex rock slope deformation and failure using numerical modeling techniques together. Discussed and stated the adequate methods for different problems.

Bye and Bell (2001) assessed stability and designed slopes at Sandsloot open pit in South Africa. Predicted failure types are planar and wedge type failures.

Rock slope deformation was analyzed by using FLAC3D program at Antaibao open pit coal mine in China. Stability was evaluated and excavation design was optimized by He et al. (2007).

MTA conducted an up-to-date study (Akbulut et al., 2007) for slope stability of EÜAŞ Kışlaköy open cast mine for new permanent slopes. MTA conducted geotechnical investigations by core drilling, sampling and laboratory analysis. 2D Limit equilibrium back-analysis was studied and weak slip layer Mohr-Coulomb

parameters are determined. This study is important that this mine is close to Çöllolar mining area in the same lignite basin.

CHAPTER 3

GENERAL INFORMATION ABOUT THE STUDY AREA AND FIELD STUDIES

3.1 History of area

Afşin-Elbistan lignite basin is in Afşin and Elbistan districts which are bound to in Kahramanmaraş, Turkey. First lignite exploration work was initiated by W.Germany technical support with MTA (Maden Tetkik Arama Gen. Md or General Directorate of Mineral Research and Exploration) in 1966. In 1967 lignite formation in the basin was detected.

The lignite basin is divided into 6 sectors which are A (Kıřlaky), B (llolar), C (Afşin), D (Kuřkayası), E (obanbey) and F.

Feasibility study of the basin was prepared in 1969. Due to the lowest depth of the coal in Kırřlaky sector and necessity of construction of power plants for other sectors, lignite extraction was decided to be started in Kırřlaky sector.

In 1971, 3 foreign and 2 Turkish firm were established a joint venture in order to work on a detailed feasibility study including the thermic power plant. Mine planning and design works were taken over by a W.Germany firm. According to the project, in Kırřlaky sector, it was planned to produce 20 million tons of lignite and 18,6 million tons of it was planned to send to the power plant for electricity production. (Yrkoęlu, 1991)

A contract was signed by Ciner Group firm, Park Enerji and EÜAŞ (Electricity Production Co. Inc) for 25 years production of lignite in Çöllolar sector in order to meet the coal consumption of Afşin-Elbistan B thermic power plant in April, 2007.

In this thesis the slope stability study was carried out for both permanent and temporary slopes of new Çöllolar sector open cast mine. Slope stability design is essential in order to establish lignite production continuity for thermic power plant.

3.2 General description of the working area

The new Çöllolar open-cast mine is located in the Afşin-Elbistan lignite basin which is surrounded by Binboga, Nurhak and Engizek mountains. The major water stream is Ceyhan River and Hurman River which is a minor part of Ceyhan River, (Figure 3.1 and 3.2).



Figure 3.1 Location of the mine

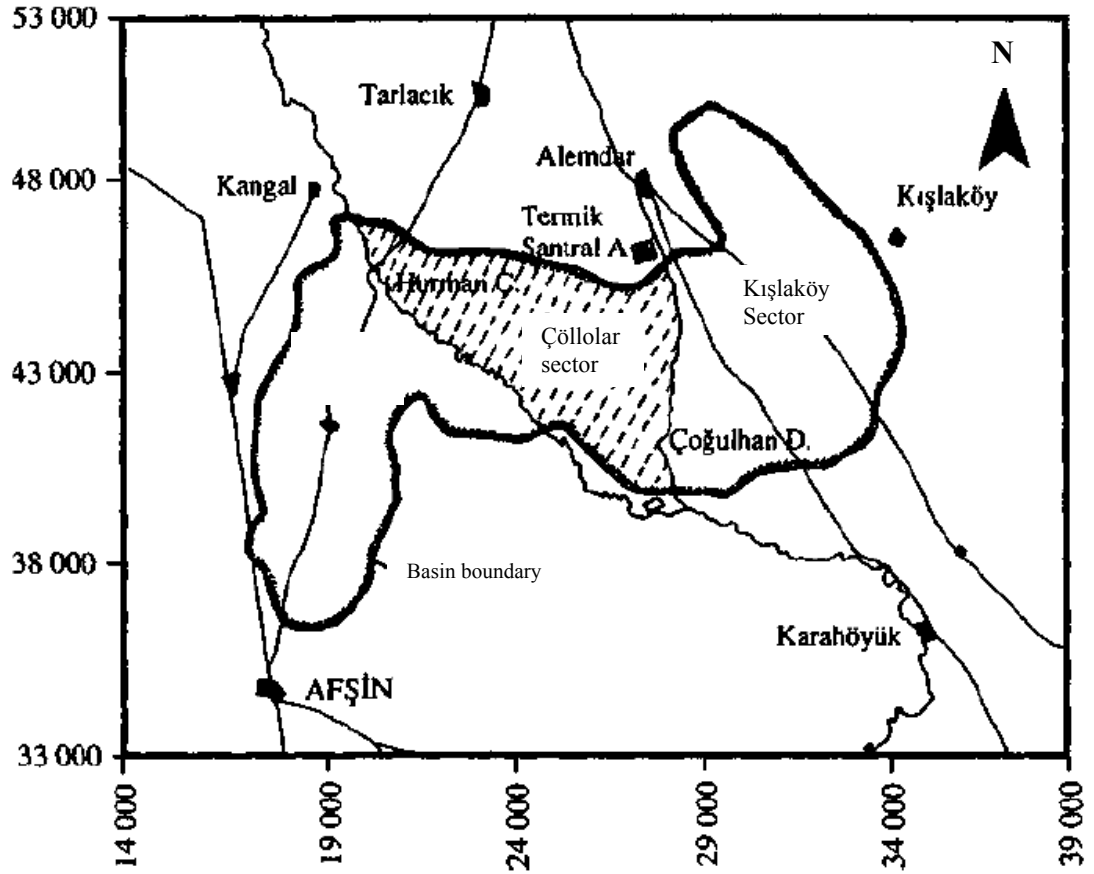


Figure 3.2 Kışlaköy and Çöllolar sectors in Afşin-Elbistan lignite basin (Otto Gold, 1969)

Çöllolar open-cast mine will be the second mining activity in the basin after active Kışlaköy open-cast mine. The new mine will meet the coal consumption of Elbistan B power plant.

3.3 Mine planning in the first five years

In the first three years, the Çöllolar mine field will be opened to get contact with the coal. Several contractors have been assigned by Park Teknik for this development work.

The mine field first will be opened with hydraulic excavators using both for excavation and loading the material on to trucks. The overburden material will be transported to the outside dump.

Firstly, a box-cut figure with a rectangular base will be formed on the south-west border of the mine field. The future mine exit will be positioned in the southern area of this box-cut.

At the end of the third year the box-cut will reach an overall expansion of approx. 260 ha at a depth of approx. 100 m. At the end of the 5th year, the mine will have been reached an expansion of 380 ha at a depth of about 145m.

After 3 years mine pit will be prepared for bucket wheel excavator usage, (Figure 3.3).



Figure 3.3 Bucket wheel excavator being used in Kışlaköy open cast mine.
(Akbulut et al., 2007)

3.4 General geology of the area

Afşin-Elbistan lignite bed is in a closed basin which is formed during the rise of the Toros Mountains after Alpine Orogeny. Region base is formed by Permo-Carboniferous old limestones (Yörükoğlu, 1991).

On the south of Kızıldağ, outcrops of Neogene formations are observed and in other places, the formations are covered by Quaternary old precipitations. The thickness is about 300-400 m. Neogene lithologies are listed from bottom to top as:

- Red, brown coarse grained clastic precipitations
- Reddish brown, sandy, marl sedimentations
- Greenish, bluish-plastic clay and marls of lignite bottom
- Lignite
- Gyttja
- Greenish, bluish, plastic clay and marls of lignite top

Typical formations and thicknesses are illustrated on the Figure 3.4.


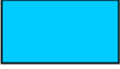



Formation		Thickness
Loam		8-20 m
Blue clay		8-30 m
Gyttja		25-45 m
Lignite		25-70 m
Footwall Clay		100-125 m

Figure 3.4 Formations and their thicknesses in Çöllolar mine

Gyttja has an importance in the area and there are transitive layers of coal and gyttja. Gyttja disappears by getting thinner by the direction of north and north-east.

Lignite which is formed in Pliocene age, is just beneath the gyttja, having a thickness of 10-80 m. The thickness of the coal increases from east to west and north to south. Faults are observed on the south of Kışlaköy sector.

3.5 Hydrogeology

Yörükoğlu (1991) reported that Ceyhan River having main branches of Hurman River, Söğütlü and Sarsap Streams as important water streams in Elbistan basin.

It is also indicated that 5 types of aquifers are present in the mining area. These are:

- Quaternary aquifer or top aquifer
- Gytja aquifer
- Artesian aquifer
- Paleozoic limestone aquifer
- Quarstic aquifer

Quaternary aquifer: This coarse grained formation performs high permeability of water. Especially, rainy seasons, ground water affects these permeable layers. Under quaternary formation, due to the blue clay existence, this ground water performs aquifer behaviour. Flow direction is from north to south.

Gyttja aquifer: Gytja being laid on the lignite layer having a thickness of 40-50 m, has high water content. Thus this situation is important from the aspect of mining and slope stability. Water trapped in the gyttja performs pressurized aquifer behaviour. Gytja has low permeability of water and does not dissipate water easily.

Artesian aquifer: This formation has no importance for mining activities and existed under the lignite layer.

Paleozoic limestone aquifer: This aquifer is not important for mining activities because of its depth and thick clay layers lying between lignite and the aquifer.

Quarstic aquifer: During tectonic movements, Kızıldağ limestones and side debris etc. established contact with lignite layer. These limestones provide permeable zones. Kızıldağ water, called as “Quarstic area”, finds access to mining area. Thus, this aquifer is very important from the point of mining activities.

3.6 Water Drainage

It is indicated that in Kışlaköy open cast mine, a slope failure occurred in 2006, the water level was high and 15 m under the surface at the top of the slope. Formations in the areas have very low permeability parameters as also being detected in laboratory which informs about drainage difficulties.

Park Teknik with the consulting firm MBEG firm plans to lower the water table 100 m below the surface within the 5th year targets. This plan may be sounded as lowering the water table under gyttja formation.

CHAPTER 4

ELBİSTAN-ÇÖLLÖLAR SLOPE STABILITY ANALYSES

4.1 Introduction

In an open pit or open cast mine stripping ratio is an essential concern. Stripping ratio informs about the cost and profit of extracted material. In an open cast mine, overall slope angle can also be important for the lignite recovery when there is a restriction of legal mine boundary.

Permanent slopes were designed in the safe range of safety factor as steep as possible. It means less excavation and transportation of the waste material and shorter time to reach the lignite.

In production slopes, bucket wheel excavators are planned to be used in the required bench and overall slope geometry. For the box-cut stripping, truck-excavator system will be utilized.

Slopes were conventionally analyzed for circular failure using a limit equilibrium method, that is, Bishop Simplified method (1955). Mining area was analyzed for circular failures and factor of safety values were calculated. Information about faulting is scarce in the Çöllölar mine field. A fault with unknown dip and dip direction is located on the line of the River Hurman. Composite failure analyses were also conducted by using limit equilibrium methods.

4.2 Geotechnical drilling

Five geotechnical boreholes enabled soil mechanics testing by taking undisturbed samples using shelby tubes. SK-1, SK-3, SK-5, SK-6, SK-11 are the names of these five boreholes. Undisturbed samples were sent to Soil Mechanics Laboratory in Civil Engineering Department, METU (Figure 4.1). Laboratory results were reported by Karpuz et al., 2008. The results are presented in the Appendix A being classified according to the type of formation.

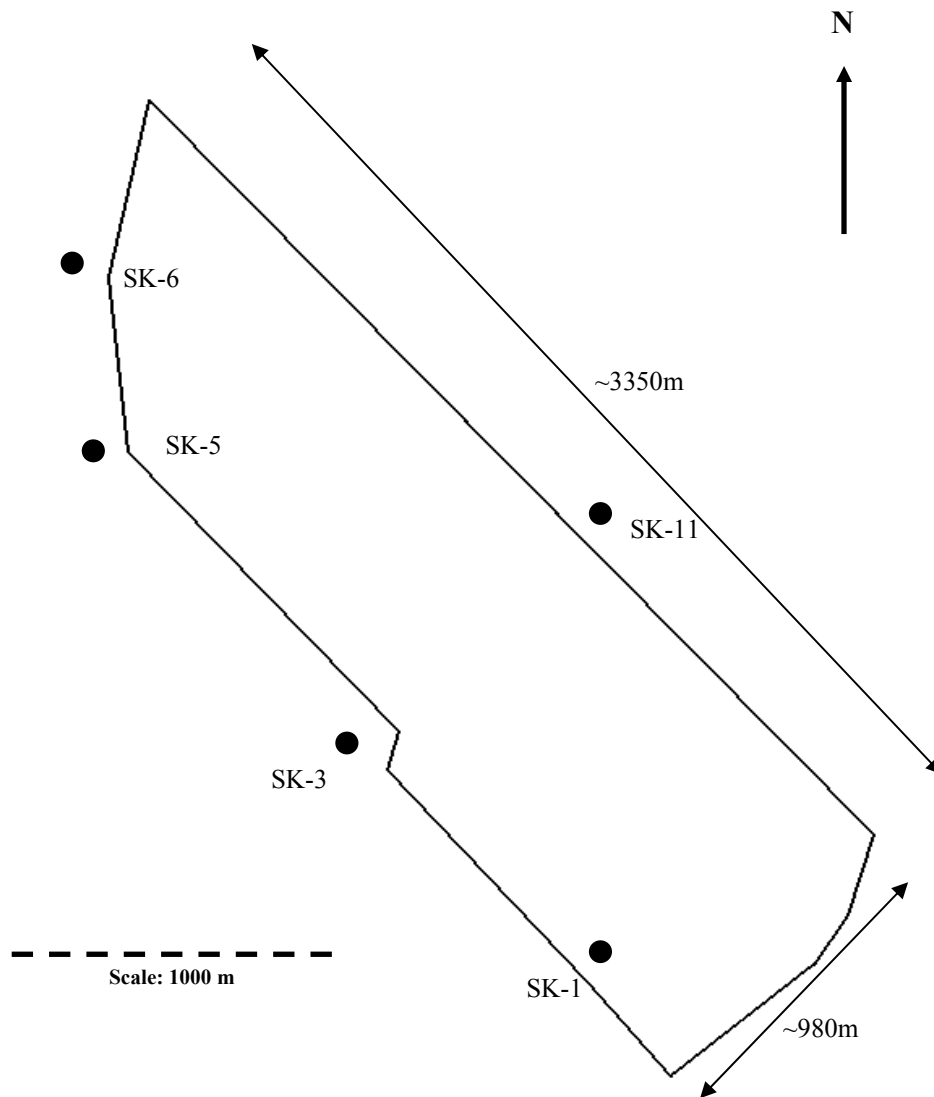


Figure 4.1 Locations of geotechnical research boreholes

Table 4.1 Coordinates of the boreholes in global coordinate system

Borehole	X	Y
SK-1	25163	42343
SK-3	24402	43063
SK-5	23542	43931
SK-6	23472	44529
SK-11	24949	43861

4.2.1 Borehole Information

SK-1 borehole is located at the side where the conveyors lie from pit to dump area. Seven undisturbed samples were recovered. Borehole has a depth of 76,5 m. six sieve analysis and hydrometers, six consolidated-drained, direct shear test, five consolidation, one unconfined strength, seven water content, unit weight, void ratio, specific gravity, four Atterberg limits and four permeability coefficient test are conducted and interpreted.

SK-1

from-to (m)

0-13.50 Top soil, gravel, loam

13.50-19.50 Blue clay

19.50-53.15 Gyttja (fossil, limestone, with coal, grey or black)

53.15-76.50 Lignite (interburdens of gyttja, with little clay or black clay bands)

SK-3 borehole is located near to Hurman river, on the middle of permanent slopes on the south-west side of the mine. Twelve undisturbed samples were recovered. Borehole has a depth of 144 m. twelve sieve analysis and hydrometers, twelve consolidated-drained, direct shear test, one consolidation, two unconfined strength, twelve water content, unit weight, one void ratio, specific gravity, eight Atterberg limits and six permeability coefficient tests are conducted and interpreted.

SK-3

from-to (m)

0-8.50	Top soil, gravel, marn
8.50-32.50	Blue clay (sand or gravel layers)
32.50-33.40	Plastic black clay
33.40-77.50	Gyttja (with lignite or fossil bands, patches of limestone)
77.50-141.50	Lignite (grey, blue, black and green clay bands)
141.50-144	Blueish green clay

SK-5 borehole is located at west side; permanent south-west and north-west slopes junction. Fifteen undisturbed samples were recovered. Borehole has a depth of 142.5 m. Twelve sieve analysis and hydrometers, fifteen consolidated-drained, direct shear test, four consolidation, four unconfined strength, fifteen water content, unit weight, four void ratio, twelve specific gravity, nine Atterberg limits and seven permeability coefficient test are conducted and interpreted.

SK-5

from-to (m)

0-10.50	Top soil, loam with gravel and silt
10.50-40.50	Greenish clay with plastic or sand layers
40.50-73.50	Gyttja (with lignite or fossils, grey-black bands)
73.50-115.00	Lignite (with gyttja, fossil and clay bands)
115.00-142.50	Grey-green clay with lignite bands

SK-6 borehole is located in the middle of north-west permanent slope. Thirteen undisturbed samples were recovered. Borehole has a depth of 94 m. Eleven sieve analysis, thirteen hydrometers, eleven consolidated-drained, direct shear test, five consolidation, four unconfined strength, thirteen water content, unit weight, five void ratio, eleven specific gravity, eleven Atterberg limits and twelve permeability coefficient test are conducted and interpreted.

SK-6

from-to (m)

0-8.00	Top soil, gravel, clay and loam
8.00-43.00	Blue clay (plastic, little plastic layers with sand or gravel bands, black clay layer
43.00-73.30	Gyttja (lignite, black-grey fossil, limestone or clay bands)
73.30-94.00	Lignite (Gyttja, fossil, clay layers, black plastic clay band)

SK-11 borehole, at the middle of production (temporary) slope borders on the north-east side. Ten undisturbed samples were recovered. Borehole has a depth of 100,5 m. Ten sieve analysis and hydrometers, ten consolidated-drained, direct shear test, seven consolidation, ten water content, unit weight, seven void ratio, specific gravity, six Atterberg limits and six permeability coefficient test are conducted and interpreted.

BH-11

from-to (m)

0-21.85	Top soil, brown clay, loam, gravel, silty bands
21.85-50.00	Blue clay (Little plastic, sandy, thin black clay layer)
50.00-76.50	Gyttja (grey clay, with fossil, limestone or black clay interburdens)
76.50-100.50	Lignite (gyttja, fossil and clay bands, limestone layers)

SK-3 and SK-5 boreholes were drilled to sub-coal levels; other three boreholes reach only up to coal levels.

4.3 Laboratory testing and results

Input parameters for slope stability analysis dedicated to the type of formations are illustrated in the Table 1.2. In the parenthesis, standard deviation values are indicated and for black clay and loam standard deviation value was not calculated due to the sample scarcity. Consolidated drained tests were carried out by shearing three samples applying three different normal stresses. Other tests were carried out by single or double repetitions.

Table 4.2 Summary of laboratory experiment results (Karpuz et al., 2007)

Material	Water content w_n (%)	Unit Weight γ_n (kN/m³)	Peak Cohesion c'_p (kPa)	Peak Internal Friction Angle ϕ'_p(°)	Residual Cohesion c'_r (kPa)	Residual Internal Friction Angle ϕ'_r(°)
Loam	36	18.66	56	15	48	11
Blue clay	31.25 (5.24)	18.06 (0.91)	34.3 (19.2)	26.3 (0.1)	21.5 (17.8)	21 (0.09)
Gyttja	78 (37.9)	15.06 (1.72)	59 (48.4)	31.8 (0,18)	41.3 (41.9)	28.33 (0.146)
Lignite	104 (45)	13.20 (2.32)	48 (19.44)	32.8 (7.28)	32.4 (17.90)	30 (9.64)
Black Clay	60	16.80	57.5	28	36	25
Green clay (Footwall clay)	47 (32.7)	16.74 (2.73)	32.83 (16)	23.17 (4.62)	15.5 (11.50)	16 (4.47)

*Standard deviation values are illustrated in the paranthesis.

4.4 Back-analysis of Kışlaköy 2006 failure

For any slope stability analyses, details of topography, geology, shear strength, groundwater conditions, external loading and a plan curvature of slope (three dimensional effects) must be known and interpreted judiciously to obtain the most representative subsurface model for analyses.

Because of the difficulties inherent in the classical design approach to slopes, back-analysis of a slope failure often provides valuable information for future design purposes. This can only be a meaningful, however, in circumstances where the majority of factors that contributed to the failure can be evaluated. Results of the back-analysis calculations should provide an unambiguous measure of the shear strength at failure. Back-analyses are conducted without adequate information being available on the mode of failure or on the pore pressure that existed at the time of failure (Abramson, 2001).

When a slope fails it can provide a useful source of information on the conditions in the slope at the time of failure as well as an opportunity to validate stability analysis methods. Because the slope has failed, the factor of safety is considered to be unity (1.0) at the time of failure (Duncan and Wright, 2005).

4.4.1 Summary of Back-analysis conducted by MTA

On 23.10.2006, due to the faulting and inclined black clay (weak layer) formations in Kışlaköy sector, a slope failure occurred having a width of 200 m on the south side and 400 m on the north side, (Figure 4.2, 4.3 and 4.4).

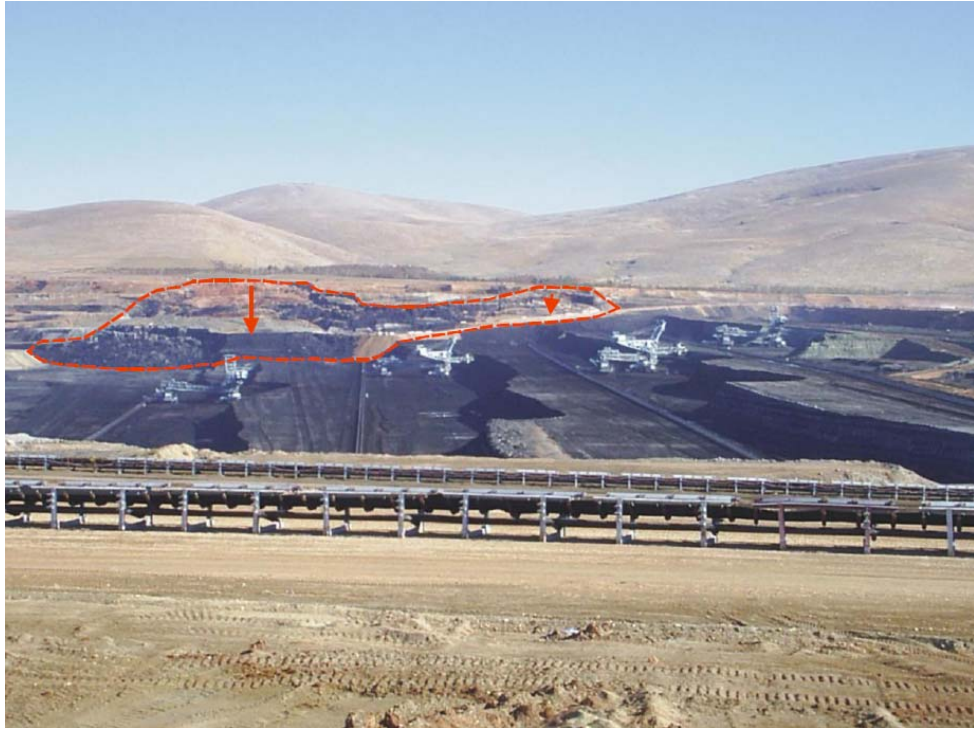


Figure 4.2 Kışlaköy 2006 slope failure.(Akbulut et al., 2007)



Figure 4.3 Kışlaköy 2006 slope failure (from Park Teknik personnel)

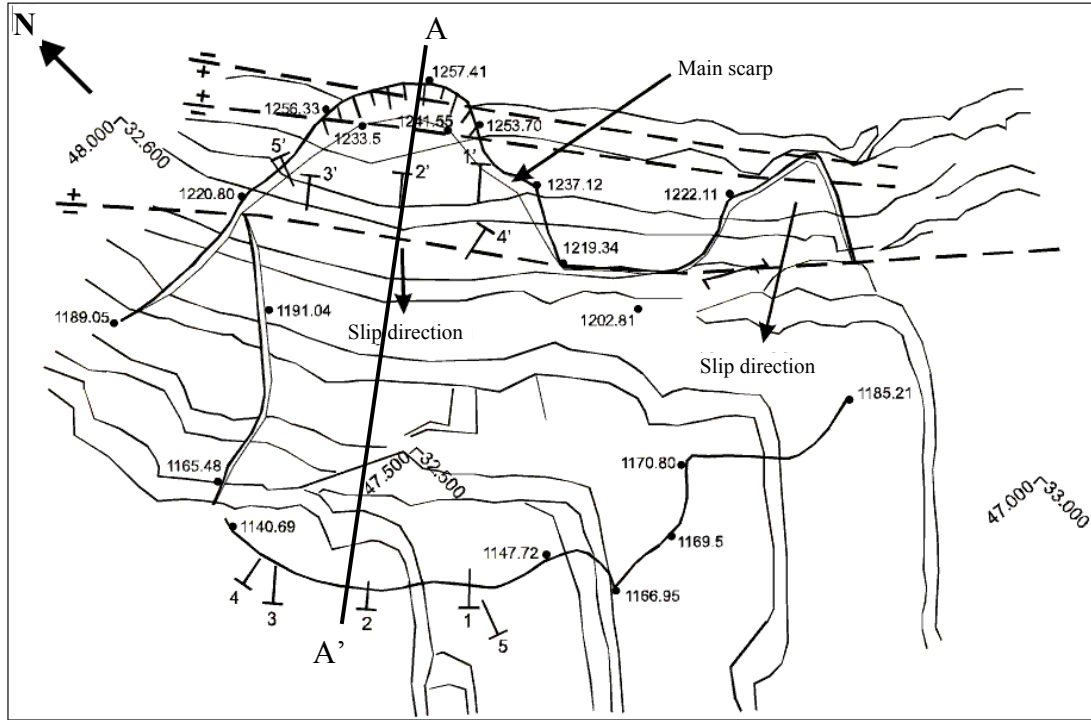


Figure 4.4 Plan view of the 2006 failure (Akbulut et al., 2007)

According to MTA report (Akbulut et al., 2007), 2006 failure developed in at least 3 stages. Starting from the tip of 2nd bench, slip has developed in the form of active passive wedge (1st stage). The back of the failure was #3 fault passing from the 2nd bench. The sliding surface of the mass was black clay on the bottom. After this slip, a steep and high slope was exposed due to the displaced mass. Because of this reason, the back side became destabilized. At the back, #2 fault passing from 1st bench and the bottom black clay consisted slip surface in the form of active-passive wedge (2nd stage). After 2nd stage, failures progresses behind #2 fault on the form of circular failures reaching up to back of the slope, (Figure 4.5).

When the factors leading to the failure are investigated, the geological structures, steepness of benches, high level of groundwater level seemed to play major roles. From the mine plan, it was estimated that east slope had an overall slope angle of 13-14° during the period of the slide.

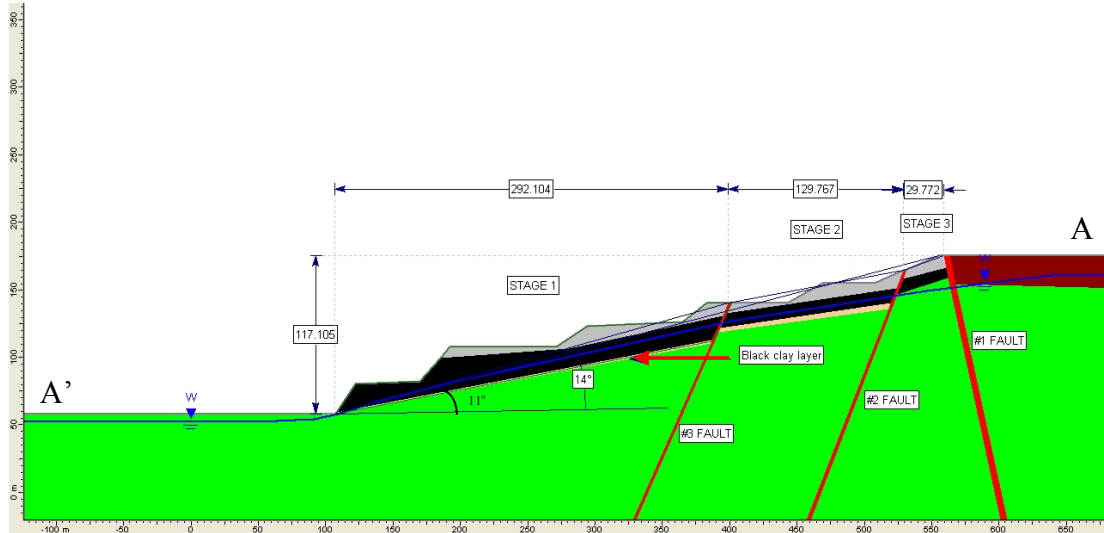


Figure 4.5 Kışlaköy 2006 failure in detail for cross section A-A'

Fault parameters are taken as $c'=0$ kPa, $\phi'=29^\circ$ and the condition satisfying the SF (factor of safety) =1 is investigated in order to back-analyze the black clay parameters. By accomplishing the back-analysis, MTA team decided to use residual shear strength parameters which are given in Table 4.2.

Table 4.2 Shear strength parameters decided to be used as design parameters by MTA (Akbulut et al., 2007)

Material	Residual Cohesion c'_r (kPa)	Residual Internal Friction Angle ϕ'_r ($^\circ$)
Black clay	23	10.5
Gyttja	20	35
Lignite	14	40
Lignite-Gyttja average	17	38
Green clay (Footwall clay)	33	14

4.4.2 Back-analysis of black clay

Conducting back-analysis of a slope failure is important in order to detect the soil engineering parameters or verify the laboratory test results. Kışlaköy 2006 failure is back analyzed by using limit equilibrium methods with Rocscience SLIDE program and 3-D finite difference analysis with Itasca FLAC3D program.

Using the MTA report (Akbulut et al., 2007) for slope stability studies for Kışlaköy open cast mine, geological cross section of the 2006 slip failure was prepared in order to initiate back analysis studies, (Figure 4.5).

It was indicated that the 2006 failure had 3 main stages. Akbulut et al.(2007) only back calculated the black clay parameters as $c'=23$ kPa ve $\phi'=10,5^\circ$ (residual strength parameters of black clay (from laboratory testing) by using limit equilibrium methods and decided to use residual shear strength parameters as design parameters by analyzing the first stage. At first stage, #3 fault was the sliding surface at the back and mass moved on the black clay layer.

In the study, firstly the black clay properties are back calculated and then properties of gyttja-lignite layer combinations are investigated. It was observed that internal friction angle values of gyttja and lignite in laboratory test results were close to each other. Also, gyttja and lignite have no sharp boundaries of transitions in the field and they were considered as single layer in the analyses.

4.5 Limit equilibrium back-analysis in 2-D

In the 1st stage of the failure, back-analysis was carried out for determining the shear strength parameters of the black clay. In the other stages, the back-calculated values are applied to the models.

4.5.1 Back-analysis of 1st stage of the 2006 Kışlaköy failure

From MTA report (Akbulut et al., 2007) geological data was collected in order to construct the model. Firstly the 1st stage of the failure was analyzed, (Figure 4.6). Here, MTA results were checked by reanalyzing the Kışlaköy 2006 slide.

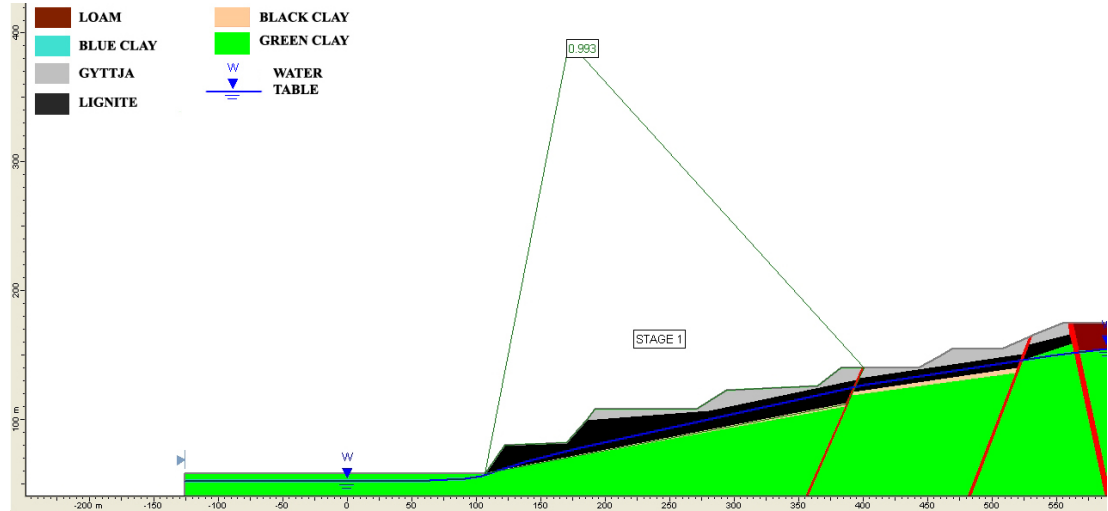


Figure 4.6 Slip surface and factor of safety plot of 1st stage of the 2006 failure
(cross section A'-A)

For the front block, factor of safety was calculated as just below 1, meaning limit or failure condition. Fault strength parameters were used as $c'=0$ ve $\phi'=29^\circ$. Strength parameters leading to the failure for black clay was confirmed as $c'=23$ kPa and $\phi'=10.5^\circ$ which are also the same as back calculated values in MTA report are the values of residual shear strength parameters obtained from laboratory testing of MTA. Thus, these parameters are concluded as back calculated as the final shear strength parameters of black clay. Shear strength parameters for the materials were shown in Table 4.2.

4.5.2 Back-analysis of 2nd stage of the 2006 Kışlaköy failure

In addition, 2nd and 3rd stages were modelled and analyzed with limit equilibrium methods. By using the parameters gathered in the 1st stage, the 2nd stage was analyzed and factor of safety was calculated as 1.15 indicating stability, (Figure 4.7).

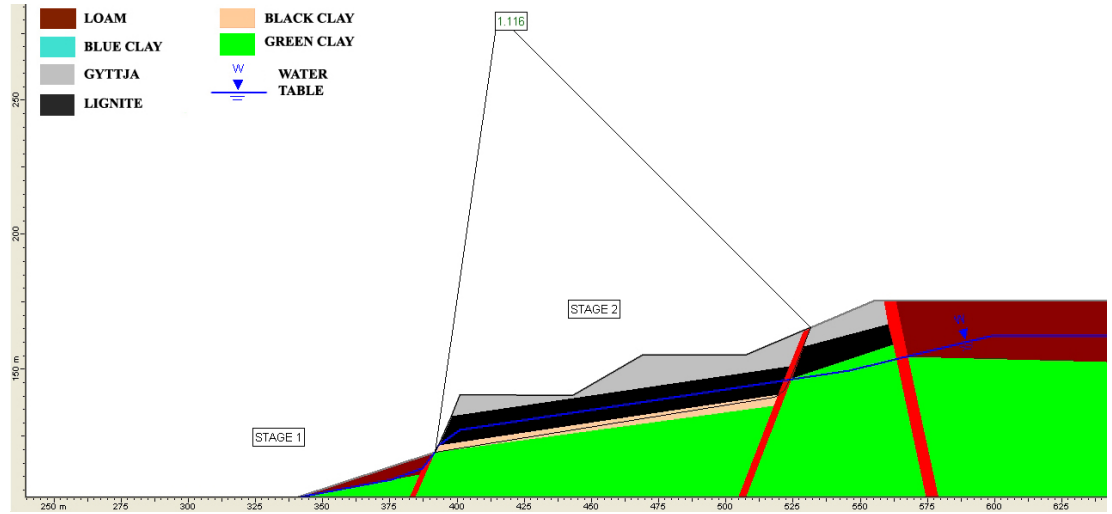


Figure 4.7 Slip surface and factor of safety plot of 2nd stage of the 2006 failure
(cross section A'-A)

This is a contradiction and showed that the parameters of black clay obtained from these two failures are different. This means that shear strength parameters of black clay are expected to be lower than $c'=23$ kPa and $\phi'=10.5^\circ$ values. Black clay weak layers are present in both Kışlaköy and Çöllolar sectors. In order to determine the strength properties of black clay and gytja-lignite layer combination more accurately in detail, 3D finite difference analysis was decided to be conducted.

4.5.3 Back-analysis of 3rd stage of the 2006 Kışlaköy failure

In 3rd stage, the circular failures occurred behind the #2 fault. The steep slip scarps that existed after the 2nd stage failure initiated circular failures, and these failures continued till reaching the clayey and gravel zones behind the slope. Cracks and splits existed. The first circular failure that was predicted to occur after 2nd stage of the failure was identified in order to verify the shear strength parameters of lignite and gyttja layer combination (Figure 4.8).

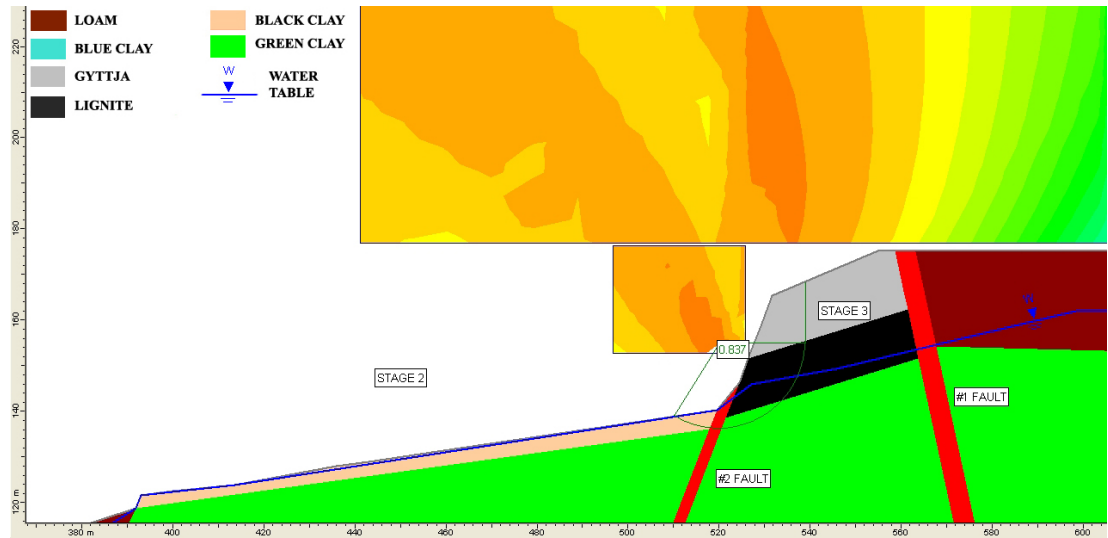


Figure 4.8 Slip surface and factor of safety plot of 3rd stage of the 2006 failure (cross section A'-A)

For this analysis the parameters used by Akbulut et al. (2007) were tried. For gyttja $c'=20$ kPa and $\phi'=35^\circ$ and for lignite formation $c'=14$ kPa and $\phi'=40^\circ$ parameters were used. However, in this case, factor of safety for the first circular slip surface behind fault #2 was found as 0.84. Failure surface pass through the footwall clay which was not the observed condition in the field. Therefore, conducting 3-D finite difference analyzes were decided to be more realistic when determining the strength parameters of black clay and gyttja and lignite layers.

4.6 Finite difference back analysis in 3-D

FLAC3D v.3.1 was used for analyzing 2006 Kışlaköy failure. The aim was to back analyze for finding black clay properties. Laboratory test samples of black clay were scarce; determining the design parameters was critical for this weak soil type. For gyttja and lignite, satisfactory laboratory tests were completed thus, back analysis of gyttja and lignite formations was not strictly necessary, but verification of these parameters was decided to be helpful.

4.6.1 Finite difference model

For black clay 29 numerical models had been cycled to obtain the solution. In order to reach the solution sometimes, up to a hundred thousand steps were required. Number of the model runs and high step numbers forced to construction of a simplified model with a coarse mesh (Figure 4.9).

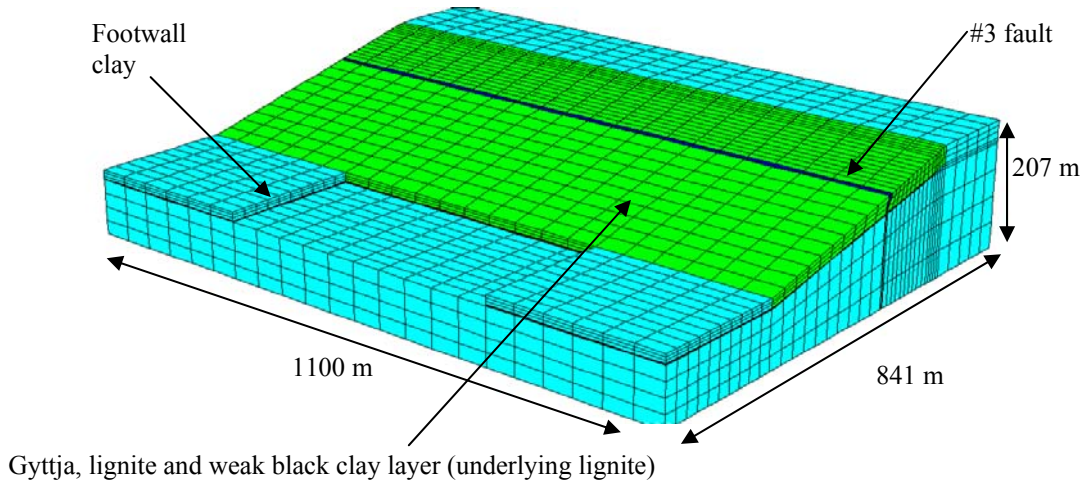


Figure 4.9 Kışlaköy 2006 slope failure, 3D model in FLAC3D, finite difference grids, dimensions and materials.

In the model, detailed benches were not constructed on the slope face; only an equivalent slope was generated by coarse finite difference grids. All those enabled running a lot of models fast and gained the time. This was safely done so, because stability analyses were concentrated on the overall slope stability rather than stability of the individual benches.

History points were located for displacements with increasing number of steps. Slope displacements of those points were recorded for both elastic and plastic stepping, (Figure 4.10).

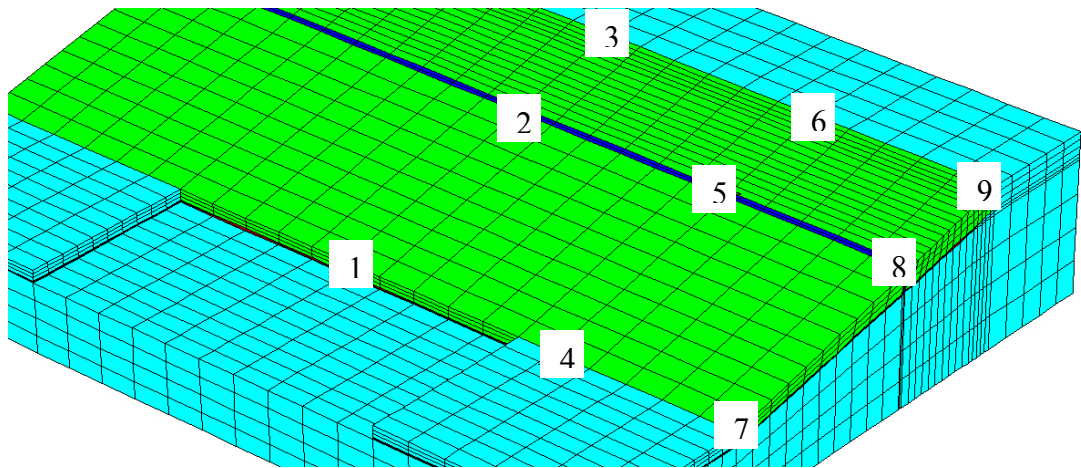


Figure 4.11 Kışlaköy 2006 slope failure 3D model in FLAC3D, history points for recording displacements during cycling for solution.

Gravitational acceleration of 9.81 m/sec^2 was applied in the direction of gravity in the model.

Base of the model was fixed for all directions. The sides of the model were fixed not to move normal to the in-plane directions of the side walls. By this way, in elastic run, model body was enabled to move under the effect of gravity and sides of the model could move freely within constrained directions, parallel to the plane but not in in-plane direction.

4.6.2 Elastic parameters

Elastic parameters are not related with slope failure or collapse but, they must be decided in order to initialize ground stress conditions. For the model, a high elastic modulus was selected. This way, model reaches equilibrium in a shorter time for solution. Poisson's ratio is important that while elastic stage is running, ground stress is being generated and the Poisson's ratio affects the horizontal stress formation.

For entire model, the same parameters were used as:

$$E = 10000 \text{ MPa}$$

$$\nu = 0.2$$

$$\gamma = 16.18 \text{ kN/m}^3$$

4.6.3 Strength parameters

Several trial runs on models were completed and calibration of the model was established. In 2006 Kışlaköy slope failure, it was observed in the field that that slip had penetrated into the footwall clay (green clay). Thus, trial runs on model showed that the use of high strength parameters for footwall clay enabled proper modelling of this condition. The parameters of the black clay were changed during the back calculations. Faults were modelled as zones of gouge material. Thus, fault zone was modelled as weak material not an interface. Strength parameters of the faults were decided to be used lower than they were used in analysis by using limit equilibrium methods after several trials. Tensile strength parameters of black clay, lignite and gyttja were taken as “zero”. Strength parameters of the fault and footwall clay were assumed as Table 4.3.

Table 4.3 Mohr-Coulomb and tensile strength parameters of the formations

Material	Cohesion, c' (kPa)	Internal Friction Angle, ϕ' ($^{\circ}$)	Tensile Strength, T_o (kPa)
Fault	0	20	0
Footwall clay (green clay)	33000	40	100

4.6.4 Back analysis of black clay

Some trial runs were conducted and in order to obtain a failure, it was determined that back calculated values of $c'=23$ kPa and $\phi'=10.5^{\circ}$ for black clay were found high and decided to be lowered. Friction angle was low enough. The lowest value of the residual cohesion value of 8 kPa (obtained from METU laboratory test results) was accepted as fixed and friction angle was back analyzed.

Two different values for gyttja and lignite were used in order to observe the effects of different parameters for gyttja and lignite. Firstly $c'=17$ kPa and $\phi'=38^{\circ}$ which were average of gyttja and lignite design parameters used by MTA (Akbulut et al., 2007) were used here too. Then $c'=54$ kPa and $\phi'=32^{\circ}$ which were the average values of gyttja and lignite laboratory tests results completed at METU, were used. While fixing $c'=8$ kPa, friction angle was changed and displacements were recorded for the history points on the model.

Horizontal displacement (towards pit bottom) vs. step plot (Figure 4.12 and 4.13) was obtained at the history point of #2. This point was located at 80 m height from the pit bottom and on the #3 fault, (Figure 4.11).

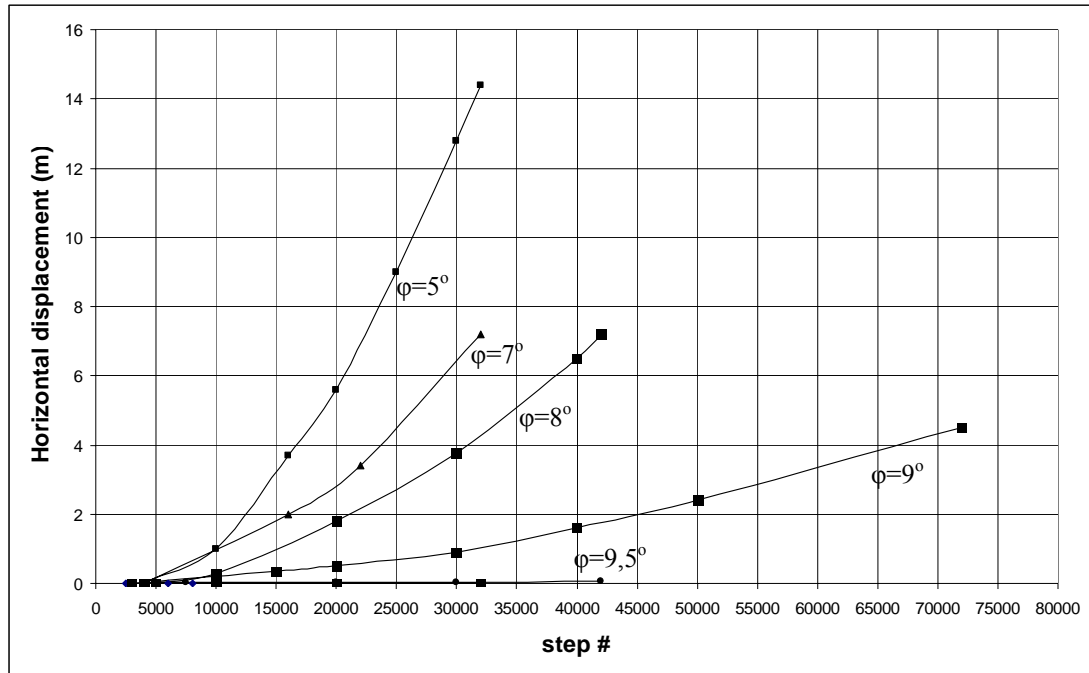


Figure 4.12 Horizontal displacements vs. solution step plot using shear strength parameters obtained from laboratory testing at MTA (Akbulut et al., 2007) gytija and lignite ($c'=17$ kPa and $\phi'=38^\circ$) keeping $c'=8$ kPa for black clay

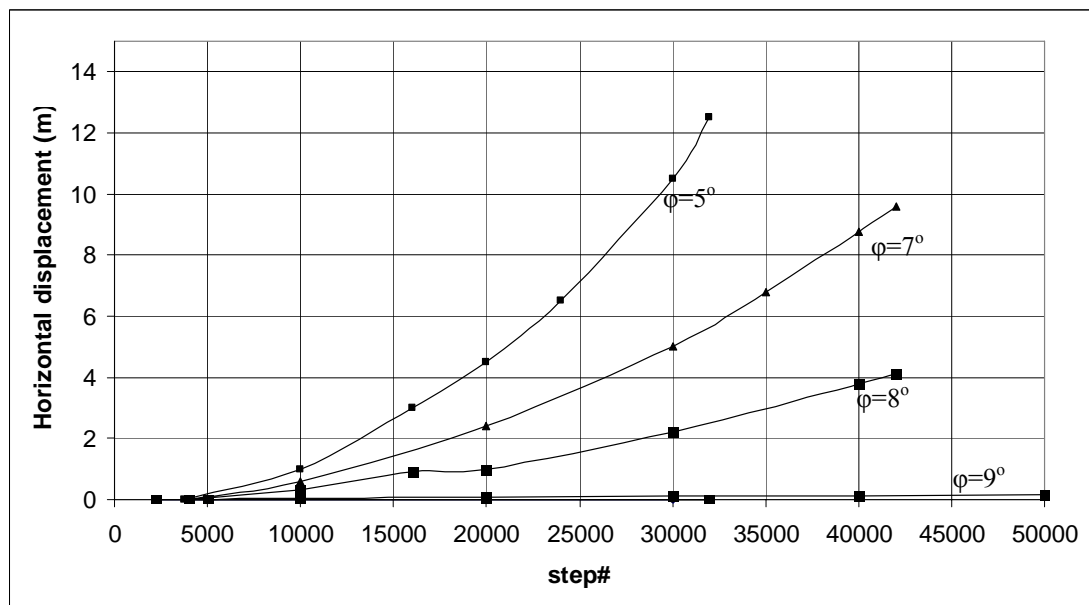


Figure 4.13 Horizontal displacements vs. solution step plot using shear strength parameters obtained from laboratory testing at METU for gytija and lignite ($c'=54$ kPa and $\phi'=32^\circ$) keeping $c'=8$ kPa for black clay

For both models, friction angle values of 10° , 9.75° and 9.5° for black clay, exhibited small displacements and movements stopped in history plots. When friction angle was lowered to 9° displacements that initiate failure were observed and movements did not stop. This point was identified as the instability point or predicted beginning point of slide from the displacement results. Lower values of the friction angles gave results of fast and large movements.

Being inspired of the shear strength reduction method, graphs were plotted for horizontal displacement vs. friction angle of black clay using two different gyttja and lignite shear strength parameters, (Figure 4.14 and 4.15).

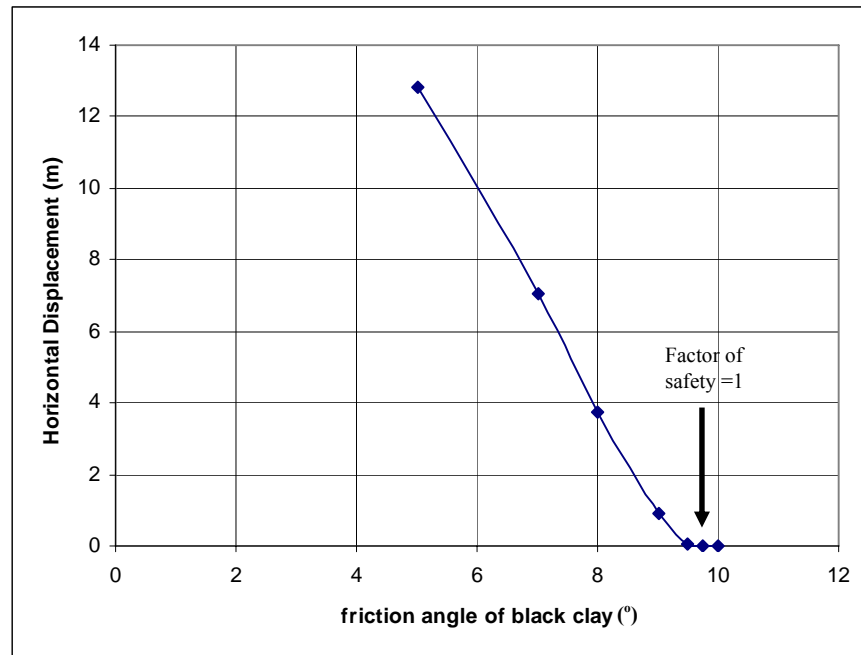


Figure 4.14 Finite difference solution convergence plot using shear strength parameters obtained from laboratory testing at MTA (Akbulut et al., 2007) gyttja and lignite ($c' = 17$ kPa and $\phi' = 38^\circ$) keeping $c' = 8$ kPa for black clay

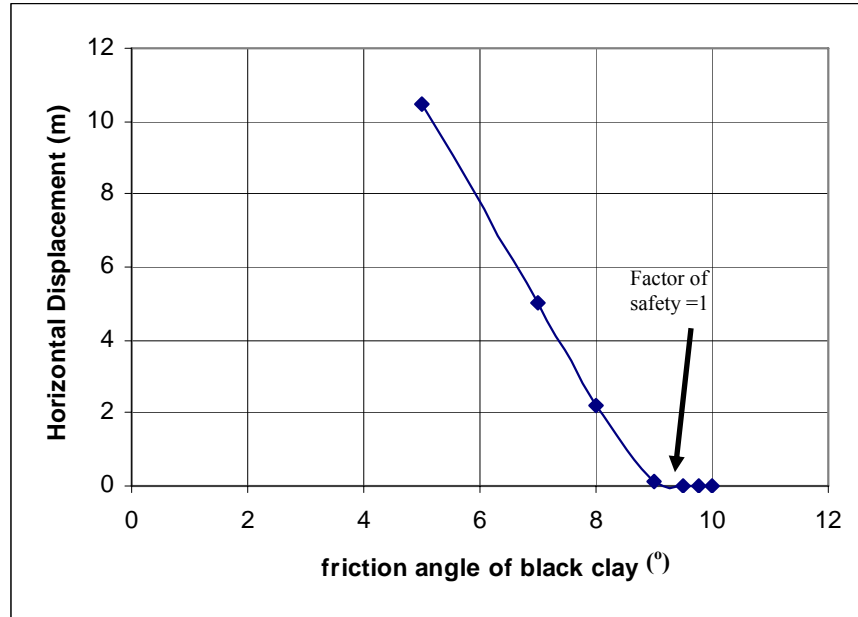


Figure 4.15 Finite difference solution convergence plot using shear strength parameters obtained from laboratory testing at METU for gyttja and lignite ($c' = 54$ kPa and $\phi' = 32^\circ$) keeping $c' = 8$ kPa for black clay

As seen from the figures for two different strength parameters of gyttja-lignite layer mobilized, black clay friction angle was back analyzed nearly the same value. In order to understand the decision on the point indicating unity for factor of safety Figures 4.16 and 4.17 are plotted for the shear strength parameters obtained from laboratory testing at METU for gyttja and lignite ($c' = 54$ kPa and $\phi' = 32^\circ$) keeping $c' = 8$ kPa for black clay.

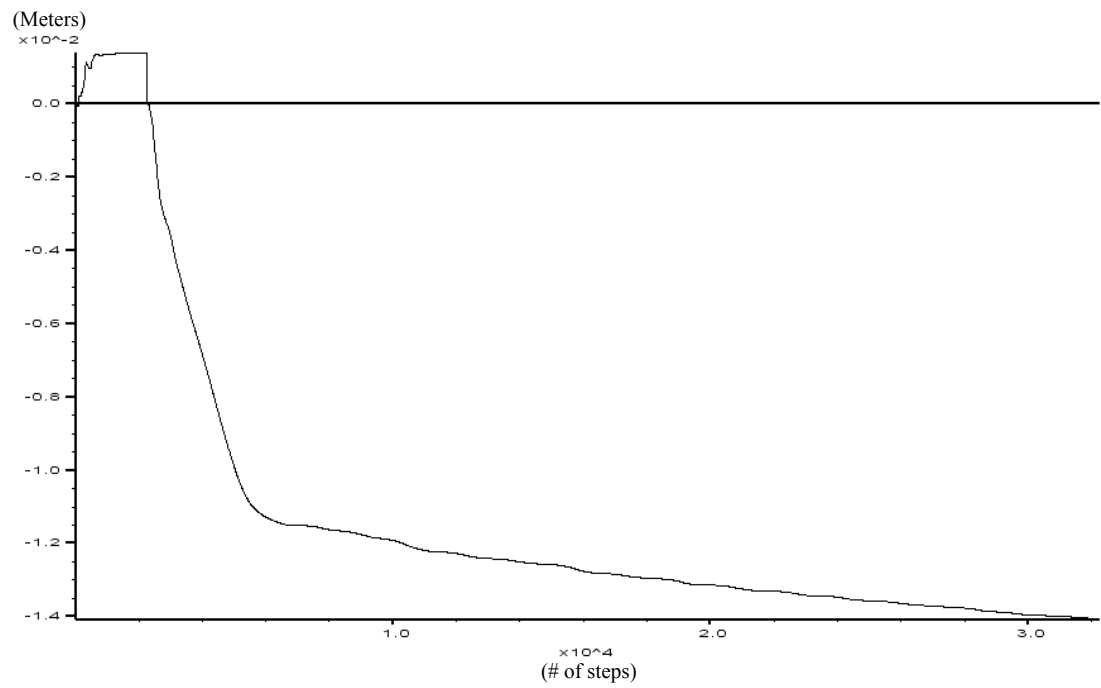


Figure 4.16 History plot for $c'=8$ kPa and $\phi'=9.5^\circ$ for black clay indicating stability

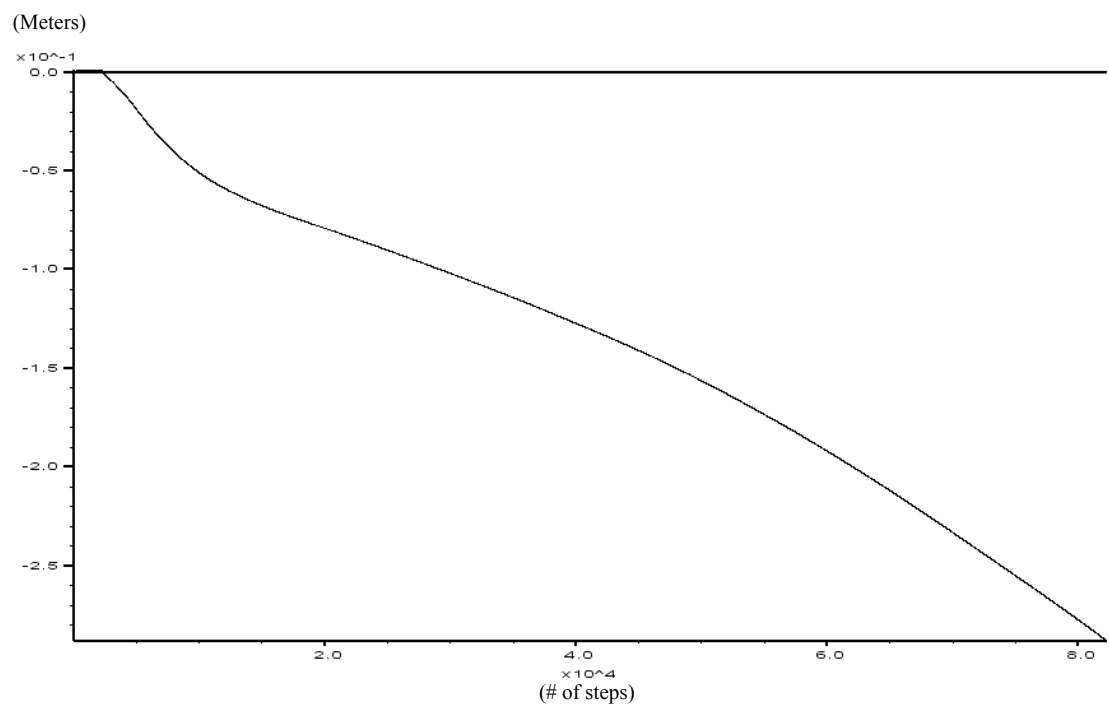


Figure 4.17 History plot for $c'=8$ kPa and $\phi'=9^\circ$ for black clay indicating instability

Figure 4.17 is the last non-equilibrium state that when the internal friction angle is lower than 9° , model is unstable and it was verified by running the model by using different values. By this way, on the Figure 4.15, the factor of safety point for one was determined.

Even if the strength parameters of gyttja and lignite was changed, consistent plots of the results (Figure 4.12, 4.13, 4.14, 4.15) indicated the back calculated parameters as $c'=8$ kPa and $\phi'=9^\circ$ for black clay. These results were found as very low when compared to back-analysis results of black clay ($c'=23$ kPa and $\phi'=10.5^\circ$) obtained by using limit equilibrium methods. In fact back-calculated values of black clay are found to be lower than the laboratory tests. In the field, water is known to be trapped in particular layers due to the low permeability of the strata and aquifer or aquiclude presence. The difference of the parameters for laboratory scale and field conditions arises from the pore pressure. In the field high pore pressures are predicted to be existed. Other consideration is related with the sampling problem that the samples may not be representative.

In order to construct a c' vs ϕ' plot, back-analyses were conducted for the cohesion values of 5, 8 and 11 kPa for black clay then internal friction angles were back-calculated.

For $c'=5$ kPa, horizontal displacement variation with respect to internal friction angle was plotted on the Figure 4.18.

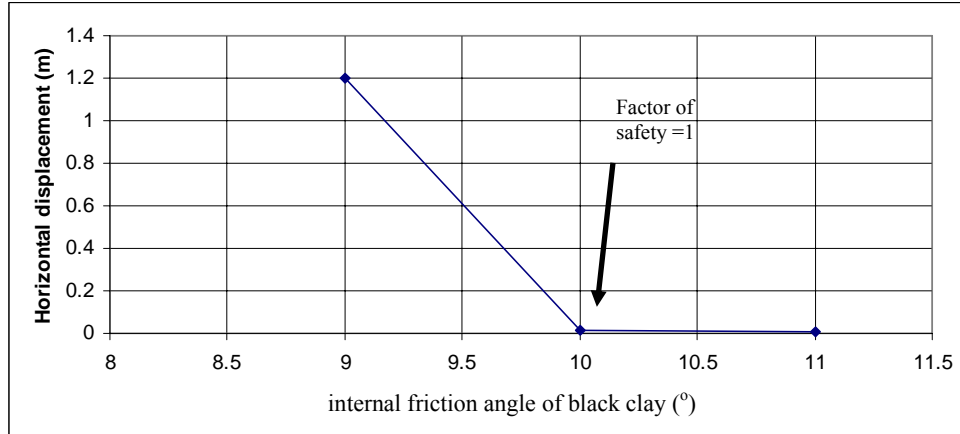


Figure 4.18 Horizontal displacement vs. friction angle of black clay with $c'=5$

$c'=5$ kPa and $\phi' = 10^\circ$ values resulted in unity in factor of safety.

Then, $c'= 11$ kPa and horizontal displacement variation with respect to internal friction angle was plotted on the Figure 4.19.

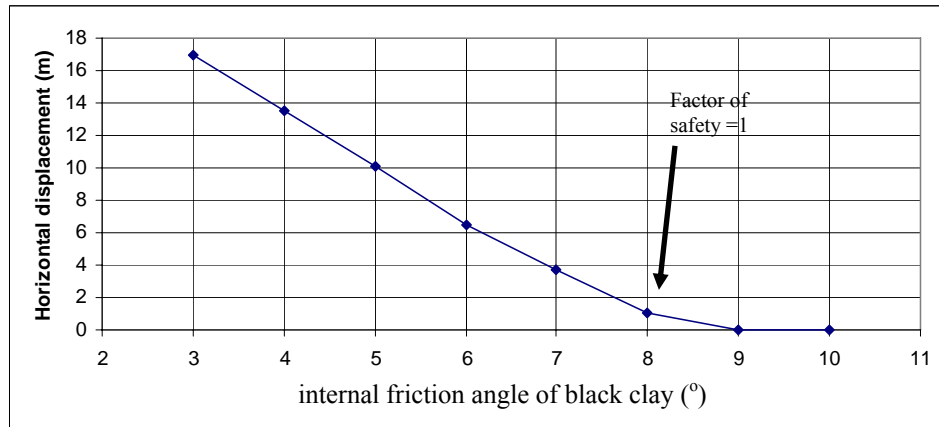


Figure 4.19 Horizontal displacement vs. friction angle of black clay

$c'=11$ kPa and $\phi' = 8^\circ$ values resulted in unity in factor of safety.

c' vs ϕ' graph is constructed on the Figure 4.20.

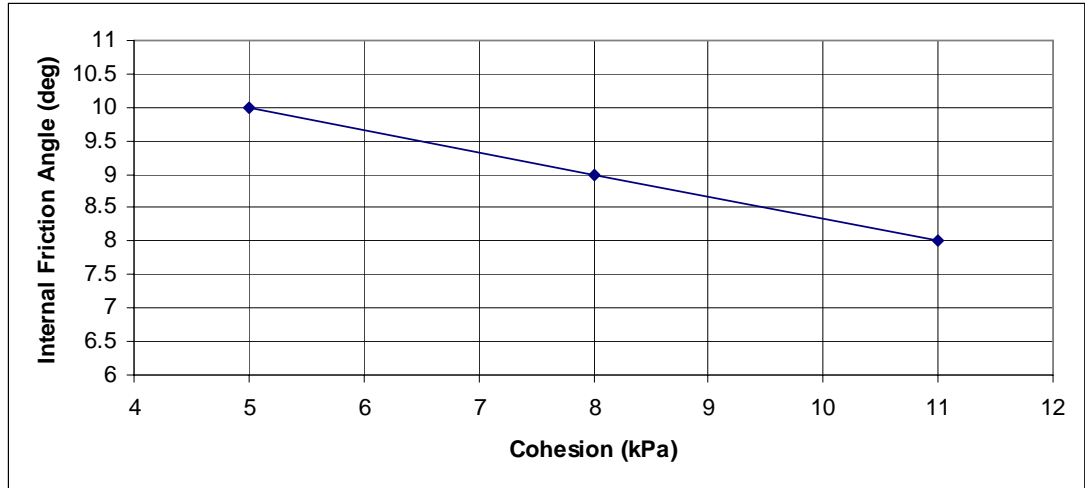


Figure 4.20 Cohesion vs. internal friction angle for black clay satisfying the condition of factor of safety=1

The equation of the cohesion and internal friction angle relation was found as:

$$\phi' = -0.3333c' + 11.667 \quad (4.1)$$

with $R^2=1$

From the equation, c' and ϕ' combination was selected for verification of the back calculated values. For $c' = 6.5$ kPa and $\phi' = 9.5^\circ$ shear strength parameters of black clay was solved by FLAC3D in order to obtain factor of safety. Factor of safety value was calculated by FLAC3D as 0.92 for the model by utilizing shear strength reduction method. Horizontal displacement contour is given on the Figure 4.21. Shear strain rate contour in the middle of the model is illustrated on the Figure 4.22.

FLAC3D 3.10

Step 6202: Model Perspective
14:21:34 Mon Aug 18 2008

Center:	Rotation:
X: 2.945e+002	X: 20.000
Y: 5.500e+002	Y: 0.000
Z: 7.149e+001	Z: 30.000
Dist: 4.561e+004	Mag.: 22.7
Increments:	Ang.: 22.500
Move: 1.144e+002	
Rot.: 10.000	

FoS

FoS value is : 0.92

Contour of X-Displacement

Magfac = 1.000e+000

-9.3836e-002 to -9.0000e-002
-9.0000e-002 to -8.0000e-002
-8.0000e-002 to -7.0000e-002
-7.0000e-002 to -6.0000e-002
-6.0000e-002 to -5.0000e-002
-5.0000e-002 to -4.0000e-002
-4.0000e-002 to -3.0000e-002
-3.0000e-002 to -2.0000e-002
-2.0000e-002 to -1.0000e-002
-1.0000e-002 to -4.0000e-003

Interval = 1.0e-002

meters

Itasca Consulting Group, Inc.
Minneapolis, MN USA

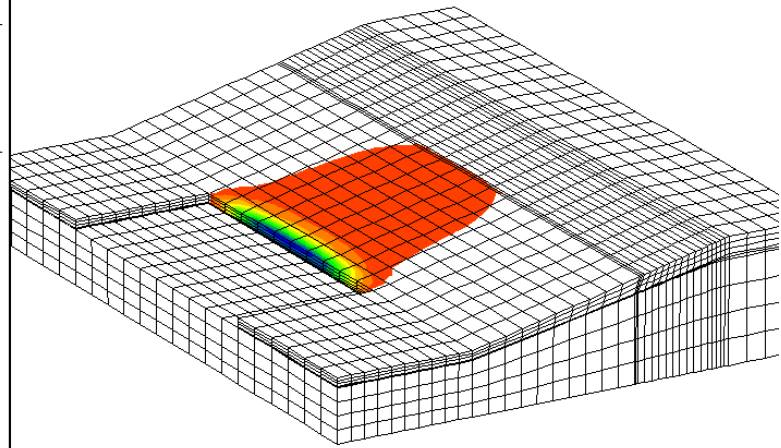


Figure 4.21 Horizontal displacement contours

FLAC3D 3.10

Step 6202: Model Perspective
14:25:26 Mon Aug 18 2008

Center:	Rotation:
X: 2.945e+002	X: 360.000
Y: 5.500e+002	Y: 0.000
Z: 7.149e+001	Z: 360.000
Dist: 2.538e+005	Mag.: 265
Increments:	Ang.: 22.500
Move: 1.144e+002	
Rot.: 10.000	

FoS

FoS value is : 0.92

Contour of Shear Strain Rate

Magfac = 1.000e+000

Gradient Calculation

2.0000e-008 to 1.0000e-006
1.0000e-008 to 2.0000e-006
2.0000e-008 to 3.0000e-006
3.0000e-008 to 4.0000e-006
4.0000e-008 to 5.0000e-006
5.0000e-008 to 6.0000e-006
6.0000e-008 to 6.1841e-006

Interval = 1.0e-006

Itasca Consulting Group, Inc.
Minneapolis, MN USA

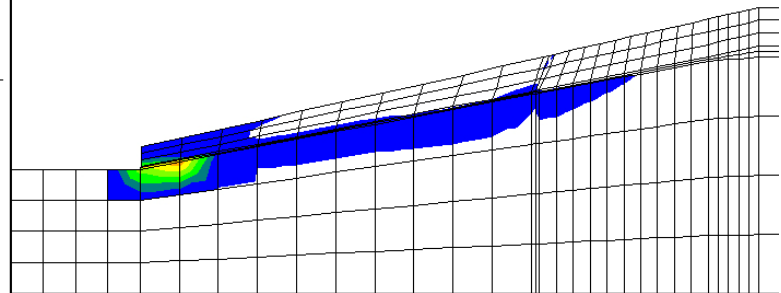


Figure 4.22 Shear strain rate contour

4.6.5 Sensitivity analysis of gyttja and lignite

After back calculation of black clay was completed, gyttja and lignite layers were started to be analyzed for sensitivity. Having no sharp boundary and being in transition of gyttja and lignite units in the field, they were considered as single layer in the analyses for modelling simplicity. In order to determine equivalent Mohr-Coulomb parameters for gyttja and lignite zone, cohesion was investigated accepting the internal friction angle fixed. The displacements of the model runs and displacement contours gave a chance to observe numerical model compare with the reality.

According to laboratory results, internal friction angle for gyttja is 32° and for lignite is 33° . The values are nearly the same. Considering the high number of experiments conducted in METU, for gyttja and lignite, 32° internal friction angle was accepted and cohesion for these two formations were changed in order to observe the model sensitivity under different values of cohesion.

For different values of cohesion for gyttja and lignite, history plot of horizontal displacement (towards pit bottom) vs. step were taken for different history points. History point #2 (Figure 4.11) was used for constructing the Figure 4.23. The history point was located at just in front of #3 fault.

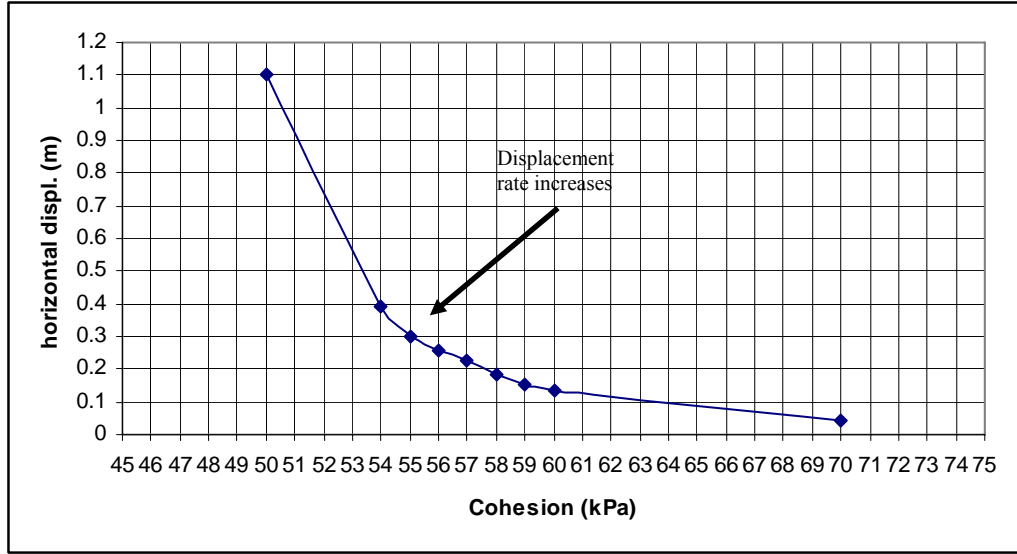


Figure 4.23 Horizontal displacements at 100000 # of steps at history point #2

In this study, a cohesion interval from 70 kPa to 50 kPa was applied and maximum displacement of corresponding cohesion was plotted. At 54-55 kPa, curve indicates initiation a possible failure that the movement rates are increased.

In laboratory tests, average cohesion for lignite and gyttja is 54 kPa. For gyttja and lignite formations, $c'=54$ kPa and $\phi'=32^\circ$ parameters were decided to be used in design.

For the combination of black clay, gyttja and lignite Mohr-coulomb parameters that simulated Kışlaköy failure, some typical FLAC3D outputs are illustrated on the Figures 4.24, 4.25 and 4.26 by using input parameters of $c'=8$ kPa and $\phi'=9^\circ$ for black clay and $c'=54$ kPa and $\phi'=32^\circ$ for gyttja-lignite combined layer.

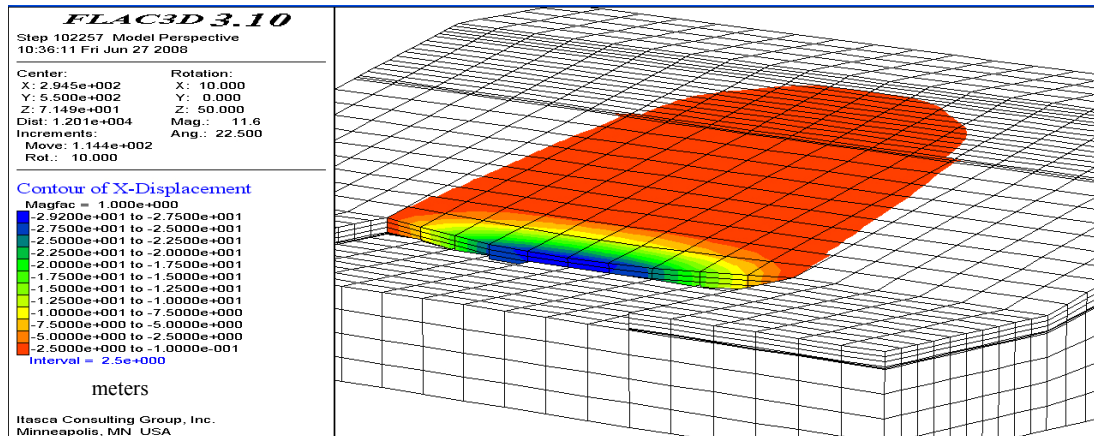


Figure 4.24 Horizontal displacement contours. Coloured range indicates failed range

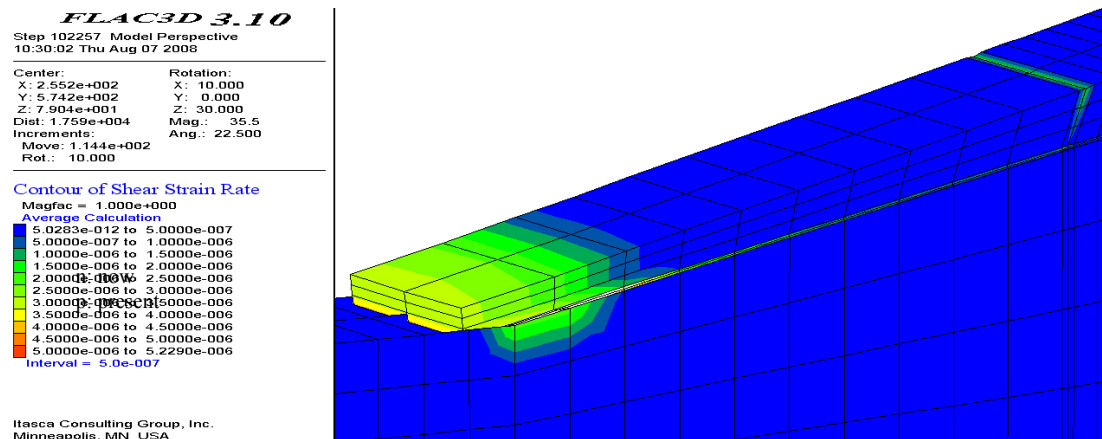


Figure 4.25 Shear strain contours are visible in front of the model, black clay and fault zone

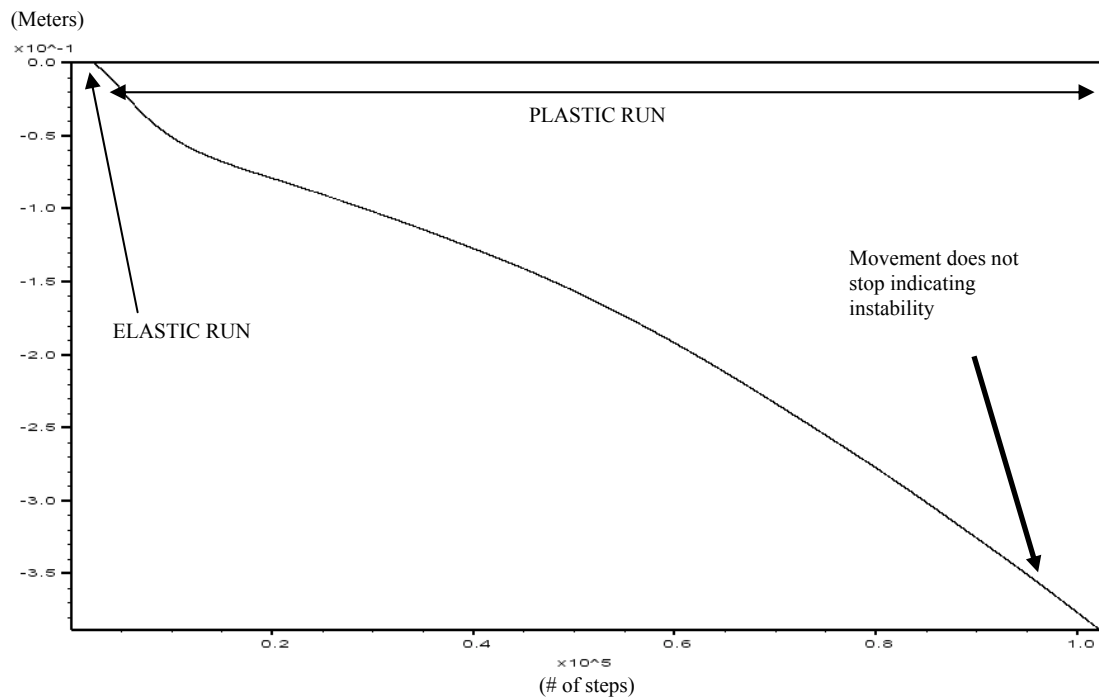


Figure 4.26 Horizontal displacement vs. solution step # plot.

4.7 Input parameters for design

Mohr-coulomb failure criterion was selected and strength parameters of the criterion were used for design stage. Effective stress parameters were investigated. Laboratory experiments and back-analysis were used for determining the design parameters. Some required modifications were done on the results in order to prevent irrelevant solutions or results and establishing model adaptation to practice and reality under engineering judgment. Input design parameters are shown on Table 4.4.

Unit weight and water content parameters were average of the laboratory results. For loam residual strength parameters of only one experiment was used. Lowest c_p' and ϕ_p' values were selected as design parameters for blue clay. 3-D back analysis led to the results illustrated on the Table 1.1 to be used as design parameters for

black clay, gyttja and black clay. Green clay laboratory values of peak average strength parameters were shown on the table 4.4.

Table 4.4 Input design parameters

Material	Unit weight (kN/m³)	Water content w_n (%)	Cohesion c' (kPa)	Internal Friction Angle φ' (°)	Hu value
Loam	18.66	36	48	11	0.36
Blue clay	18.06	31	13	18	0.31
Gyttja	15.06	78	54	32	0.78
Lignite	13.20	104	54	32	1.00
Black clay	14.50	87	8	9	0.87
Green clay (footwall clay)	16.74	47	33	23	0.47

Water content is the ratio of water weight to solid weight. Hu value is used in limit equilibrium analysis by SLIDE software. It is a factor for regulation of the pore pressure. Water unit weight is multiplied by depth of a particular point and Hu factor then the pore pressure is found at that particular point. Hu factors are assumed as water content values in the limit equilibrium analysis.

Water content values may be considered as high especially for lignite unit. Unit weight of the lignite is low and void ratio is high having water inside. Thus water content over 100% is valid.

Modelling was completed by establishing 21° overall slope angle as planned with an ultimate excavation depth reaching 145 m for South-west permanent slopes and

North-west permanent slopes. 5 benches were modelled. Conveyor region was planned to have a lower overall slope angle but a factor of safety was checked for that region.

Park Teknik planned to drain water down to the top of lignite layer that some critical technical conditions were taken account in order to reach dewatering target. The stratum in the mining area was investigated and considered to have low permeability. Thus, the strata dissipate water very slowly and some water can stay trapped in some parts of the layer. Thus, dewatering target may not be obtained precisely. Moreover, dewatering target may not be reached due to technical problems (pumps, pipes etc.) Although the dewatering target is lowering the water table 100 m under the surface, in the models, 85 m depth from the surface is used. This will compensate the effect of undrained or water trapped parts of the strata. In order to observe the effect of dewatering, a water table of 50 m deep from surface and a water table on the surface level at the crest of the slope were assumed and calculations were conducted. On the mining area there are small water streams and Hurman River on the west side of the mine area. The river is simply parallel to south-west permanent slopes. It is logical to assume water table is on the surface if the mining area is not dewatered.

4.8 Cross sections

Park Teknik prepared 3D geological model of the area by using boreholes drilled for different purposes. 2D cross-sections were prepared in order to analyze slope stability by using limit equilibrium methods, (Figure 4.27). Also, some 3D models have been extruded from 2D cross-sections. For south-west permanent slopes and north-east production slopes, 6 cross-sections (#1, 2, 3, 4, 5, 6) were taken. For north-west permanent slopes, 1 (#7) and for conveyor region 1 cross-sections (#8) were taken.

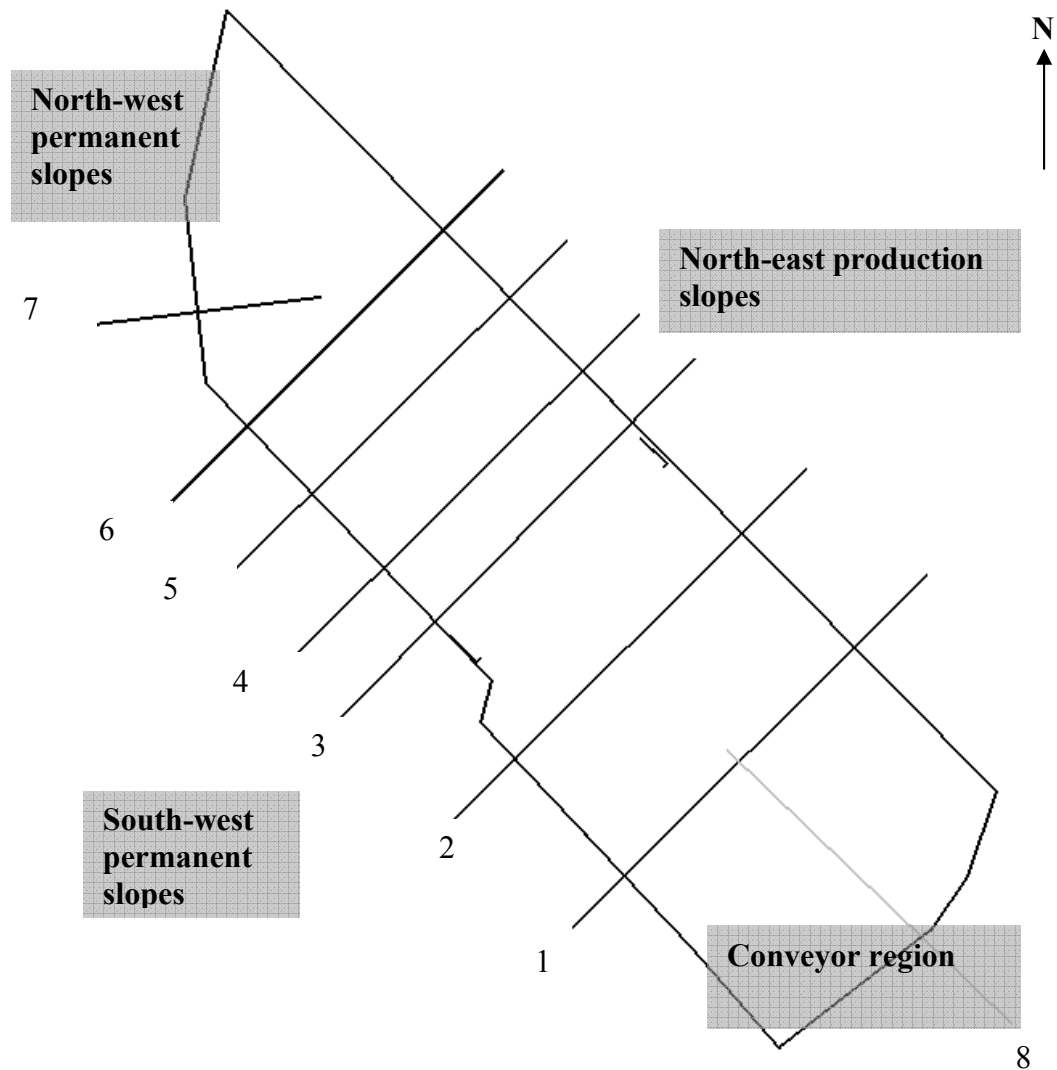


Figure 4.27 Cross-sections taken for analysis

4.9 Limit equilibrium analysis of permanent slopes in 2-D

4.9.1 Circular failure analysis of permanent slopes

South-west permanent slopes and north-west permanent slopes were analyzed by using SLIDE software on the sections of #1, #2, #3, #4, #5, #6, and #7. Bishop Simplified (1955) method was used as a popular method in circular failure

analysis. A factor of safety value of 1.50 for permanent slopes (Hoek and Bray, 1981) was decided to be satisfied for planned water table level. 7 sections with 21° overall slope angle having 5 benches were analyzed. The slip surface having lowest factor of safety was detected, (Table 4.5). The slip surface has to be affected overall stability not a local bench failure thus, local failures taken out of consideration.

Table 4.5 Factor of safety analysis of permanent slopes with a water level 85 m beneath the surface

Section #	Factor of safety
1	1.75
2	1.55
3	1.47
4	1.48
5	1.54
6	1.50
7	1.50

Section #3 had the lowest factor of safety, 1.47 (= ~1.50). Analysis outputs of the models having a water table depth of 85 m are presented in Appendix B. Slip circle and analysis output is illustrated in the Figure 4.28. Other section analysis outputs are presented.

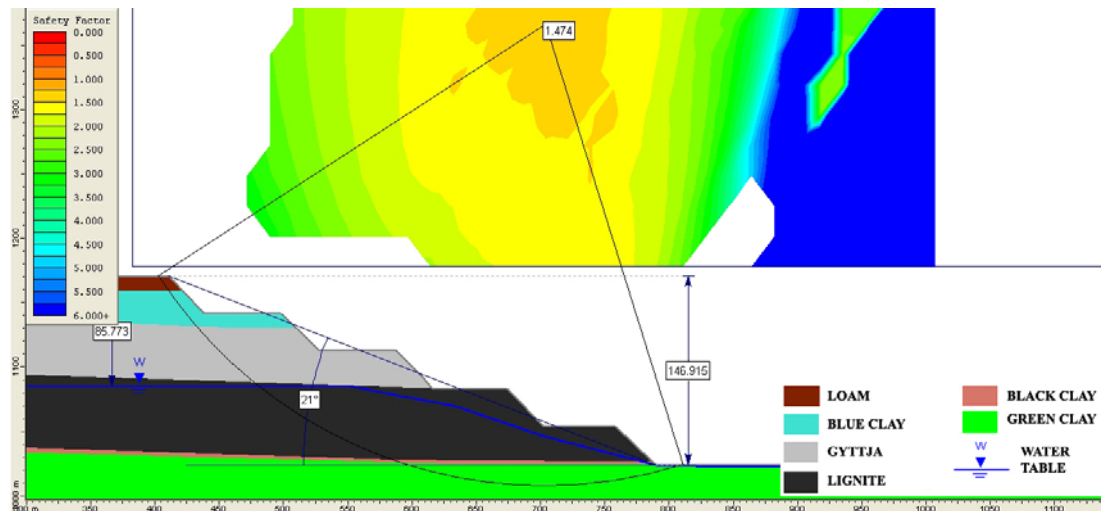


Figure 4.28 Section #3, slip circle of lowest factor of safety.

If an overall slope having 21° angle is established and dewatering target is not satisfied, the situation must be foreseen. Thus, a water table level which was 50 m deep from the surface and a water table on the surface was constructed on to the models and circular failure analyses were conducted. The slip surfaces having lowest factor of safety was detected for two distinct dewatering conditions, (Table 4.6 and Table 4.7). Analysis outputs of the cross sections are presented in the Appendix C).

Table 4.6 Factor of safety analysis of permanent slopes with a water level 50 m beneath the surface

Section #	Factor of safety
1	1.59
2	1.26
3	1.17
4	1.18
5	1.26
6	1.19
7	1.24

Analysis outputs of the cross sections are presented in the Appendix D).

Table 4.7 Factor of safety analysis of permanent slopes with a water level on the surface

Section #	Factor of safety
1	1.05
2	0.97
3	1.01
4	1.04
5	1.10
6	1.07
7	1.24

For these two conditions, slip circles and analysis outputs are illustrated in the Figure 4.29 and Figure 4.30.

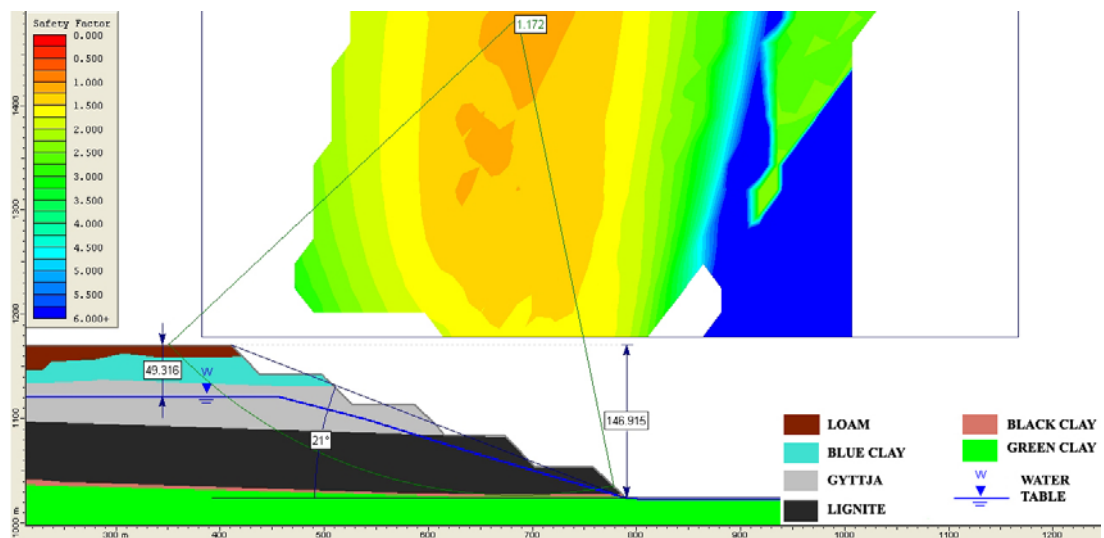


Figure 4.29 Section #3, slip circle of lowest factor of safety with a ground water table 50 m beneath the surface

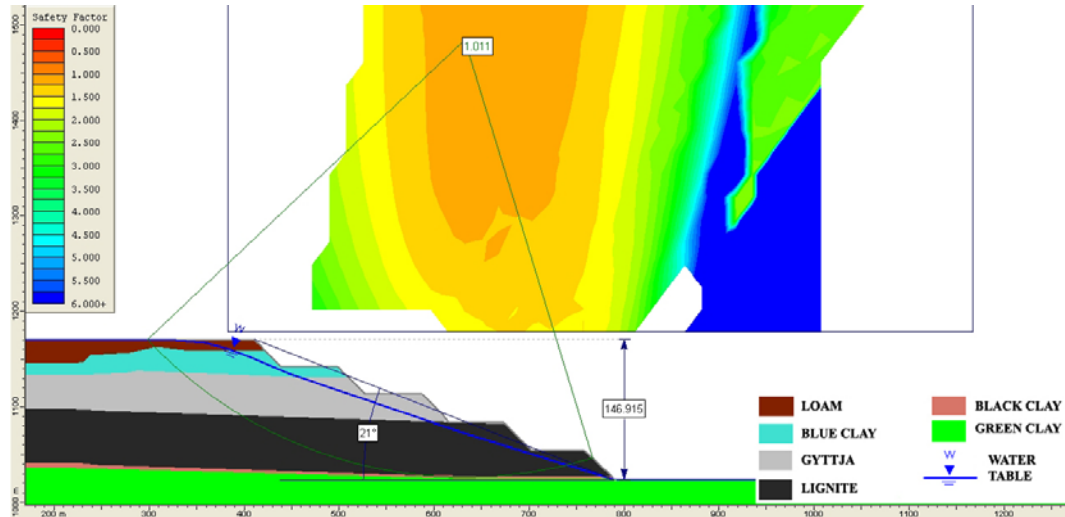


Figure 4.30 Section #3, slip circle of lowest factor of safety with a ground water table on the surface

A graph was constructed for permanent slopes (section #3) having an overall slope angle of 21° with changing depth of water levels and corresponding factor of safeties, (Figure 4.31).

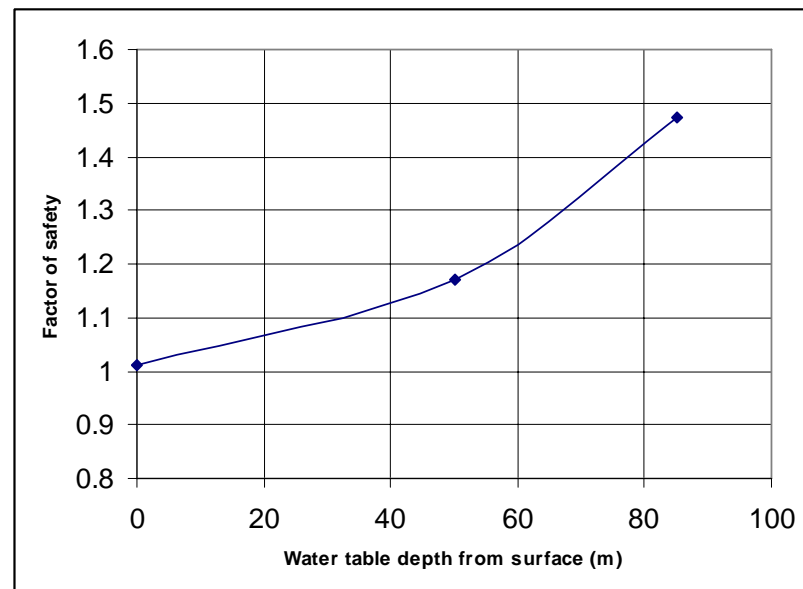


Figure 4.31 Factor of safety vs. water table depth from surface graph for 21° overall slope angle for section #3

If dewatering targets are satisfied, 21° overall slope angle provides acceptable factor of safety value of ~ 1.50 . Unless dewatering is realized, factor of safety value converges to 1 which can initiate instability as a boundary value for safety.

An analysis by using section #3 was conducted for different levels of water table in order to satisfy 1.50 factor of safety. Slip circles and analysis results are illustrated on the figures (Figure 4.32 and Figure 4.33)

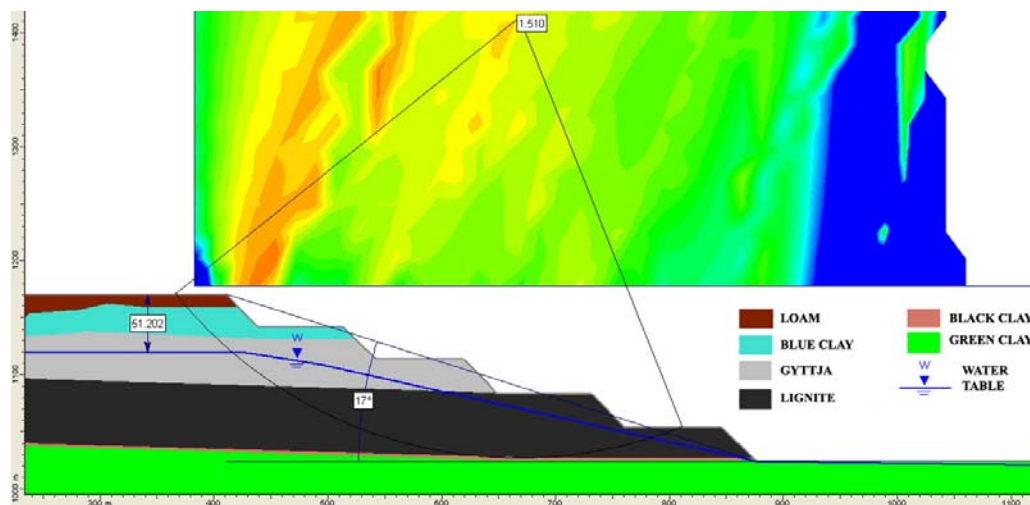


Figure 4.32 Slope with overall slope angle of 17° having a water table having a depth of 50 m from the surface

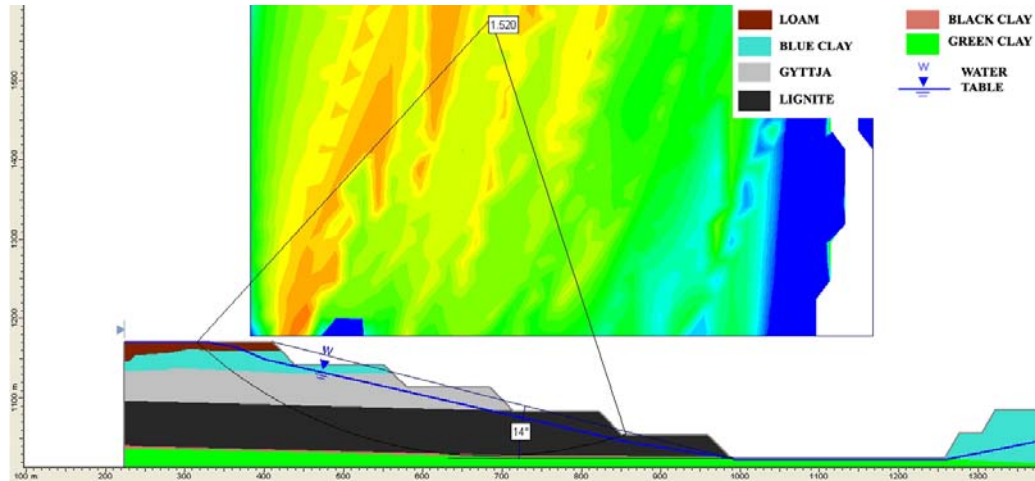


Figure 4.33 Slope with overall slope angle of 14° having a water table on the surface

In order to satisfy 1.50 factor of safety value, overall slope angles had to be reduced if dewatering target (lowering the water table 85 m beneath the surface) is not attained. Figure 4.35 is constructed for necessary overall slope angles on the conditions of different water table depths.

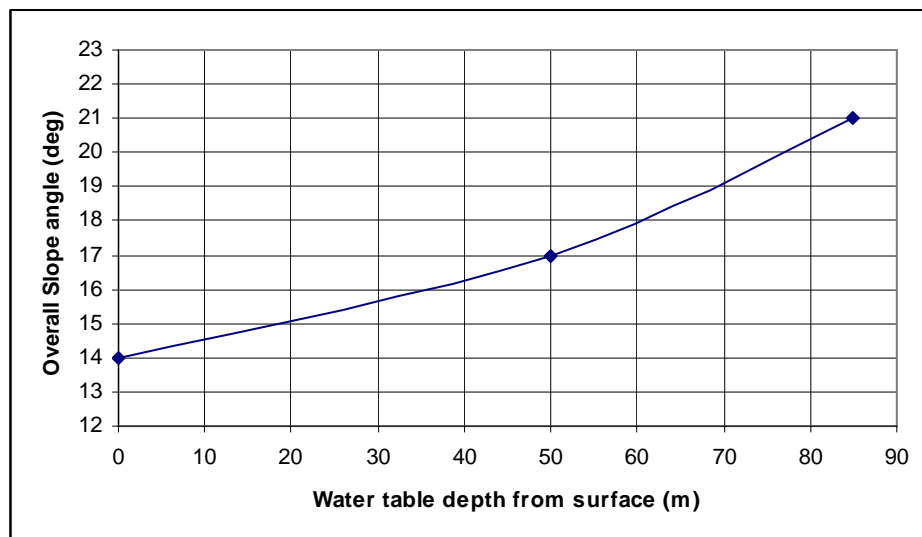


Figure 4.35 Overall slope angle vs. water table depth plot to reach 1.5 factor of safety value

4.9.2 Composite failure analysis around fault

In 2006, slope failure was occurred in Kışlaköy open cast mine operated by EÜAŞ (Electricity Production Co. Inc.) in a composite form. Weak black clay layer underlying the lignite layer caused overlying mass to move. These movements reached instability conditions and at the back, faulting established the back side of the failure. The first movement aroused from the inclined black clay layer, (Figure 4.5). Firstly the overlying block was moved then the block is separated from the fault.

In order to prevent this type of failure in Çöllolar mine field, composite failure analyses were conducted. On the line of the Hurman River, a fault existence was stated by Koçak et al., (2003). No information was obtained about the dip and dip direction of the fault. When cross section #6 was examined some fault indicators may be observed. In the cross section, black clay layer has an inclination of 5° . This cross section had to be analyzed by constructing a non-circular composite failure analysis. The failure surface was assumed to be passed through fault and black clay layer. In fact, from an engineering view, black clay layer having 9° friction angle, may not initiate a considerable slip when the inclination of the black clay layer has an inclination of 5° , (Figure 4.35). However, limit equilibrium analysis was conducted.

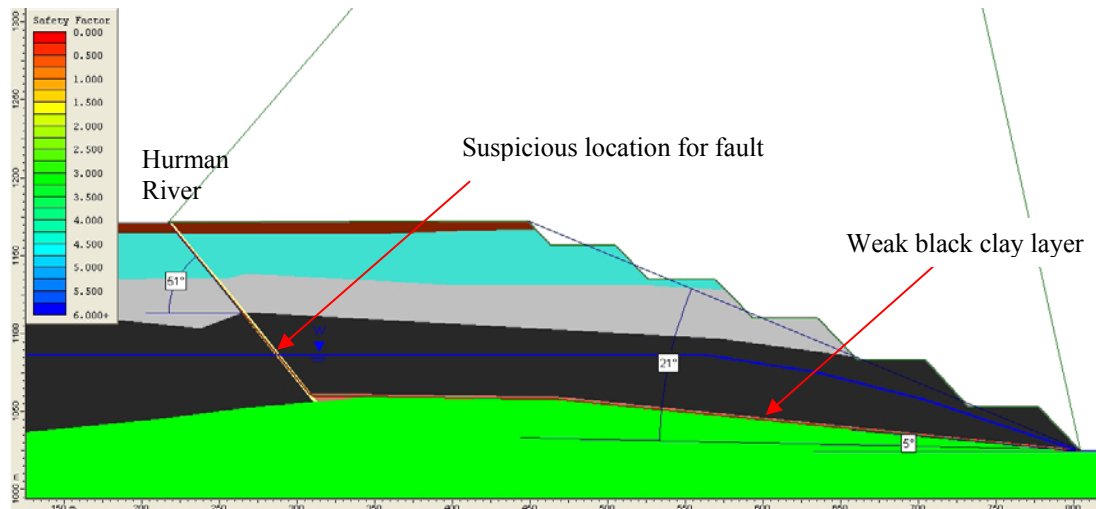


Figure 4.35 Inclination of black clay and possible fault is shown on cross section

#6

At the point where Hurman River passes through, the fault daylights. The fault was constructed by connecting the line from Hurman River to anomaly point in the section. Suspicious location of the fault is shown on the Figure 4.35. A conjectural fault having 51° dip angle was modeled in order to analyze a risky situation. Factor of safety calculation was carried out, (Figure 4.36).

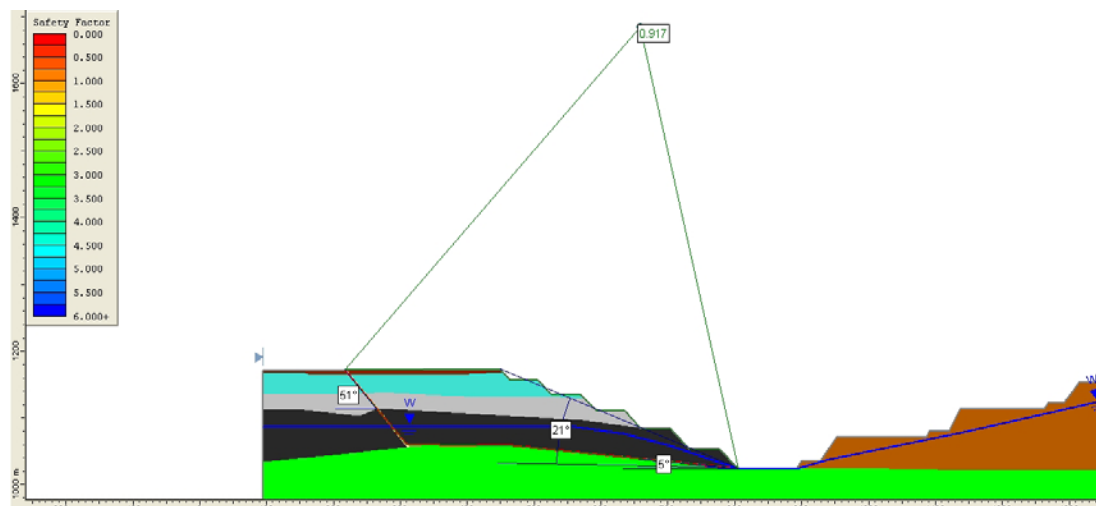


Figure 4.36 Slip surface and factor of safety output

Slip surface and factor of safety output is illustrated and factor of safety value was found as 0.92 by using Janbu simplified (1968) method. The calculated factor of safety is a warning for Park Teknik to launch geological investigations aiming to acquire information about the fault.

4.10 Finite difference analysis of permanent slopes in 3-D

3D numerical models are superior to limit equilibrium methods that they include material failure, plastic deformation and elastic-plastic deformation analysis. Also, field stresses can be implemented and used on the contrary to limit equilibrium methods. South-west permanent slopes were modeled in 3-D for numerical analysis.

4.10.1 Model

Model was constructed having 5 benches and 145 m height. $\sim 21^\circ$ overall slope angle was imposed to the model. Grids were generated fine in sensitive parts of the model and coarse in insensitive parts. For south-west permanent slopes, finite difference grids, model dimensions and material boundaries are illustrated on the Figure 4.37.

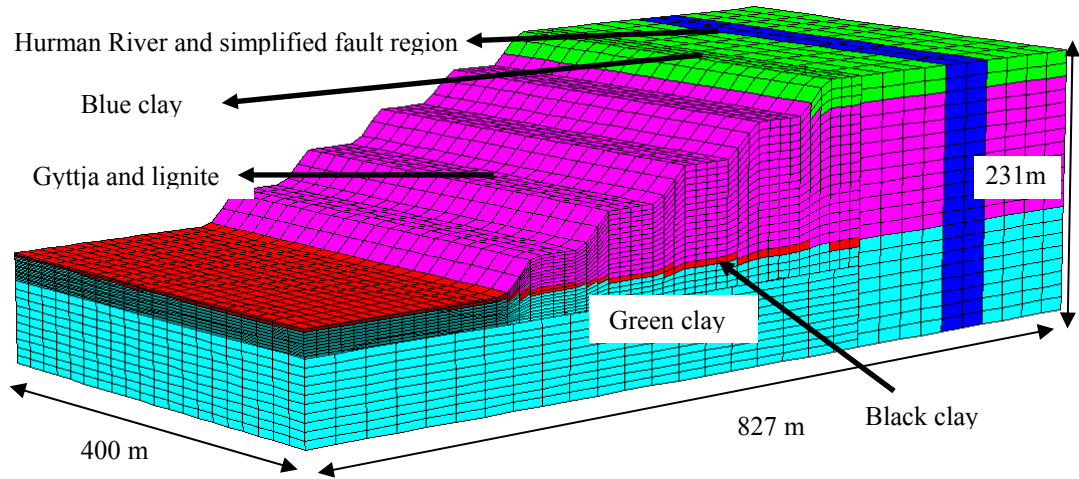


Figure 4.37 FLAC3D model in 3D, finite difference grids, dimensions and materials of the south-west permanent slopes in Çöllolar open cast mine

Thicknesses of the layers used in FLAC3D are tabled on the Table 4.8.

Table 4.8 Thickness of layers in the model

Material	Layer Thickness (m)
Loam	4
Blue Clay	21
Gyttja	56
Lignite	57
Black Clay	5

The fault was also implemented to the model having 50 m thickness as material not an interface. Thickness of fault material enabled failure to find its own way within weak fault material zone thus, the failure line was not restricted.

Water table level was used as it is planned by Park Teknik shown on the Figure 4.38.

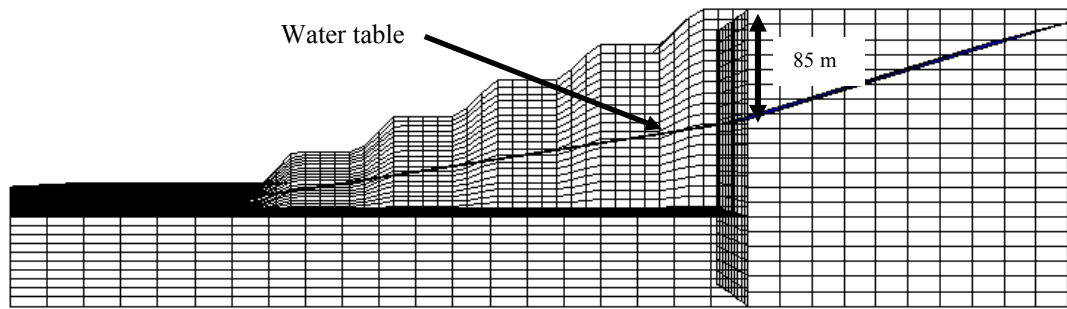


Figure 4.38 Water table geometry

History points were located for displacements corresponding number of steps. Slope displacements were recorded both in elastic and plastic stepping, (Figure 4.39).

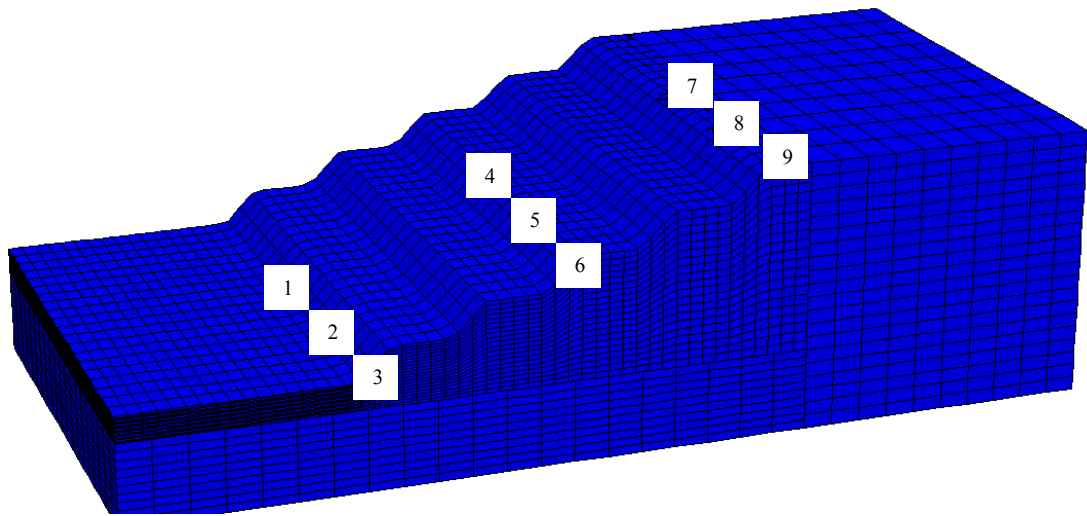


Figure 4.39 History points for recording displacements during stepping (or cycling) for solution

Gravitational acceleration of 9.81m/sec^2 was applied in the direction of gravity on the model.

Base of the model was fixed for all directions. The sides of the model were fixed not to move normal to the in-plane directions of the side walls. By this way, in elastic run, model body was enabled to move under the effect of gravity and sides of the model could move freely within constrained directions, parallel to the plane but not in in-plane direction.

4.10.1.1 Input elastic parameters

Elastic parameters are not related with slope failure or collapse but, they must be decided carefully to initialize field stress conditions. For the model, a high elastic modulus was selected to reach to the equilibrium in a shorter time for solution. Poisson's ratio is important that while elastic stage is running the Poisson's ratio affects the horizontal stress formation.

For entire model, the same parameters were used and average density was selected as:

$$E = 10000 \text{ MPa} \qquad \nu = 0.2 \qquad \gamma = 15.99 \text{ kN/m}^3$$

4.10.1.2 Input strength parameters

In Chapter 4, shear strength parameters of black clay were back analyzed and Mohr-coulomb parameters were investigated. For blue clay lowest values of peak strength parameters in laboratory results were taken into consideration. For loam, lowest residual parameters were used. Average values of peak parameters were used for footwall clay (green clay). Fault shear strength parameters were used as same values as in the back analysis. The used values are listed on the Table 4.9

Table 4.9 Shear strength (Mohr-Coulomb) parameters used in the model.

Material	Cohesion, c' (kPa)	Internal Friction Angle, ϕ' (°)
Loam	48	11
Blue Clay	13	18
Gyttja	54	32
Lignite	54	32
Black Clay	8	9
Green Clay (Footwall clay)	33	23
Fault Zone	0	20

Tensile strength of the entire model was used as “zero”.

4.10.2 Analysis of permanent slopes in 3-D

In numerical analysis, there were several outputs to consider. History plots were observed.

Horizontal displacement contours are illustrated on the Figure 4.40. Some movements were observed on the black clay and fault zones.

FLAC3D 3.10
Step 14134: Model Perspective
15:56:19 Sun Jul 27 2008

Center: X: 2.365e+002 Y: 2.000e+002 Z: 1.046e+003
Rotation: X: 10.000 Y: 0.000 Z: 30.000
Dist: 2.487e+003 Mag.: 1.95
Increments: Move: 9.893e+001 Ang.: 22.500
Rot.: 10.000

Contour of X-Displacement

Magfac = 0.000e+000
-1.0102e-002 to -1.0000e-002
-1.0000e-002 to -9.0000e-003
-9.0000e-003 to -8.0000e-003
-8.0000e-003 to -7.0000e-003
-7.0000e-003 to -6.0000e-003
-6.0000e-003 to -5.0000e-003
-5.0000e-003 to -4.0000e-003
-4.0000e-003 to -3.0000e-003
-3.0000e-003 to -2.0000e-003
-2.0000e-003 to -1.0000e-003
-1.0000e-003 to 0.0000e+000
0.0000e+000 to 0.0000e+000
Interval = 1.0e-003
(Meters)

Itasca Consulting Group, Inc.
Minneapolis, MN USA

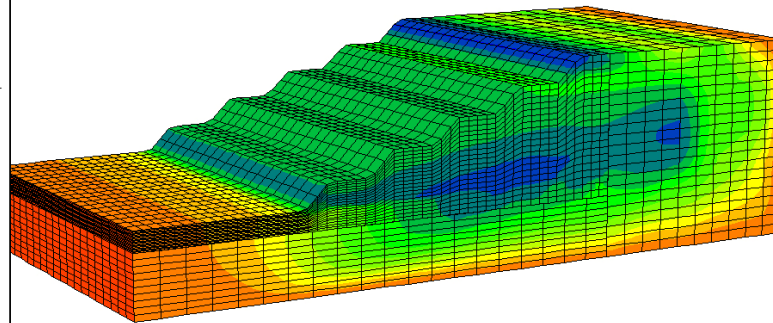


Figure 4.40 Horizontal displacement contours

Shear strain rate illustrates important information about shear failure and mechanism of the failure, (Figure 4.41). Movements were intensified on black clay layer. Thickness of the black clay layer was exaggerated on the model which can lead material failure due to very low Mohr-Coulomb parameters ($c'=8$ kPa and $\phi'=9^\circ$).

FLAC3D 3.10
Step 14134: Model Perspective
16:04:29 Sun Jul 27 2008

Center: X: 1.944e+002 Y: 2.243e+002 Z: 1.046e+003
Rotation: X: 10.000 Y: 0.000 Z: 30.000
Dist: 2.487e+003 Mag.: 3.05
Increments: Move: 9.893e+001 Ang.: 22.500
Rot.: 10.000

Contour of Shear Strain Rate

Magfac = 0.000e+000
Gradient Calculation
-3.0260e-012 to 0.0000e+000
0.0000e+000 to 2.5000e-010
2.5000e-010 to 5.0000e-010
5.0000e-010 to 7.5000e-010
7.5000e-010 to 1.0000e-009
1.0000e-009 to 1.2500e-009
1.2500e-009 to 1.5000e-009
1.5000e-009 to 1.7500e-009
1.7500e-009 to 2.0000e-009
2.0000e-009 to 2.2500e-009
2.2500e-009 to 2.4966e-009
Interval = 2.5e-010

Itasca Consulting Group, Inc.
Minneapolis, MN USA

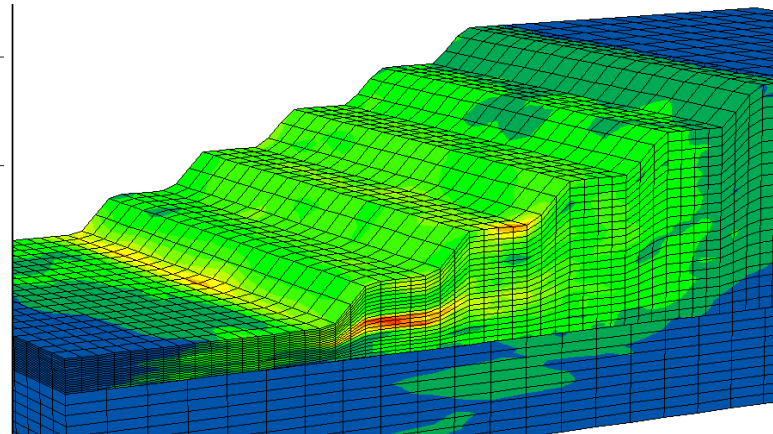


Figure 4.41 Shear strain rate contours

X-displacements vs. solution steps were taken by allocated history points. History points #4 and # 7 (on Figure 4.39) were used in construction of Figure 4.42 and Figure 4.43.

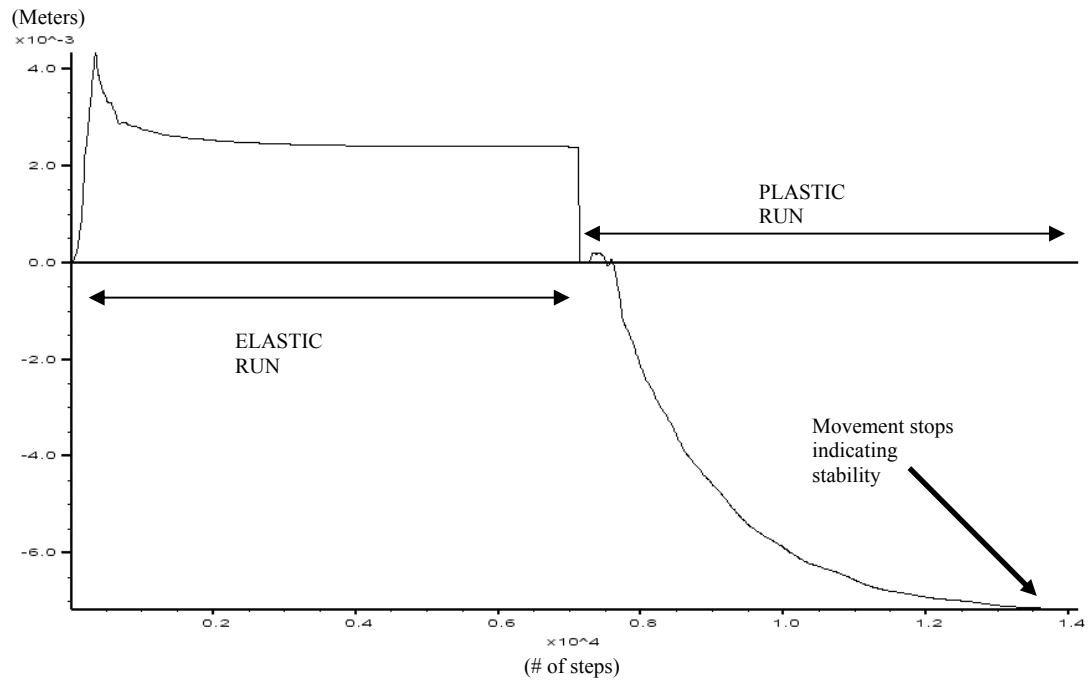


Figure 4.42 History point of #4

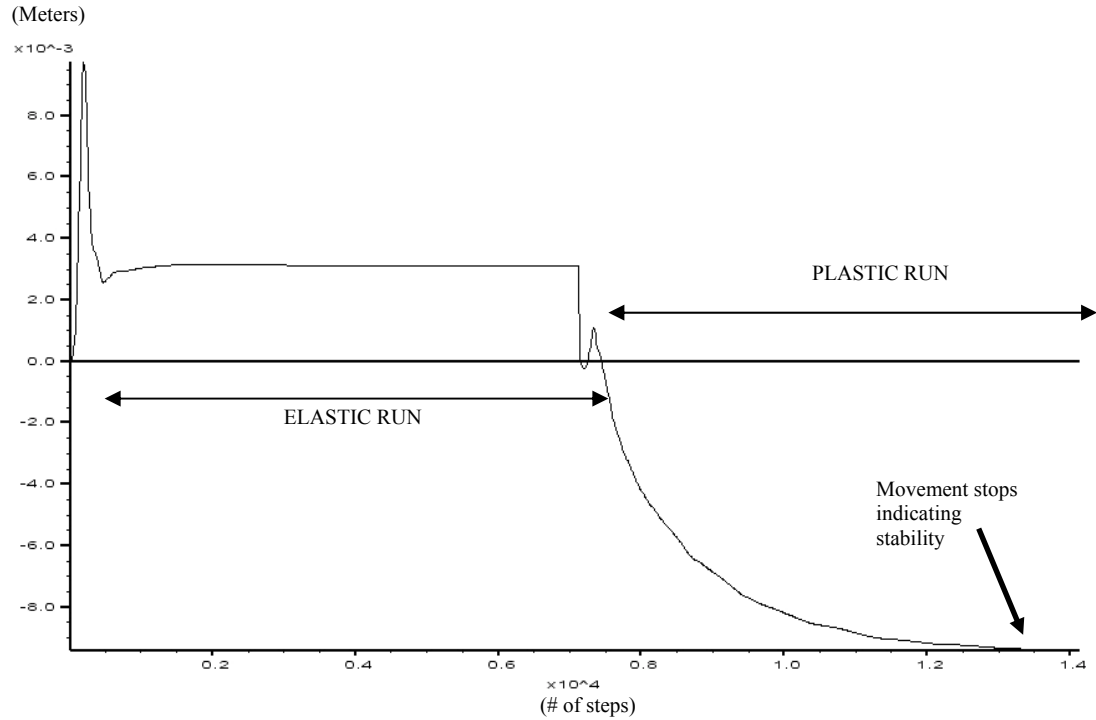


Figure 4.43 History point of #7

Displacements were stopped after a small movement occurred. Movement magnitudes were small and indicating stability. The slope was considered as stable and safe.

4.10.3 Factor of safety analysis by using finite difference method manually

Factor of safety analysis was conducted by manual implementation of the basic principles of shear strength reduction method by using FLAC3D software.

In this specific model, some special conditions were taken into consideration. In Kışlaköy overall slope failure, mechanism did not include footwall clay (green clay). The slip occurred on black clay. In this model, it was assumed that a failure extension did not reach and form a failure surface including footwall clay. Thus, shear strength parameters of footwall clay was not reduced not to allow model to

result in a deep seated failure. Fault parameter was also not reduced that strength parameters are so low ($c'=0$ kPa and $\phi'=20^\circ$) and it was logical to assume fault strength parameters fixed.

In the model, shear strength parameters (both cohesion and internal friction angle) were reduced by a factor and displacements at same particular solution step were recorded. Horizontal displacements were obtained by using history points of #4 on Figure 4.38.

Shear strength parameters of black clay, gyttja, lignite and blue clay were reduced in a factor (reduction factor) and the point indicating instability (slope collapse) was determined. The point indicating instability denotes factor of safety by reduction factor, (Figure 4.44). Manual application of shear strength reduction principles enabled Figure 4.44 to be constructed.

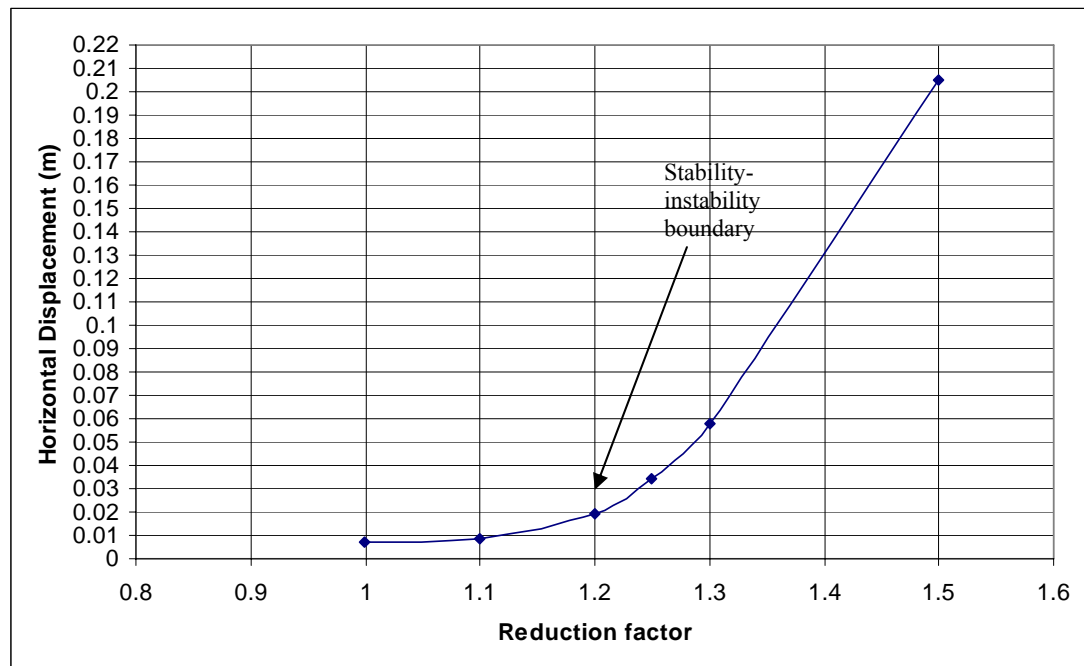


Figure 4.44 Horizontal displacement vs. reduction factor plot at 5000 steps of plastic solution cycling.

From the graph on Figure 4.44, it was determined that the factor of safety of the slope have a factor of safety of ~ 1.20 .

When deciding the stability-instability boundary, some graphical outputs were found to be beneficial. Displacement contour, shear strain rate contour, horizontal displacement history corresponding to solution steps were illustrated, (Figure 4.45, 4.46, 4.47 for reduction factor of 1.20 and Figure 4.48, 4.49, 4.50 for the reduction factor of 1.2).

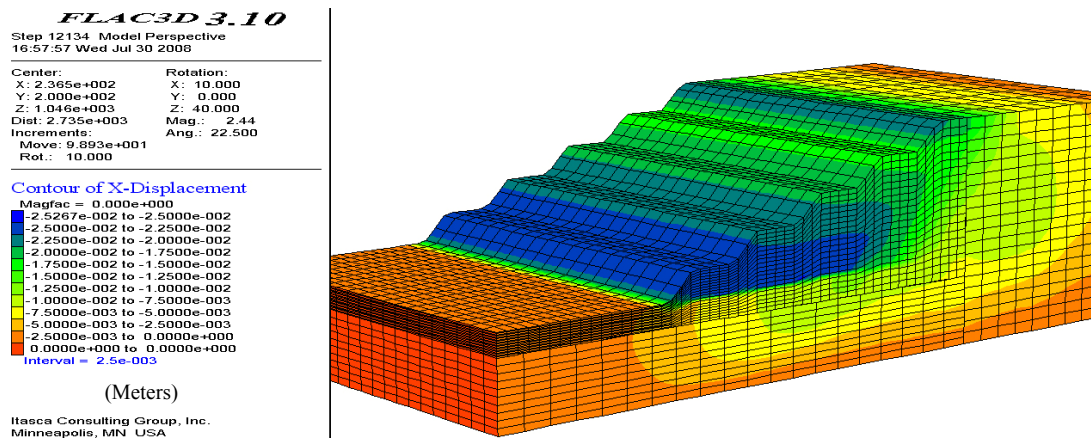


Figure 4.45 Horizontal displacement contour (Reduction factor of 1.20)

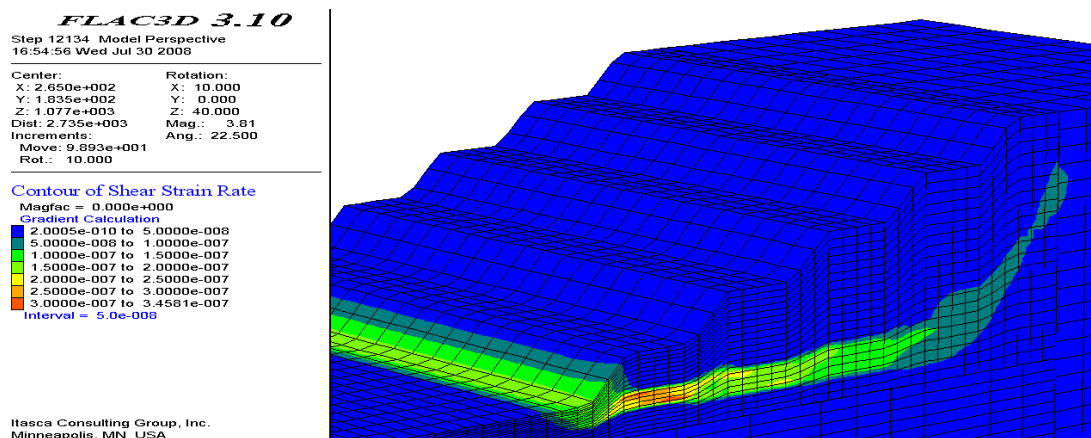


Figure 4.46 Shear strain rate contour (Reduction factor of 1.20)

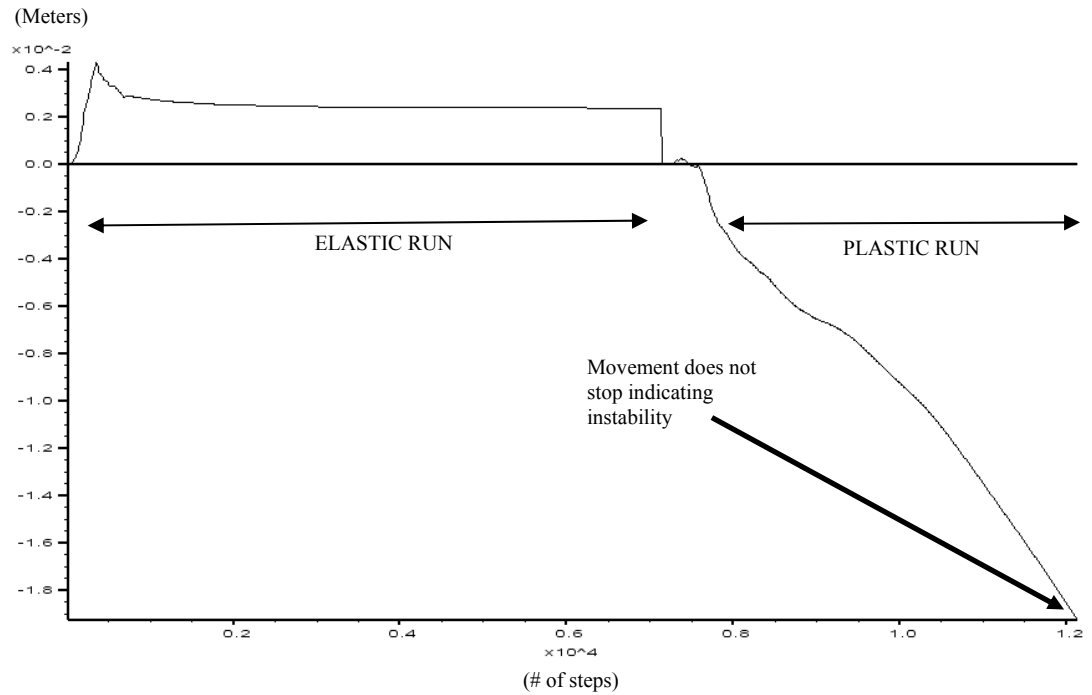


Figure 4.47 Horizontal displacement vs. solution steps graph (Reduction factor of 1.20)

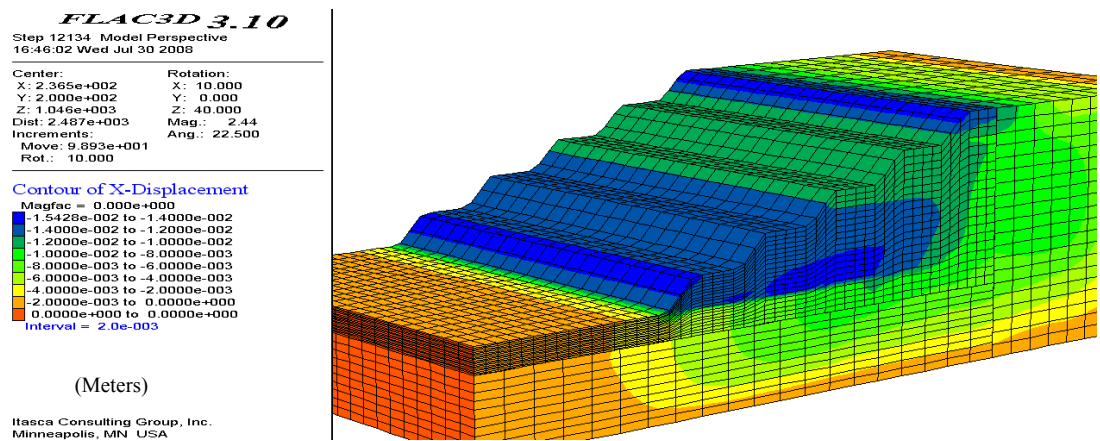


Figure 4.48 Horizontal displacement contour (Reduction factor of 1.10)

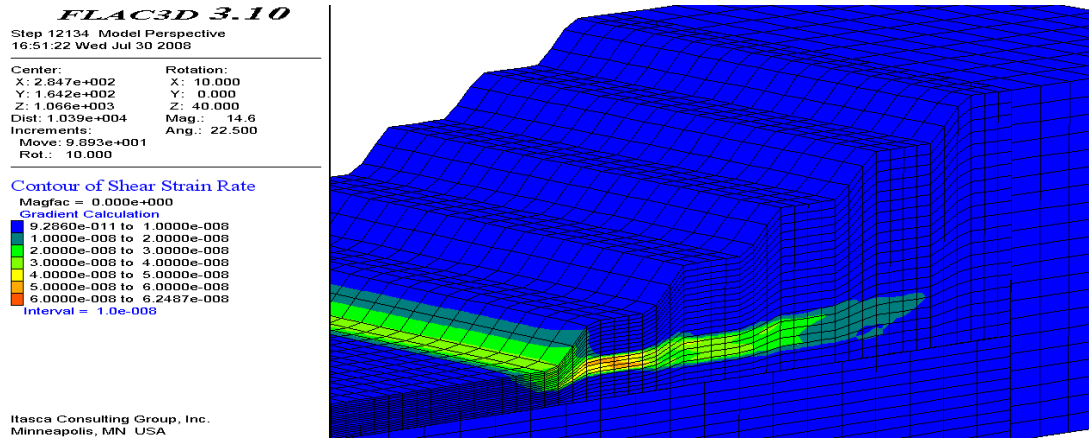


Figure 4.49 Shear strain rate contour (Reduction factor of 1.10)

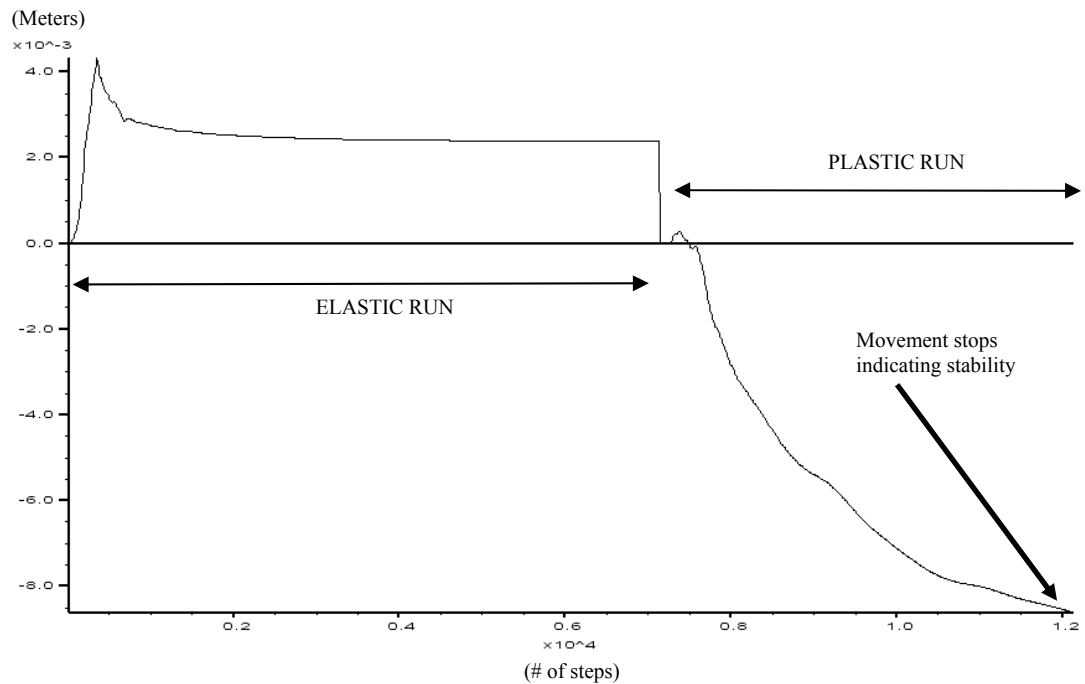


Figure 4.50 Horizontal displacement vs. solution steps graph (Reduction factor of 1.10)

4.10.3.1 Factor of safety calculation by using FLAC3D

The strength reduction method for determining factor of safety was implemented in FLAC3D by SOLVE fos command. FLAC3D found 1.22 factor of safety value

for permanent slopes having $\sim 21^\circ$ overall slope angle which is the same value (~ 1.20) found in manual implementation. Last non-equilibrium state was saved in FLAC3D software and important graphical outputs are illustrated in the Figures 4.51, 4.52 and 4.53.

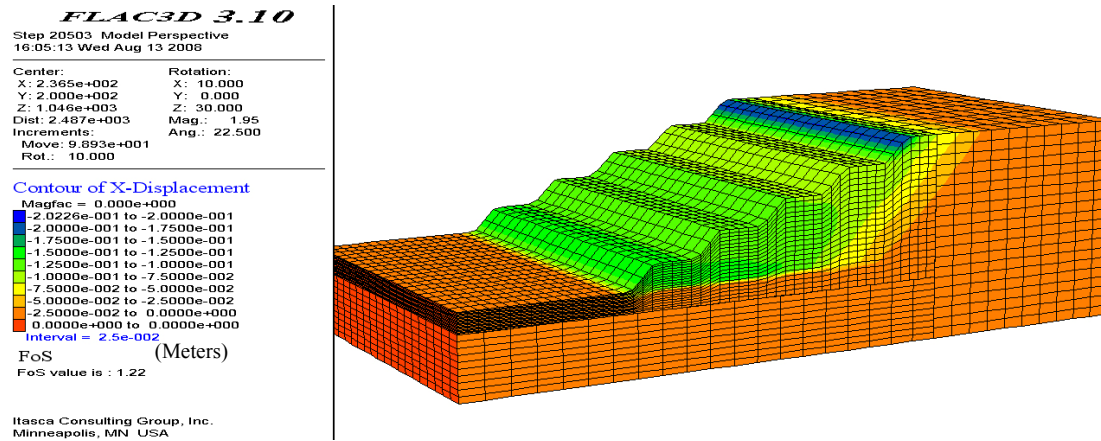


Figure 4.51 Horizontal displacement contour of last non-equilibrium state

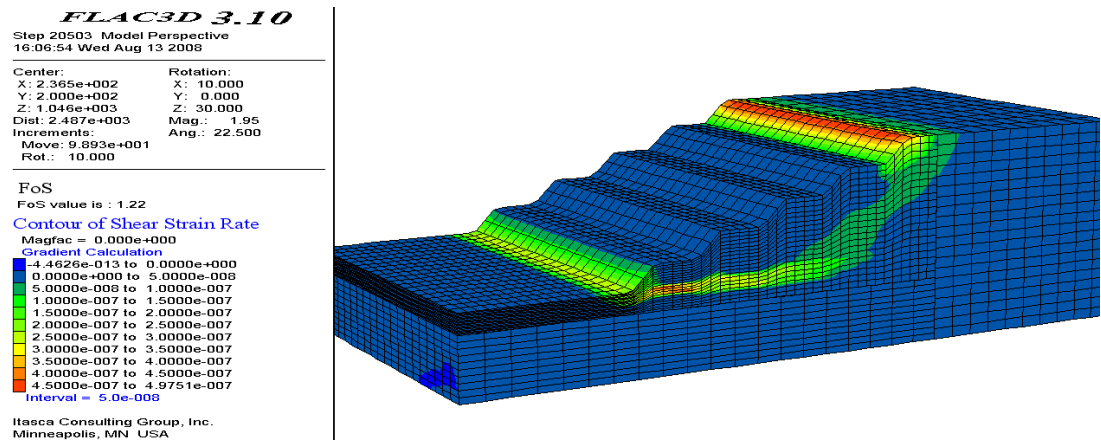


Figure 4.52 Shear strain contours of last non-equilibrium state

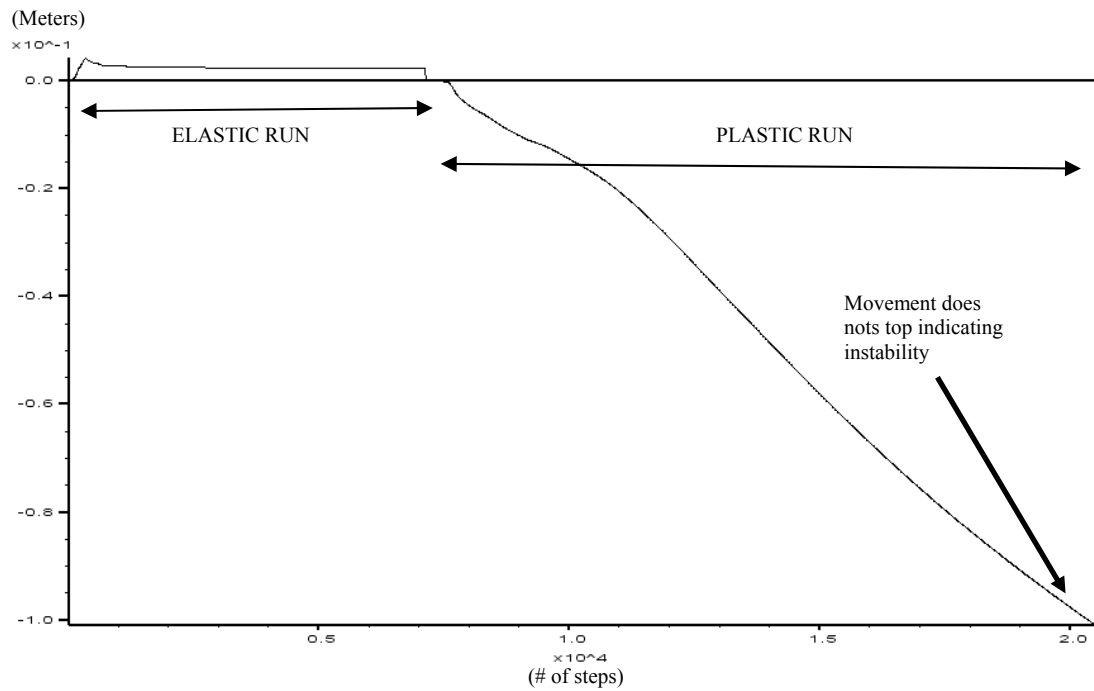


Figure 4.53 Horizontal displacement vs. solution steps graph of last non-equilibrium state at history point #4

Factor of safety calculated in manual implementation (1.20) and by FLAC3D solution (1.22) is same.

4.10.3.2 Comparison of the numerical analysis with limit equilibrium analysis

In limit equilibrium analysis, researcher designates the failure surface. Researcher must be careful on constructing the failure surface that probable failure surface must be used in the analysis. In finite difference analysis, failure line or zone finds its own way and researcher does not designate a failure path to be followed. Shear strain rate contour informs about the failure surface or zone. Although circular failure analyses were conducted and critical slip circles were determined, a different failure line was existed in the finite difference analysis.

Failure surface was determined and implemented on SLIDE software in order to calculate the factor of safety by a limit equilibrium method. Janbu Simplified (1968) method was used in the analysis, (Figure 4.54 and 4.55).

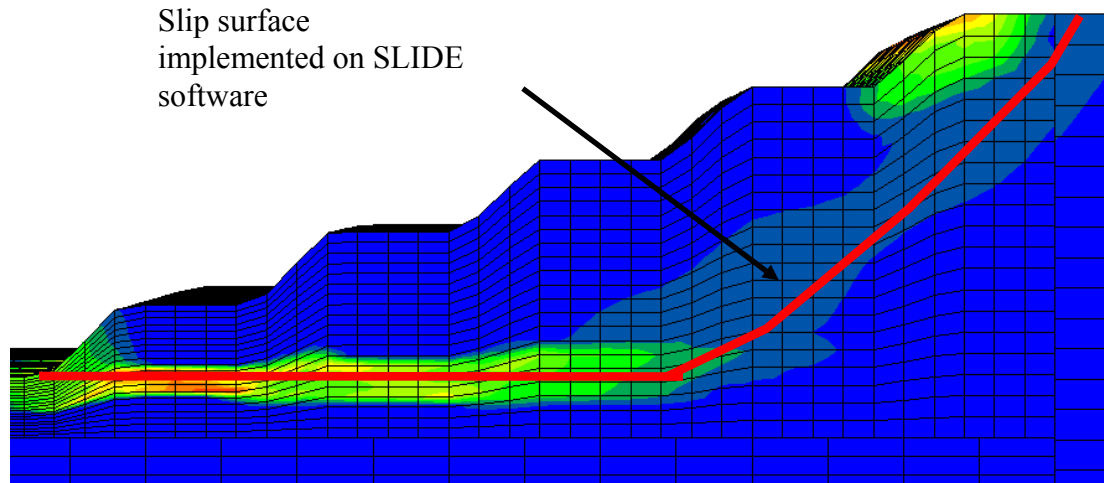


Figure 4.54 Shear strain contour of the numerical model and slip surface used in limit analysis

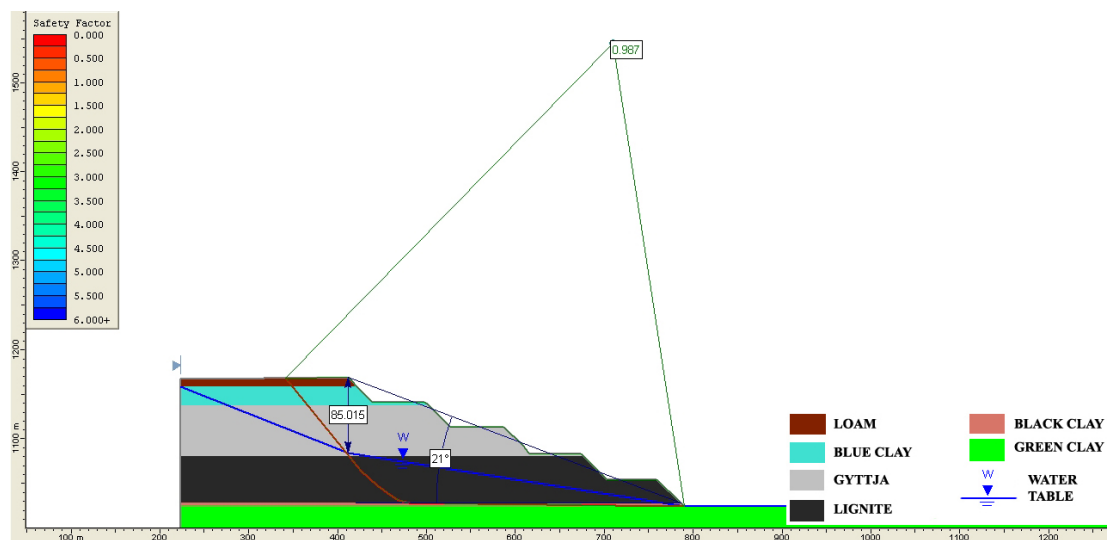


Figure 4.55 Non-circular failure surface analyzed for the same model properties as implemented in FLAC3D

Janbu Simplified method (1968) calculated a factor of safety value of 0.99 for the non-circular failure surface. Shear strength reduction method had given ~ 1.20 for the same case. This result might be raised from stress confinement in 3D numerical model and absence of the field stress in limit equilibrium analysis.

4.10.4 Impact of overall slope angle to stability in the case

Finite difference model was modified for different overall slope angles and the effect was investigated when the overall slope angle is steepened. Overall slope angles of 21° , 27° , 35° and 36° were modeled. At 5000 steps of solution cycling history plots were taken from history point #4 on Figure 4.39 and a graph was plotted, (Figure 4.56). Factor of safety calculations by FLAC3D commands were also illustrated on the Figure (4.56).

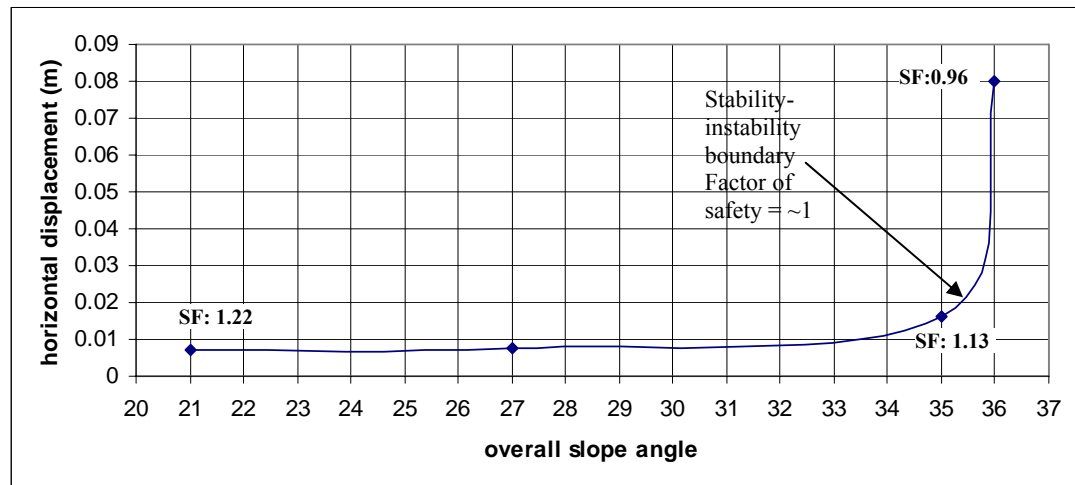


Figure 4.56 Overall slope angle vs. Horizontal displacement graph

When the model had overall slope angle of 35° , was still stable and 36° was found as a boundary for stability. When the angle was raised to 36° instability drastically increased and a collapse could be predicted. It was understood that factor of safety was ~ 1.00 when the overall slope angle is between 35° and 36° .

When deciding the stability-instability boundary, some graphical outputs are considered as beneficial. Displacement contour, shear strain rate contour, horizontal displacement history corresponding to solution steps are illustrated, (Figure 4.57, 4.58, 4.59 for overall slope angle 36° and Figure 4.60, 4.61, 4.62 for overall slope angle 35°).

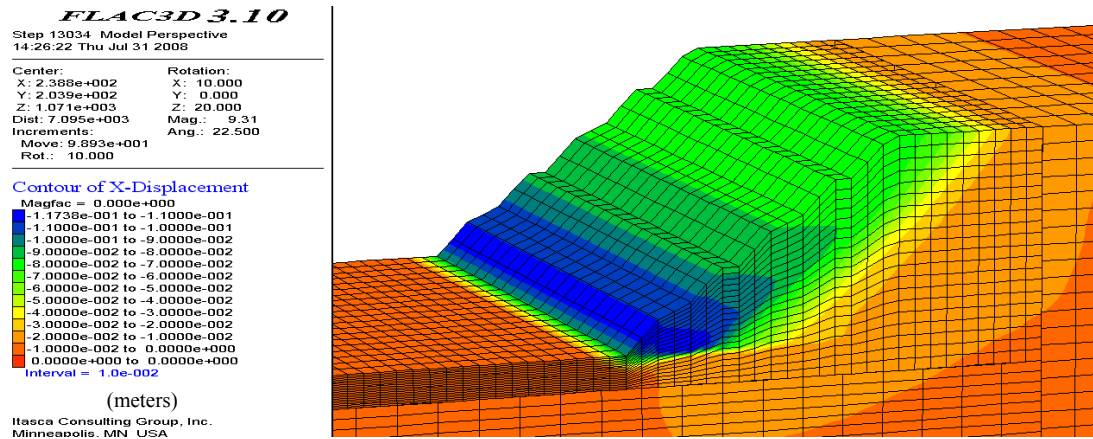


Figure 4.57 Horizontal displacement contour (overall slope angle 36°)

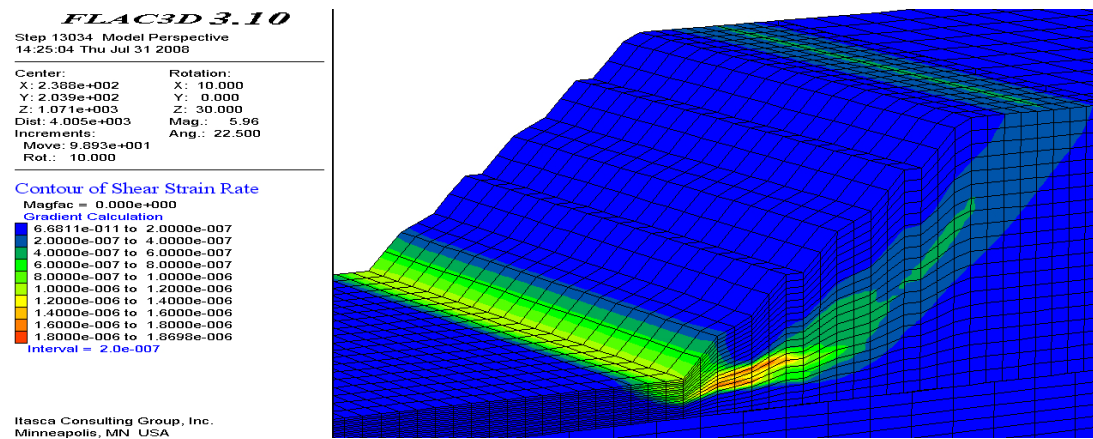


Figure 4.58 Shear strain rate contour (overall slope angle 36°)

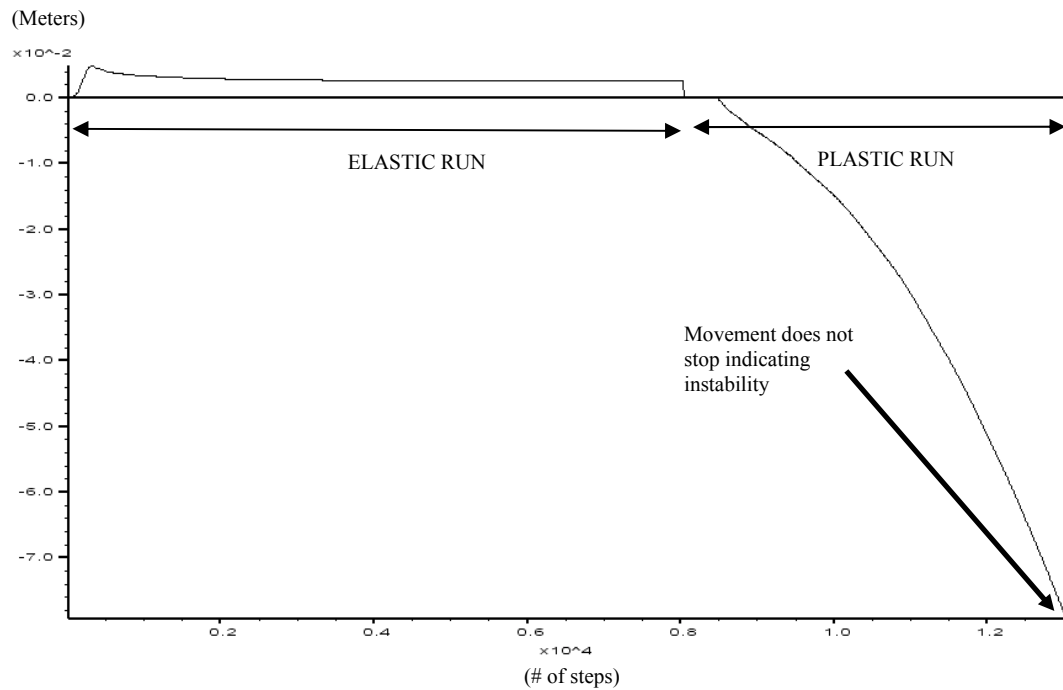


Figure 4.59 Horizontal displacement vs. solution steps graph (overall slope angle 36°)

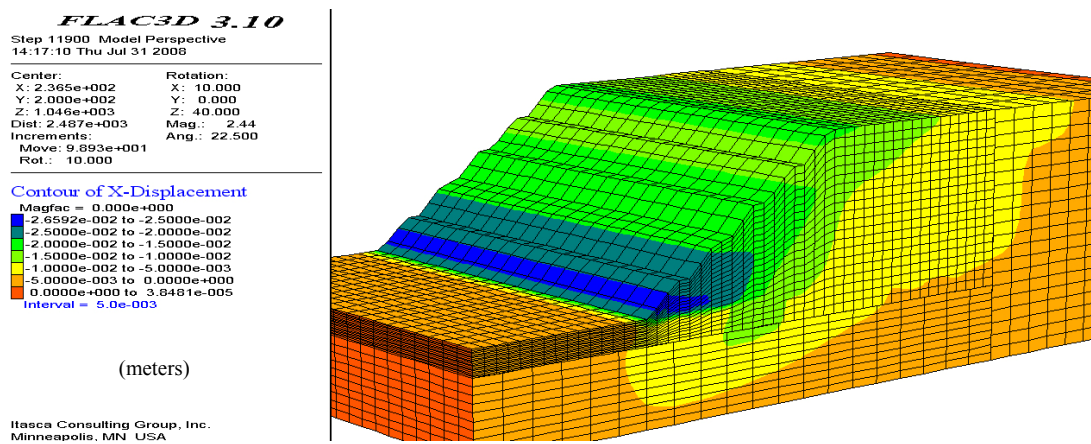


Figure 4.60 Horizontal displacement contour (overall slope angle 35°)

FLAC3D 3.10
 Step 11900 Model Perspective
 14:20:03 Thu Jul 31 2008

Center:	Rotation:
X: 2.140e+002	X: 10.000
Y: 2.130e+002	Y: 0.000
Z: 1.046e+003	Z: 30.000
Dist: 3.009e+003	Mag.: 3.81
Increments:	Ang.: 22.500
Move: 9.893e+001	
Rot.: 10.000	

Contour of Shear Strain Rate
 Magfac = 0.000e+000
 Gradient Calculation

7.6687e-012 to 0.0000e+000
0.0000e+000 to 2.0000e-010
2.0000e-010 to 4.0000e-010
4.0000e-010 to 6.0000e-010
6.0000e-010 to 8.0000e-010
8.0000e-010 to 1.0000e-009
1.0000e-009 to 1.2000e-009
1.2000e-009 to 1.4000e-009
1.4000e-009 to 1.4204e-009

Interval = 2.0e-010

Itasca Consulting Group, Inc.
 Minneapolis, MN USA

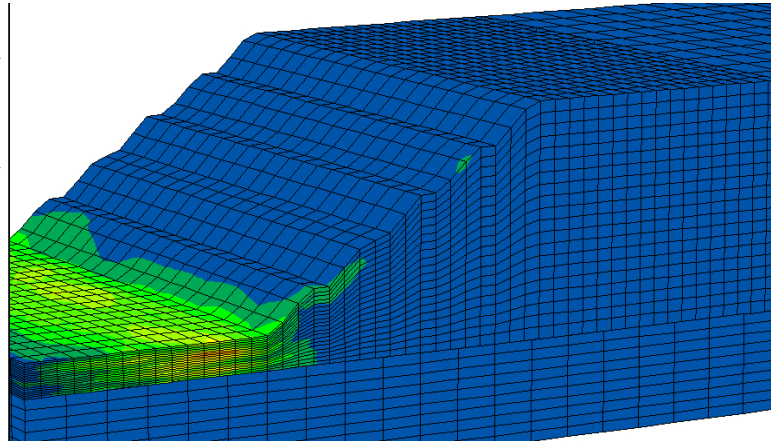


Figure 4.61 Shear strain rate contour (overall slope angle 35°)

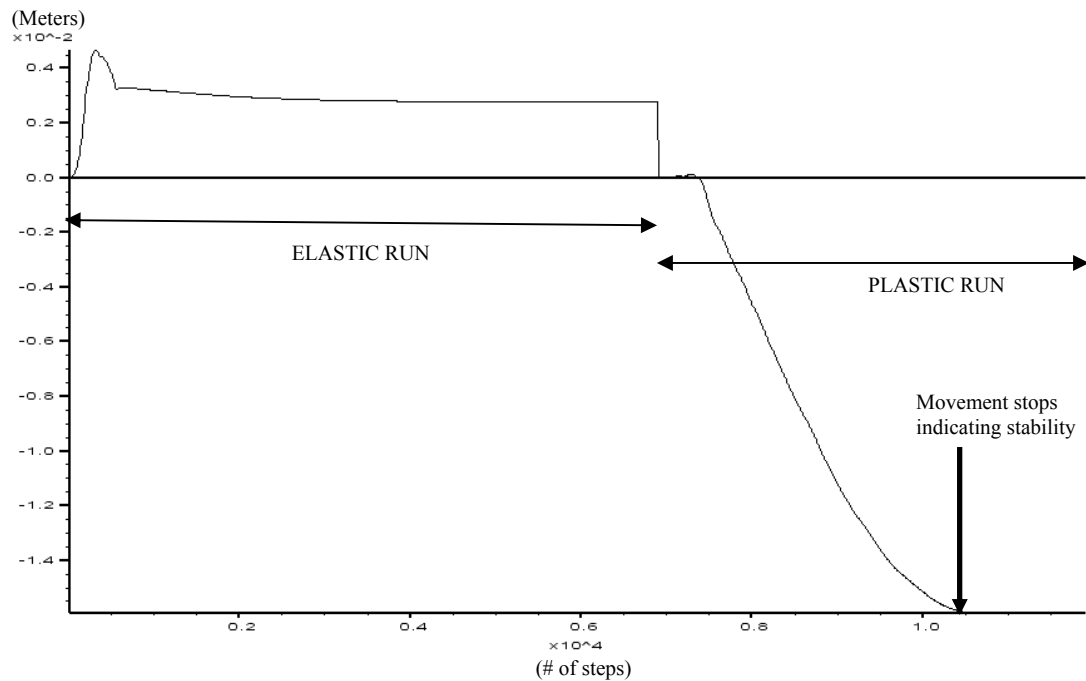


Figure 4.62 Horizontal displacement vs. solution steps graph (overall slope angle 35°)

Factor of safety analysis of slopes having 35° and 36° overall slope angles were computed by using FLAC3D software. FLAC3D computed 1.13 for 35° and 0.96 factor of safety for 36° overall slope angle. Factor of safety values for 21°, 35° and 36° slope angles are summarized on the Figure 4.63 by using FLAC3D factor of

safety calculation property. A drastic change is also take attention between the overall slope angles of 35° and 36° . The slip surfaces were found in FLAC3D results by inspecting shear strain rate contours. The slip surfaces are applied to SLIDE software and results are summarized in the plot 4.63.

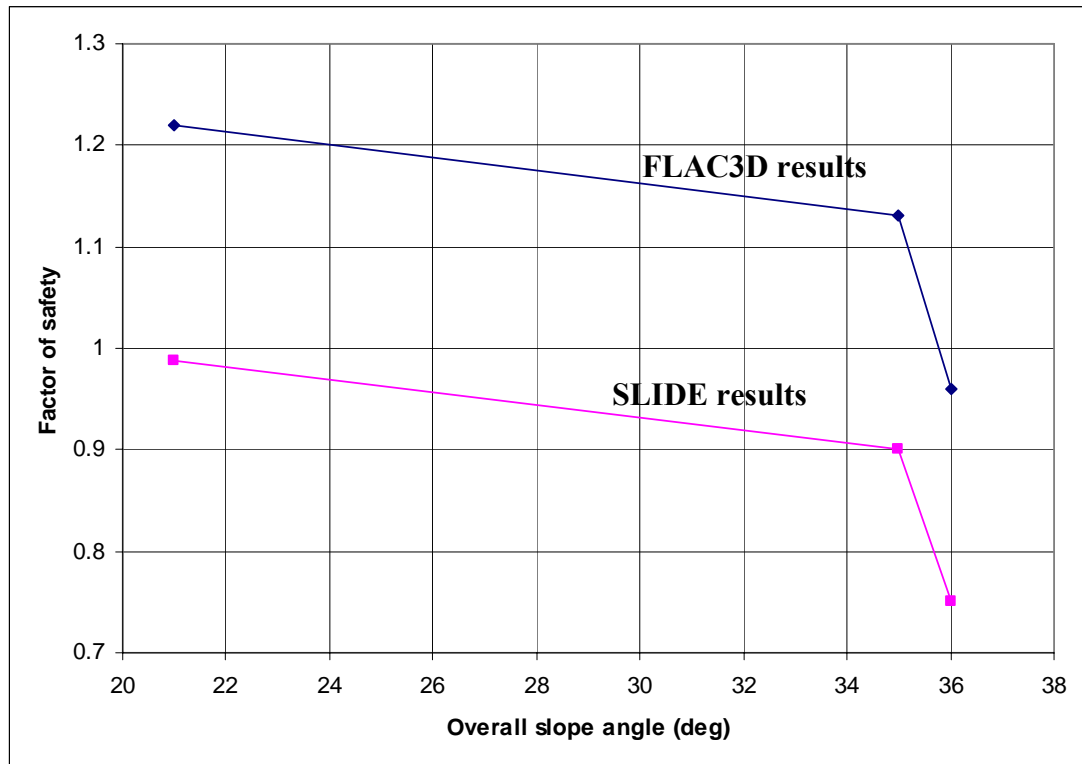


Figure 4.63 Factor of safety variation with respect to overall slope angle

Results of FLAC3D/SLIDE for factor of safety results ratio is ~ 1.26 . It is observed that the results calculated by SLIDE is lower than the FLAC3D results.

4.10.4.1 Comparison of the numerical analysis with limit equilibrium analysis

A comparison of limit equilibrium method and finite difference method was also studied in section 4.10.3. For the same purpose, limit equilibrium analysis was carried out for the slope having 35° overall slope angle. Failure surface was impressed from the shear strain rate contour of the finite difference analysis and Janbu Simplified method (1968) was used in the analysis, (Figure 4.64 and 4.65).

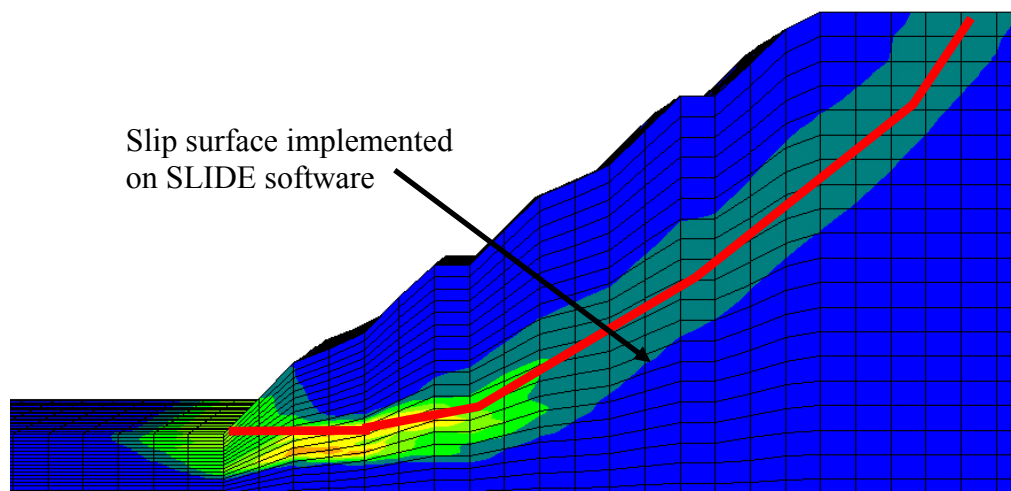


Figure 4.64 Shear strain contour of the numerical model and slip surface applied in the limit analysis

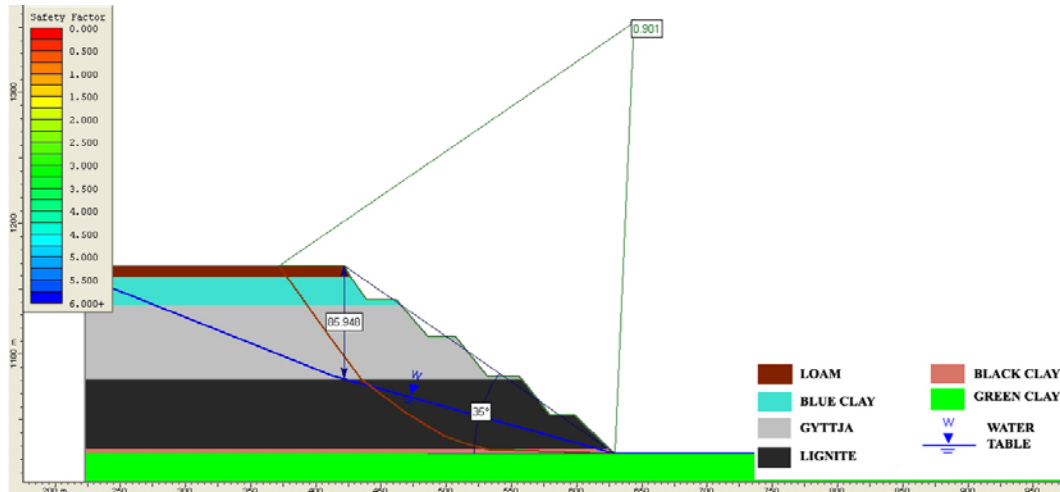


Figure 4.65 Non-circular failure surface analyzed for the same model properties as implemented in FLAC3D

Factor of safety value of 0.90 was obtained from the analysis. When 35° overall slope angle was formed, limit equilibrium analysis resulted in instability while finite difference analysis resulted in approximately unity of safety factor. The results were verified each other.

4.11 Limit Equilibrium analysis of temporary slopes in 2-D

4.11.1 Bucket wheel excavator production slopes

Figure 4.1 illustrates the slopes and north-east production slopes are the permanent slopes to be analyzed. These slopes will be formed allowing bucket wheel excavators to work safely. Production slope geometry was given by Park Teknik considering the bucket wheel excavators require specific bench geometry.

Ground water table level was accepted as on the surface and circular failure analyses were conducted and the lowest factor of safety values obtained by slip circles are illustrated on Table 4.10. All sections and analyses are presented in Appendix E. Required factor of safety value is 1.30 in permanent slopes (Hoek and Bray, 1981). Shear strength parameters on Table 4.9 were used in the analysis.

Table 4.10 Factor of safety analysis of bucket wheel excavator working slopes
with a water level on the surface

Section #	Factor of safety
1	1.63
2	1.72
3	1.53
4	1.56
5	1.44
6	1.58

Lowest factor of safety value was obtained from the section #5. Slip circle and factor of safety value is given on the Figure 4.65.

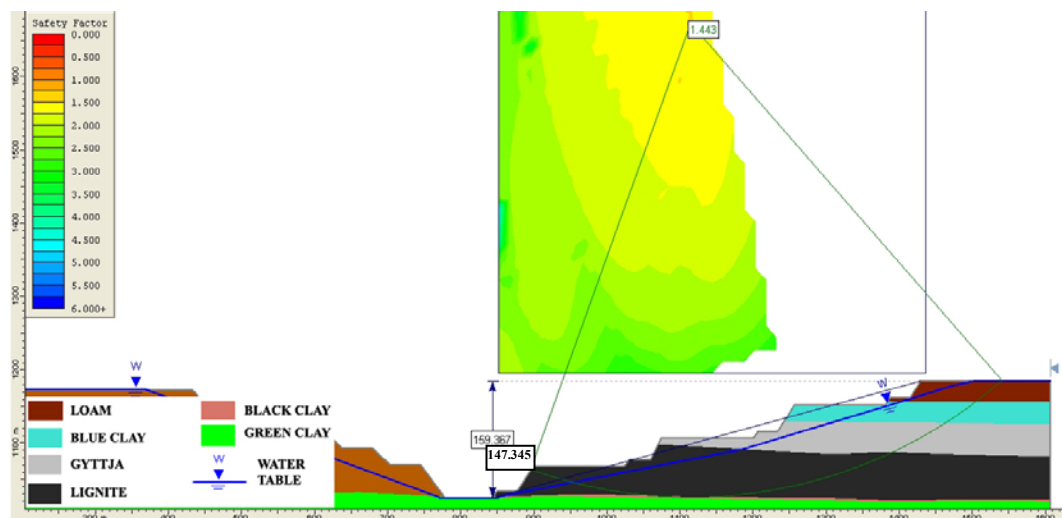


Figure 4.65 Slip circle and factor of safety is shown
with an overall slope angle of 15°

Even if the water table was assumed as on the surface at the slope crest, factor of safety values were obtained as higher than 1.30. These slopes can be considered as safe having a factor of safety greater than 1.30. In fact this approach may be

adequate because strata traps water in pressure and it is not easy to dissipate its water or in restricted time successful drainage may not take place.

A detailed pretentious dewatering project was prepared by German consulting firm of Park Teknik. Thus, different ground water table levels were also analysed.

Section #5 was used (due to having the lowest factor of safety) and ground water tables were lowered 50 m and 85 m below the surface at the slope crest, (Figure 4.66 and Figure 4.67).

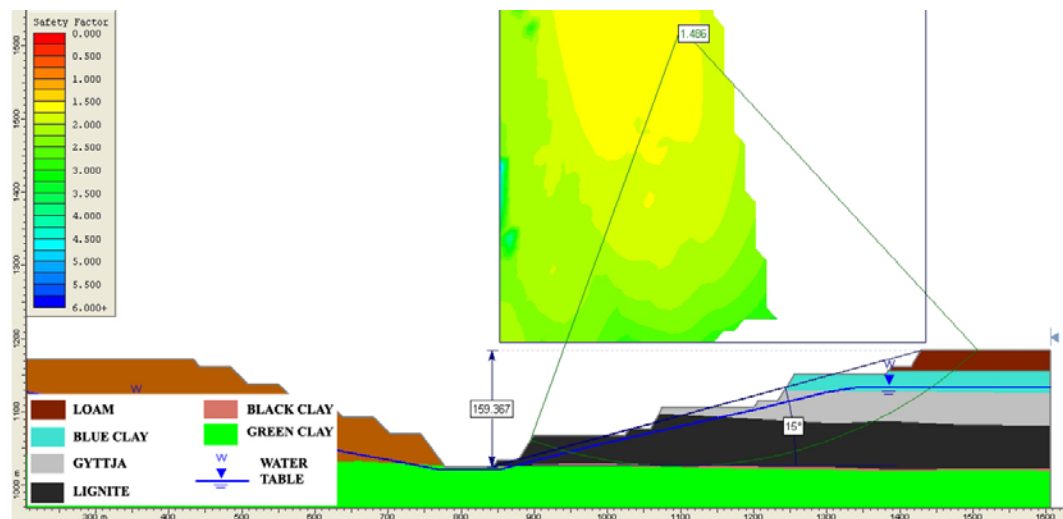


Figure 4.66 Section #5, slip circle of lowest factor of safety with a ground water table 50 m beneath the surface

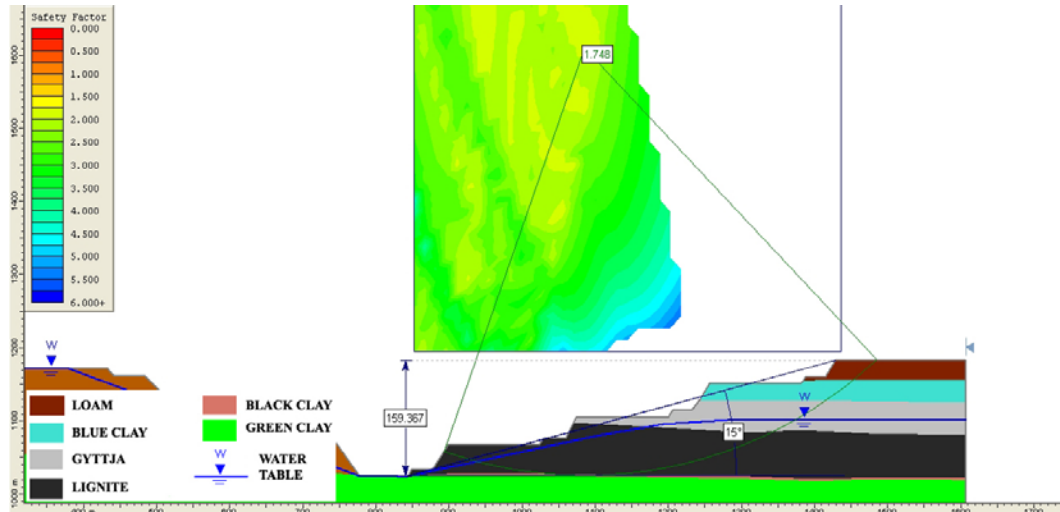


Figure 4.67 Section #5, slip circle of lowest factor of safety with a ground water table 85 m beneath the surface

A graph was constructed for permanent slopes having an overall slope angle of 15° with changing depth of water levels and corresponding factor of safeties, (Figure 4.68).

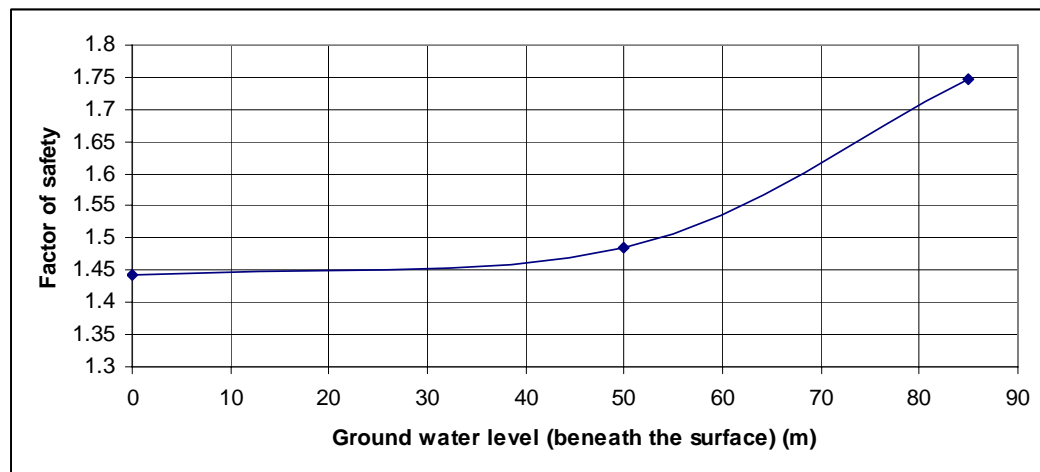


Figure 4.68 Factor of safety vs. water table depth from surface graph for 15° overall slope angle

When the Figure 4.67 was observed, it was concluded that if dewatering aims were obtained, factor of safety reached 1.75 indicating a satisfactory safety and also lowest factor of safety of 1.44.

4.11.2 “Box-cut” slopes

In the first three years, by assigning several contractors, Çöllolar mine field will be opened in order to establish the access to the coal.

The mine field will be started to be excavated by using hydraulic excavators which are used in also loading. Then, trucks will be used in hauling. Outside dump will be utilized for collecting the overburden material. Within three years box-cut excavation will be formed as primary excavation and after three years, pit geometry will be adequate for bucket wheel excavator production.

Permanent slopes are designed considering the 1.30 factor of safety to be satisfied, (Hoek and Bray, 1981) and limit equilibrium analyses were carried out by using Bishop Simplified Method (1955) for different ground water levels. As illustrated on the Table 4.7, cross section resulting in the lowest factor of safety is #5. In box-cut stability analyses, section #5 was used. Figures 4.69, 4.70 and 4.71 are illustrated for the factor of safety values with respect to water table depth.

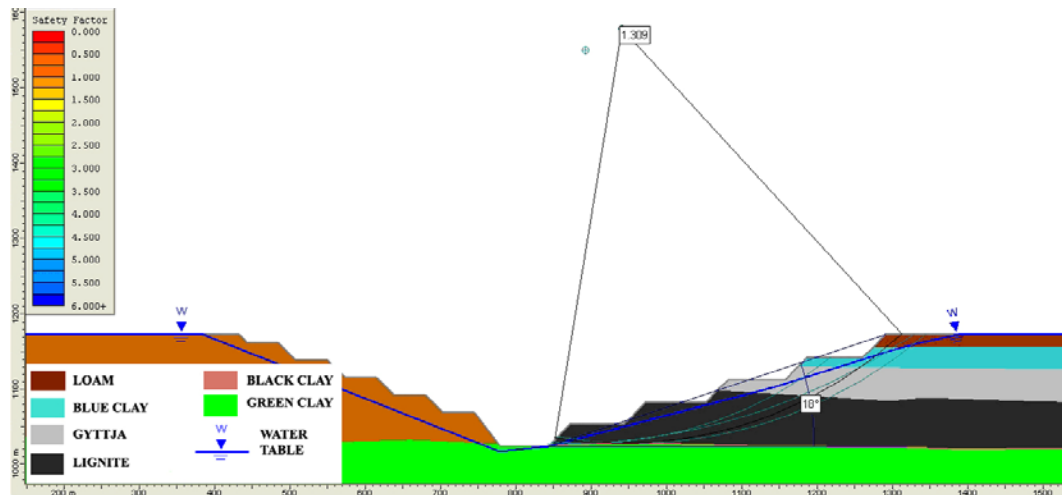


Figure 4.69 Temporary slope having 18° overall slope angle with a ground water level at the surface

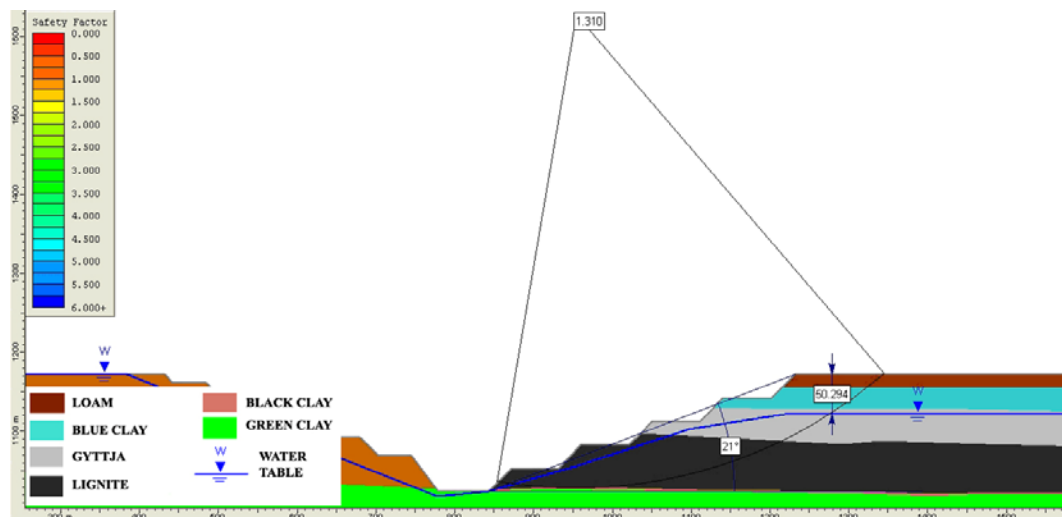


Figure 4.70 Temporary slope having 21° overall slope angle with a ground water level having a 50 m depth from surface

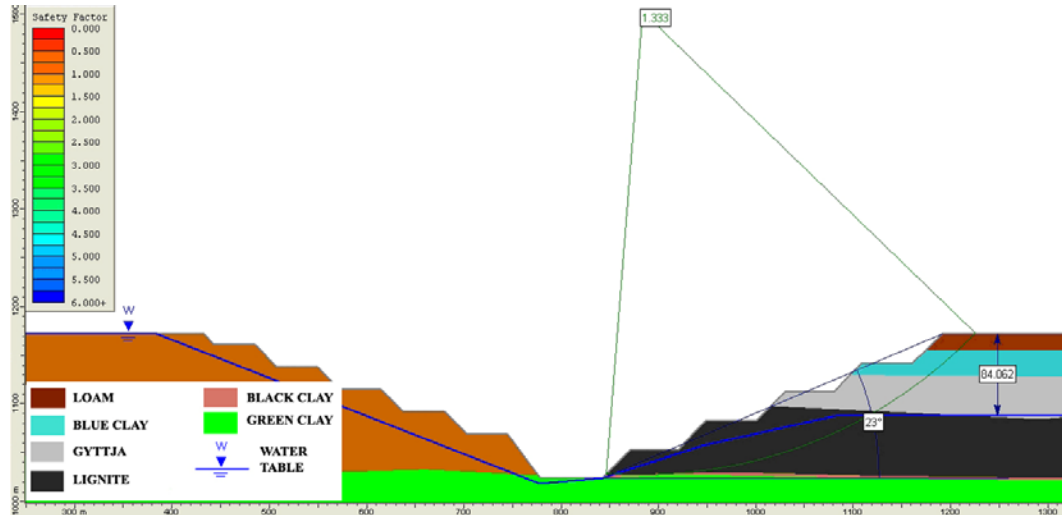


Figure 4.71 Temporary slope having 23° overall slope angle with a ground water level having a 85 m depth from surface

Variation of overall slope angle responding to ground water level is illustrated on the Figure 4.71.

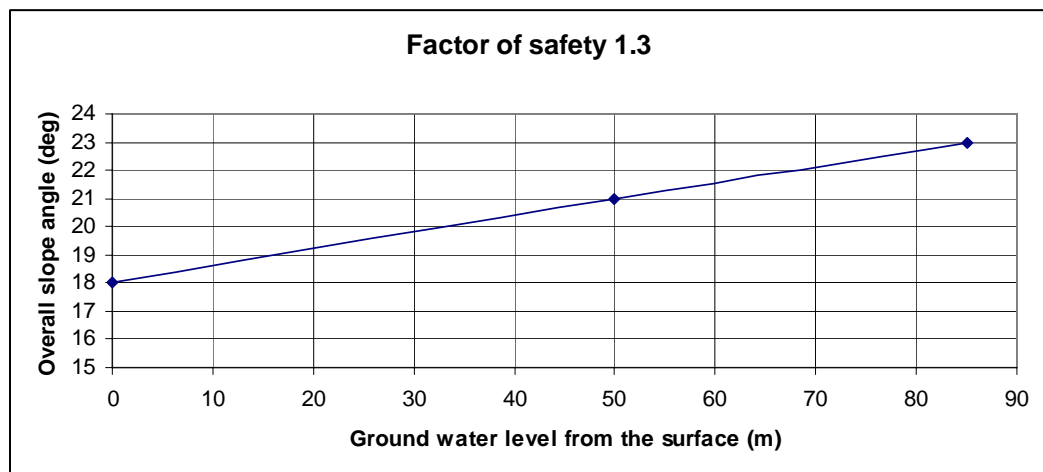


Figure 4.72 Overall slope angle vs. ground water level satisfying 1.30 factor of safety.

If dewatering aims are realized, it is safe to excavate a slope having overall slope angle of 23° .

4.12 Finite difference analysis of temporary slopes in 3-D

Although the bucket wheel excavator production slopes were analyzed and considered as safe (factor of safety > 1.30), finite difference analysis was carried out in order to observe displacements and confirmation of the stability of the slope.

4.12.1 Model

Model has a total width of 400 m and 975 m length. On the Figure 4.73, model, material boundaries, finite difference grids and dimensions of the model are illustrated.

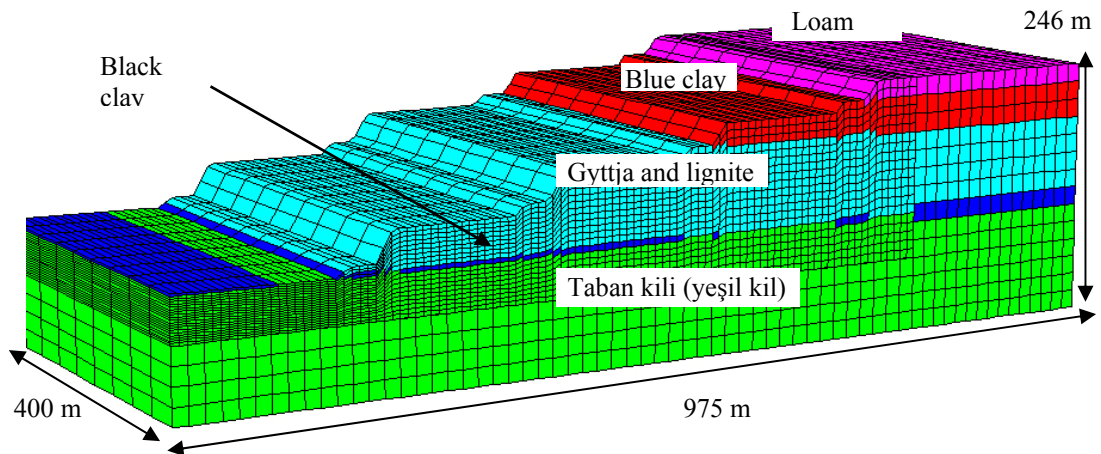


Figure 4.73 Finite difference grids and material boundaries with dimensions

History points were located for displacements corresponding number of steps. Slope displacements were recorded both in elastic and plastic stepping, (Figure 4.74).

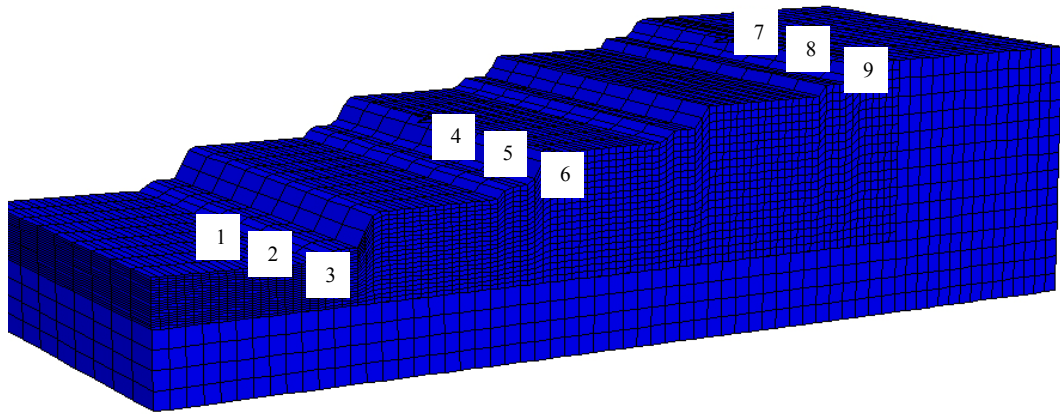


Figure 4.74 History points for recording displacements during stepping (or cycling) for solution.

Displacement history plot of point #7 is illustrated on the Figure 4.75.

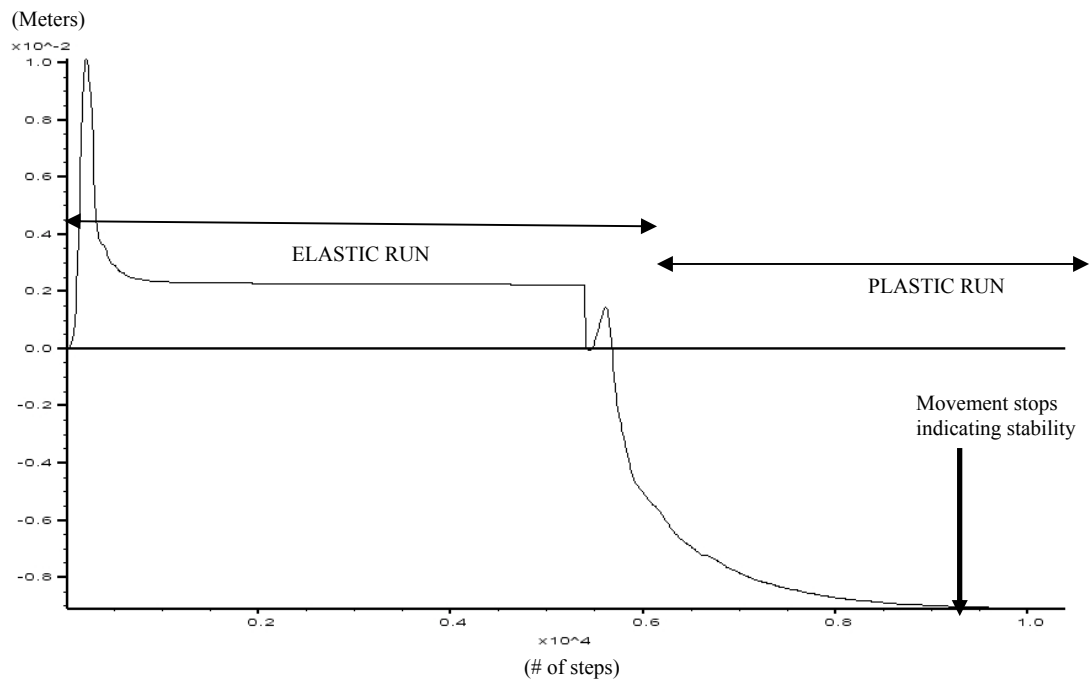


Figure 4.75 Horizontal displacement vs. solution steps graph

On the Figure 4.75, displacement stops at ~9 mm which indicated stability of the model. Horizontal displacement contour is illustrated on the Figure 4.76.

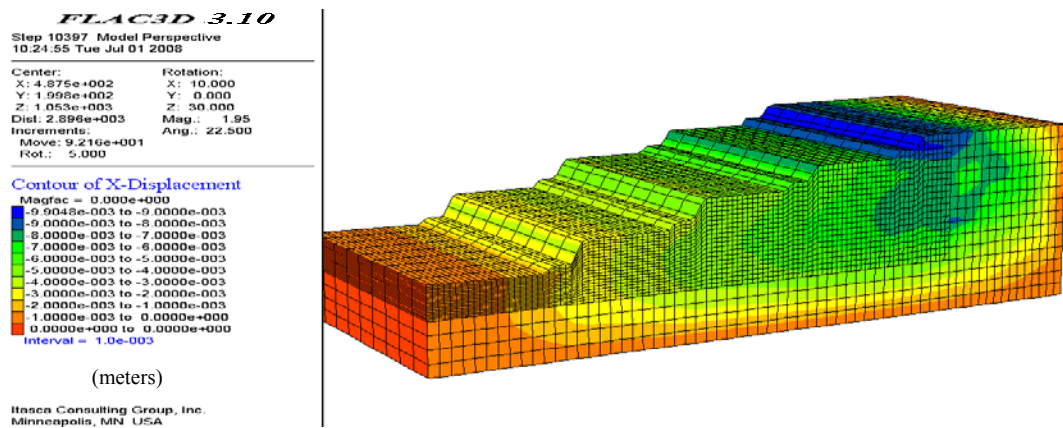


Figure 4.76 Horizontal displacement contours

Shear strain contour of the model is presented on the Figure 4.77.

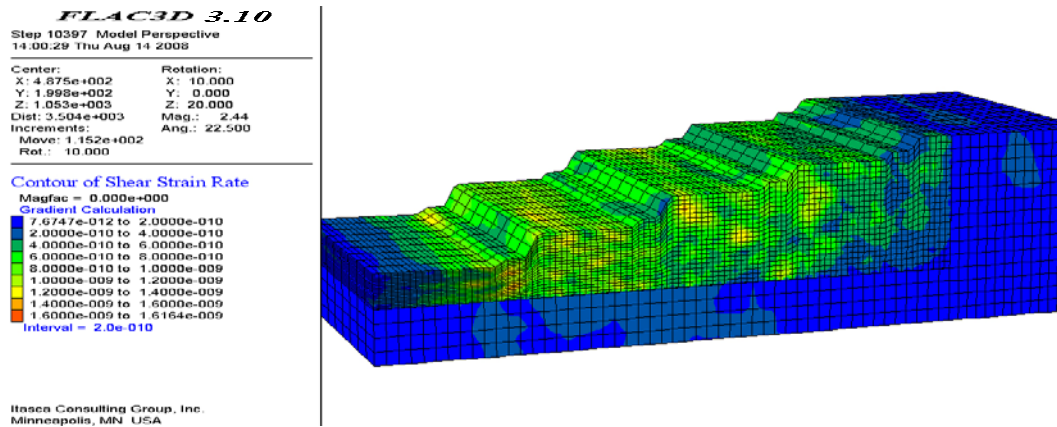


Figure 4.77 Shear strain rate of the model

Shear strain rate contour did not exhibit a failure zone or failure surface existed in the computation of FLAC3D.

Bucket wheel excavator production slopes were determined as safe with an overall slope angle of $\sim 15^\circ$.

Factor of safety calculation of production slopes were carried out by using FLAC3D commands resulting in 1.56 factor of safety. Horizontal displacement contour and shear strain contour is illustrated on the Figure 4.78 and 4.79.

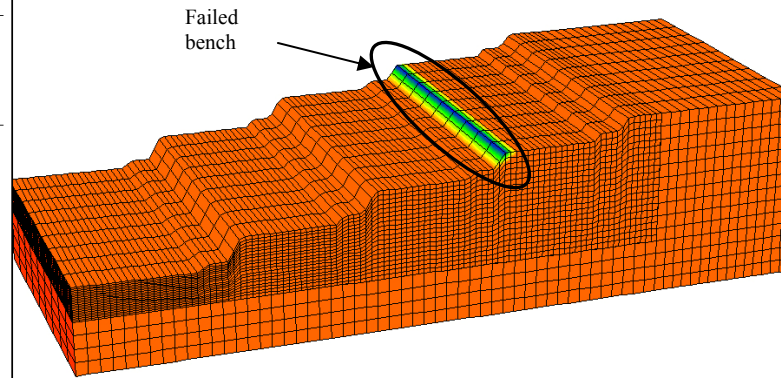
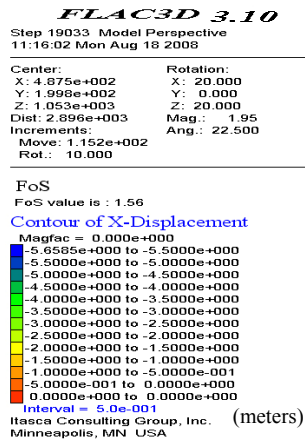


Figure 4.78 Horizontal displacement contour

Figure 4.78 expresses that the when the shear strength parameters were reduced by a factor of 1.56, only local bench failures were existed.

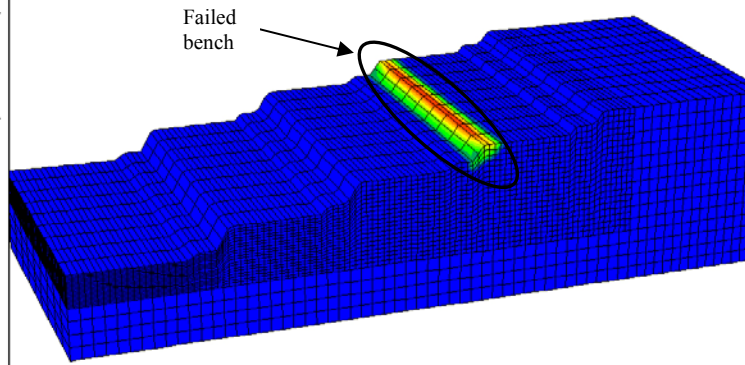
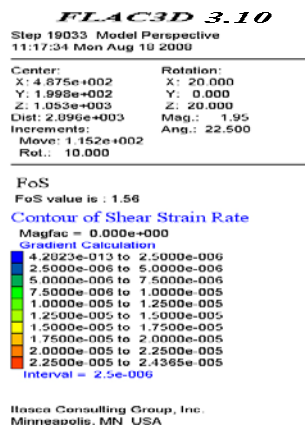


Figure 4.79 Shear strain rate contour

Shear strain rate contours gave information about the failure path or surface generated within the bench. On the Figure 4.79, failure of the bench can be observed clearly. Factor of safety of the weakest part was analyzed by FLAC3D software of the model and 1.56 factor of safety is calculated. This value is the factor of safety of indicated bench on the Figure 4.79. In fact factor of safety value

is higher for an overall instability condition. Thus, calculations conclude satisfactory safety for bucket wheel excavation slopes.

4.13 Summary of the analysis results

Back-analysis and sensitivity analysis results are summarized in the Table 4.11.

Table 4.11 Back-analysis and sensitivity analysis results

Back-calculated shear strength parameters of black clay for Kışlaköy 2006 failure by Limit equilibrium method	$c' = 23 \text{ kPa}$ and $\phi' = 10.5^\circ$
Back-calculated shear strength parameters of black clay for Kışlaköy 2006 failure by Finite difference method	$c' = 8 \text{ kPa}$ and $\phi' = 9^\circ$
Shear strength parameters of Gytja and Lignite verified by sensitivity analysis by Finite Difference method	$c' = 54 \text{ kPa}$ and $\phi' = 32^\circ$

Factor of safety analysis of permanent slopes with respect to three different ground water levels by limit analysis (circular failure) are illustrated in Table 4.12.

Table 4.12 Factor of safety analysis of permanent slopes with respect to three different ground water levels by limit analysis (circular failure)

	Factor of safety		
Ground water level from surface	85 m	50 m	0 m
Section #			
1	1.75	1.59	1.05
2	1.55	1.26	0.97
3	1.47	1.17	1.01
4	1.48	1.18	1.04
5	1.54	1.26	1.10
6	1.50	1.19	1.07
7	1.50	1.24	1.24

Overall slope angles vs. water table depth plot to keep 1.5 factor of safety are presented in the Table 4.13.

Table 4.13 Overall slope angles vs. water table depth plot to keep 1.5 factor of safety

Overall slope angle (°)	Water table depth (m)
14	85
17	50
21	0

Composite failure analysis around fault for cross section #6 is shown on the Table 4.14.

Table 4.14 Composite failure analysis around fault for cross section #6

Factor of safety in Limit Equilibrium Method	0.92
---	------

Finite Difference Analysis of permanent slopes for different overall slope angles and finite difference and limit equilibrium methods results comparison are illustrated on the Tables 4.15 and 4.16.

Table 4.15 Finite Difference Analysis of permanent slopes for different overall slope angles

Overall slope angle (°)	Factor of safety
21	1.22
35	1.13
36	0.96

Table 4.16 Finite difference and limit equilibrium methods result comparison (Slip surfaces are the same with FLAC3D failure zones)

Overall slope angle (°)	Factor of safety by FLAC3D	Factor of safety by Limit Equilibrium
21	1.22	0.99
35	1.13	0.90
36	0.96	0.75

Results dedicated to temporary slopes are presented in the Tables 4.17, 4.18, 4.19 and 4.20.

Table 4.17 Factor of safety analysis of bucket wheel excavator working slopes with a water level on the surface by limit analysis (circular failure)

Section #	Factor of safety
1	1.63
2	1.72
3	1.53
4	1.56
5	1.44
6	1.58

Table 4.18 Factor of safety vs. water table depth from surface graph for 15° overall slope angle by Limit equilibrium analysis (for circular failure)

Factor of safety	Ground water depth (m)
1.75	85
1.49	50
1.44	0

Table 4.19 Overall slope angle vs. ground water level satisfying 1.30 factor of safety for temporary slopes

Overall slope angle (°)	Ground water level (m)
23	85
21	50
18	0

Table 4.20 Finite Difference analysis, factor of safety calculation by FLAC3D for bucket wheel excavator production slopes

Factor of safety	1.56
------------------	------

CHAPTER 5

CONCLUSION AND RECOMMENDATIONS

This study covers the safe slope design at the Çöllolar sector that will be mined by PARK Teknik A.Ş., the studies have been completed. Both two and three dimensional solutions were utilized.

The main conclusions drawn from this work and recommendations for future studies are given below:

- 1- Laboratory tests carried out at the Soil Mechanics laboratory of the civil Engineering Department of METU. The results are presented in the text, in detail. The shear strength parameters of the dominant units were as: $c_p'=59$ kPa and $\phi_p'=31.8^\circ$ for gyttja, $c_p'=48$ kPa and $\phi_p'=32.8^\circ$ for lignite, $c_p'=57.5$ kPa and $\phi_p'=28^\circ$ for black clay
- 2- The failure occurred at the Kışlaköy sector was utilized by back-analysis, to verify the small scale laboratory test results. The shear strength parameters of black clay obtained from back-analysis were quite lower than lab results while the other units have compatible values.
- 3- After evaluation, in the analyses, $c'=54$ kPa and $\phi'=32^\circ$ for gyttja, $c'=54$ kPa and $\phi'=32^\circ$ for lignite, $c'=8$ kPa and $\phi'=9^\circ$ for black clay were used.
- 4- For the permanent slopes, considering the factor of safety as 1.5, the maximum safe slope angle was determined as 21° when the water table is lowered down to a depth of 85 m. The corresponding maximum safe slope angle for temporary slopes was calculated as 23° .
- 5- As it is obviously expected, ground water level affects the stability and in this case, for the permanent slopes, maximum safe slope angle decreased to 14°

when the ground water table is at the top. In other words, if there is no dewatering process. The corresponding safe slope angle for the temporary slopes was 18° .

6- Overall slope angle of 15° for Bucket Wheel Excavator panels are planned by the mine management is safe enough with a factor of safety of 1.46 even in fully saturated condition.

7- The factor of safety (reduction factor) of 1.22 was obtained in FLAC3D analysis. Corresponding factor of safety of 1.5 was calculated by limit analysis (circular failure). The factor of safety of 1.22 found in FLAC3D provided permanent overall slope angle of 21° , when factor of safety decreased to 1.00, the maximum safe slope angle $\sim 35.5^{\circ}$.

8- Failure paths obtained from FLAC3D was compared in SLIDE by imposing the failure path. While FLAC3D has given 1.22 factor of safety for 21° permanent slope, SLIDE analysis resulted in 0.99. This is due to the confinement effect of the FLAC3D which generates 3-D field stresses while limit equilibrium methods assume in-plane stresses as zero and no field stresses.

9- Factor of safety analysis of Bucket Wheel Excavator slopes in FLAC3D software resulted in 1.56 value. This corresponds to the lowest safety factor of the weakest part of the model: local bench failure not an overall instability. FLAC3D factor of safety solver was unable to find overall factor of safety. Because a failure zone or surface affecting overall stability could exist when reduction factor was higher than 1.56. Practically for this case, it is unnecessary to calculate factor of safety for overall stability while it is greater than required value, 1.3. For conditions constituting local weaker parts like benches, manual implementation of shear strength reduction principles on FLAC3D will result in finding a factor of safety dedicated to overall stability. Moreover, FLAC3D may be upgraded for different options for finding factor of safety for this kind of particular conditions as considered.

REFERENCES

- Anon 2003a: U.S. Army Corps of Engineers, *Engineer Manual*. [Online]
Available:
<http://www.usace.army.mil/publications/eng-manuals/em1110-2-1902/entire.pdf>,
2003 (Last accessed date: 10.08.08)
- Anon 2003b: Rocscience Inc. 2-D Limit Equilibrium slope Stability for soil and
Rock Slopes, 2003
- Anon 2006: ITASCA FLAC3D version 3.1 *User's guide*. Third Edition, 2006
- Anon 2007a: ITASCA 3DEC version 4.1 *User's guide*. Third Edition, 2007
- Anon 2007b: Tagasoft software website:
<http://www.tagasoft.com/TAGAsoft/TAGAsoft/docs/tslope/b2.html> (Last accessed
date: 24.04.2007)
- Abramson, L.W., Lee, T.S., Sharma, S. and Boyce, G.M. *Slope Stability and
Stabilization Methods*. 2nd edition, John Wiley & Sons, 712 p., 2001
- Akbulut, İ., Aksoy, T., Çağlan, D., Ölmez, T., *Afşin-Elbistan Kışlaköy Açık Kömür
İşletmesi Şev Stabilitesi Çalışması*. Maden Tetkik Arama Gen. Müd., Ankara, 130
p., 2007
- Baker R., *A relation between safety factors with respect to strength and height of
slopes / technical communication*. Computers and Geotechnics 33 pp. 275–277,
2006

Bishop, A. W. and Bjerrum, L., *The relevance of the triaxial test to the solution of Stability problems*, Proc. ASCE Research Conference on Shear Strength of Cohesive Soils, Boulder, Colorado, pp. 503-532., 1960

Bye, A.R., Bell, F.G., *Stability assessment and slope design at Sandsloot open pit, South Africa*. International Journal of Rock Mechanics & Mining Sciences 38 (2001) 449–466)

Cala M., Flisiak J., Tajdus A., *Slope stability analysis with modified shear strength reduction technique*. Proc. of Landslides '04, Rio de Janeiro. (ed. Lacerda, Ehrlich, Fontoura, Sayao), 2004

Cala M., Flisiak J., Tajdus A., *Slope stability with FLAC in 2D and 3D*. 4th Int. Symp. FLAC and Numerical Modeling in Geomechanics, (2006)

Carvalho, J.L., *Slope Stability Analysis for Open Pits*. Golder Associates Ltd. Mississauga, CANADA, 15 p., 2002

Cheng, Y.M., *Location of critical failure surface and some further studies on slope stability analysis*, Computers and Geotechnics 30 pp. 255–267, 2003

Duncan, J.M. and Wright, S.G., *Soil Strength and Slope Stability*. John Wiley & Sons, Inc., 309 p., 2005

Eberhardt, E., *Rock Slope stability Analysis - Utilization of advanced numerical techniques*. Vancouver/CANADA, 41 p., 2003

Hack, R. *An Evaluation of Slope Stability Classification*, ISRM EUROCK'2002, Portugal, Madeira, Funchal, 32 p., 25-28 November 2002

Hammah, R.E., Curran, J.H., Yacoub, T., Corkum, B., *Stability Analysis of Rock Slopes using the Finite Element Method*, EUROCK 2004 & 53rd Geomechanics Colloquium. Schubert (ed.), 6 p., © 2004 VGE

He, M.C., Feng, J.L., Sun, X.M., *Stability evaluation and optimal excavated design of rock slope at Antaibao open pit coal mine*. China. Int J Rock Mech Mining Sci (2007), Article in press, 14 p., doi:10.1016/j.ijrmms.2007.05.007)

Hoek, E. and Bray, J., *Rock Slope Engineering*. Revised Third Edition, The Institution of Mining and Metallurgy, London, 358 p., 1981

Jiang J-C, Yamagami T, *A new back analysis of strength parameters from single slips*, Comput Geotech, doi:10.1016/j.compgeo.2007.09.004, 2007

Kempfert, H.G. and Gebreselassie, B. *Excavations and Foundations in Soft Soils*. Springer-Verlag Berlin Heidelberg, 576 p., 2006

Koçak Ç., Kürkçü S.N., Yılmaz S., *Afşin-Elbistan linyit havzasının değerlendirilmesi ve linyit kaynakları arasındaki yeri.*, Report, 11 p., 2003.

Leshchinsky, D., *Design Dilemma: Use peak or residual strength of soil*. Geotextiles and Geomembranes 19 111 125 p., 2001

OTTO GOLD, *Lignite Deposit of Afsin-Elbistan Feasibility Report, Vol 1*, Köln, 123 p., 1969

Rocscience, *A New Era in Slope Stability Analysis: Shear Strength Reduction Finite Element Technique*. Article, 10 p., 2004

Rocscience, *SLIDE version 5.0 User's manual*, 2006

Sjöberg, J., *Large Scale Slope Stability in Open Pit Mining – A Review*. Lulea University of Technology, Division of Rock mechanics, 215 p., 1996

Sonmez, H., Ulusay, R., *Modifications to the geological strength index (GSI) and their applicability to stability of slopes.*, International Journal of Rock Mechanics and Mining Sciences 36 pp. 743-760, 1999

Sonmez, H., Ulusay, R., Gökçeoğlu, C., *A Practical Procedure for the Back Analysis of Slope Failures in Closely Jointed Rock*, Int. J. Rock Mech. Min. Sci. Vol. 35, No. 2, pp. 219-233, 1998

Stead, D., Eberhardt, E., Coggan, J.S., *Developments in the characterization of complex rock slope deformation and failure using numerical modelling techniques*, Engineering Geology 83, pp. 217–235, 2006

Wang, C., Tannanta, D.D., Lilly, P.A., *Numerical analysis of the stability of heavily jointed rock slopes using PFC2D*, International Journal of Rock Mechanics & Mining Sciences 40, pp. 415–424, 2003

Verrujit, A., *Soil Mechanics*, Delft University of Technology, pp. 255-258, 2006

Yörükoğlu M., *Afşin-Elbistan Mining Project and Mining Activities at AELI Establishment of TKİ*. Madencilik Dergisi, pp. 13-29, September 1991, #3

APPENDIX A

LABORATORY TEST RESULTS

Laboratory test results with respect to geological units. Tests were conducted in Soil Mechanics Laboratory, Civil Engineering Department at METU and reported by Karpuz et al. (2008).

Table A.1 Laboratory test results of Loam

Boring No	Sample No	Depth (m.)	w _n (%)	γ _n kN/m ³	G _s	Void Ratio e _o	Direct Shear Test (CD)				Permeability Coeff. k (m/sec)	Unconfined Comp. Test q _u (kPa)
							Peak Shear Strength		Residual Shear Strength			
							C _p	φ _p	C _r	φ _r		
							(kPa)	(deg)	(kPa)	(deg)		
SK-11	UD-1	14.00- 14.50	36	18.66	2.645	1.1088	56	15	48	11	-	-

Table A.2 Laboratory test results of Blue Clay

Boring No	Sample No	Depth (m.)	w _n (%)	γ _n kN/m ³	G _s	Void Ratio e _o	Direct Shear Test (CD)				Permeability Coeff. k (m/sec)	Unconfined Comp. Test q _u (kPa)
							Peak Shear Strength		Residuel Shear Strength			
							C _p	φ _p	C _r	φ _r		
							(kPa)	(deg)	(kPa)	(deg)		
SK-1	UD-1	16.50- 16.85	26	-	2.668	-	-	-	-	-	-	
SK-3	UD-1	10.00- 10.40	24	18.15	2.718	-	32	35	21	22	2.964 x 10 ⁻⁹	-
SK-3	UD-2	19.00- 19.50	35	17.51	2.686	-	23	26	10	25	1.188 x 10 ⁻⁹	-
SK-3	UD-3	25.00- 25.50	34	19.15	2.665	-	43	26	37	22	5.606 x 10 ⁻¹⁰	-
SK-6	UD-1	10.00- 10.30	30	17.50	2.759	-	16	29	6	25	-	-
SK-6	UD-2	13.00- 13.40	38	17.08	2.765	-	40	29	18	27	7.069 x 10 ⁻⁹	-
SK-6	UD-3	19.00- 19.40	29	19.52	-	-	-	-	-	-	5.270 x 10 ⁻⁸	-
SK-6	UD-4	25.00- 25.50	33	17.01	2.725	-	85	20	67	16	8.637 x 10 ⁻⁹	78
SK-6	UD-5	31.00- 31.30	31	18.44	2.772	-	26	18	9	11	6.707 x 10 ⁻¹⁰	-
SK-11	UD-2	22.50- 23.00	32	19.27	2.075	-	31	25	23	20	3.768 x 10 ⁻¹⁰	-
SK-11	UD-3	28.50- 29.00	40	17.40	2.179	-	34	28	20	20	-	-
SK-11	UD-4	37.50- 38.00	23	17.66	2.212	-	13	25	4	21	-	-

Table A.3 Laboratory test results of Gytja

Boring No	Sample No	Depth (m.)	w _n (%)	γ _n kN/m ³	G _s	Void Ratio e _o	Direct Shear Test (CD)				Permeability Coeff. k (m/sec)	Unconfined Comp. Test q _u (kPa)
							Peak Shear Strength		Residual Shear Strength			
							C _p	φ _p	C _r	φ _r		
							(kPa)	(deg)	(kPa)	(deg)		
SK-1	UD-2	25.50-25.85	155	13.46	1.658	2.5835	91	14	63	13	2.396 x 10 ⁻⁹	-
SK-1	UD-3	31.50-31.90	66	16.11	1.873	3.5776	35	36	18	31	4.527 x 10 ⁻⁹	-
SK-1	UD-4	43.50-44.00	66	16.08	2.489	1.7921	85	30	77	26	2.263 x 10 ⁻⁹	175
SK-1	UD-5	49.50-49.90	61	14.90	2.090	0.9962	21	34	17	33	1.986 x 10 ⁻⁹	-
SK-1	UD-6	55.50-55.75	179	11.44	1.510	2.7858	59	29	29	27	-	-
SK-3	UD-5	39.00-39.20	49	14.91	2.248	-	34	32	30	29	-	-
SK-3	UD-6	48.00-48.50	53	17.27	2.616	-	30	40	20	39	-	-
SK-3	UD-7	61.00-61.50	82	15.89	2.590	3.7732	26	30	18	28	2.013 x 10 ⁻⁹	-
SK-3	UD-8	75.00-75.20	114	12.59	2.405	-	33	42	6	35	-	-
SK-5	UD-6	40.50-40.80	45	18.30	2.744	1.3655	14	22	7	20	8.5 x 10 ⁻¹¹	-
SK-5	UD-7	52.50-52.75	141	11.59	2.060	2.2246	12	32	9	30	-	-
SK-5	UD-8	58.50-58.80	82	15.86	2.215	1.5945	26	39	11	32	2.814 x 10 ⁻⁹	-
SK-5	UD-9	64.50-65.75	56	15.72	2.445	3.1072	134	18	128	17	3.385 x 10 ⁻⁹	-
SK-6	UD-7	43.50-44.00	27	16.87	2.664	1.4968	87	32	57	31	8.655 x 10 ⁻⁹	80
SK-6	UD-8	49.50-49.80	51	16.33	2.593	1.6231	217	19	169	18	2.170 x 10 ⁻⁹	-
SK-6	UD-10	61.00-61.30	118	16.01	2.519	-	91	27	67	25	7.434 x 10 ⁻⁹	-
SK-6	UD-11	67.00-67.30	83	14.67	2.567	2.3469	29	34	24	31	3.429 x 10 ⁻⁹	-
SK-6	UD-12	73.00-73.30	93	15.14	2.558	2.4792	27	32	11	28	1.471 x 10 ⁻⁹	-
SK-6	UD-13	85.00-85.50	61	15.31	2.629	1.5954	136	48	48	38	2.185 x 10 ⁻⁹	182
SK-11	UD-5	56.60-57.00	51	12.16	2.515	2.2350	28	31	-	-	8.049 x 10 ⁻¹⁰	-
SK-11	UD-6	64.50-65.00	61	14.68	2.401	1.6479	19	30	16	28	-	-
SK-11	UD-7	70.50-71.00	60	15.51	2.268	1.8755	48	36	-	-	3.861 x 10 ⁻⁹	-
SK-11	UD-8	76.50-77.00	56	15.10	2.050	1.2197	46	31	-	-	2.219 x 10 ⁻⁹	-

Table A.4 Laboratory test results of Lignite

Boring No	Sample No	Depth (m.)	w _n (%)	γ _n kN/m ³	G _s	Void Ratio e _o	Direct Shear Test (CD)				Permeability Coeff. k (m/sec)	Unconfined Comp.Test q _u (kPa)
							Peak Shear Strength		Residuel Shear Strength			
							C _p	φ p	C _r	φ _r		
							(kPa)	(deg)	(kPa)	(deg)		
SK-1	UD-7	73.50-73.85	166	12.04	-	-	74	31	61	29	-	-
SK-3	UD-12	135.00-135.20	78	14.75	1.830	-	38	24	25	18	-	-
SK-5	UD-10	73.50-73.70	93	11.74	-	-	30	46	16	45	-	-
SK-5	UD-11	79.50-79.75	140	10.20	-	-	33	34	22	29	-	-
SK-5	UD-12	85.50-85.80	142	11.78	-	-	42	32	38	29	-	-
SK-6	UD-9	55.00-55.40	44	16.25	-	-	-	-	-	-	5.659 x 10 ⁻⁹	-
SK-11	UD-9	82.50-83.00	68	15.66	2.270	1.4184	71	30	-	-	2.263 x 10 ⁻⁹	-

Table A.5 Laboratory test results of Black clay

Boring No	Sample No	Depth (m.)	w _n (%)	γ _n kN/m ³	G _s	Void Ratio e _o	Direct Shear Test (CD)				Permeability Coeff. k (m/sec)	Unconfined Comp. Test q _u (kPa)
							Peak Shear Strength		Residual Shear Strength			
							C _p	φ _p	C _r	φ _r		
							(kPa)	(deg)	(kPa)	(deg)		
SK-3	UD-4	33.00-33.50	87	14.52	2.612	-	41	24	8	23	1,408 x 10 ⁻⁹	-
SK-6	UD-6	37.50-38.00	32	19.08	2.753	-	74	32	64	27	7,111 x 10 ⁻¹⁰	238

Table A.6 Laboratory test results of Green clay (Footwall clay)

Boring No	Sample No	Depth (m.)	w _n (%)	γ _n kN/m ³	G _s	Void Ratio e _o	Direct Shear Test (CD)				Permeability Coeff. k (m/sec)	Unconfined Comp.Test q _u (kPa)
							Peak Shear Strength		Residuel Shear Strength			
							C _p	φ _p	C _r	φ _r		
							(kPa)	(deg)	(kPa)	(deg)		
SK-3	UD-10	114.00- 114.50	47	18.02	2.463	-	56	23	36	21	-	-
SK-3	UD-11	126.00- 126.50	34	16.07	2.680	-	48	20	19	11	5.434 x 10 ⁻¹⁰	63.2
SK-3	UD-13	144.00- 144.50	33	18.40	2.714	-	32	17	4	13	-	546
SK-5	UD-13	118.50- 118.70	111	11.65	1.249	-	24	29	15	20	-	-
SK-5	UD-14	130.50- 130.80	20	19.26	2.594	-	15	28	6	19	3.071 x 10 ⁻⁸	-
SK-5	UD-15	139.50- 140.00	35	17.03	2.649	-	22	22	13	12	-	41

APPENDIX B

SLIDE SOFTWARE GRAPHICAL OUTPUTS FOR PERMANENT SLOPES HAVING GROUND WATER LEVEL OF 85 m BELOW THE SURFACE

Limit equilibrium analyses graphical outputs illustrating the slip circles and factor of safety values when the ground water level has a depth of 85 m from the slope crest.

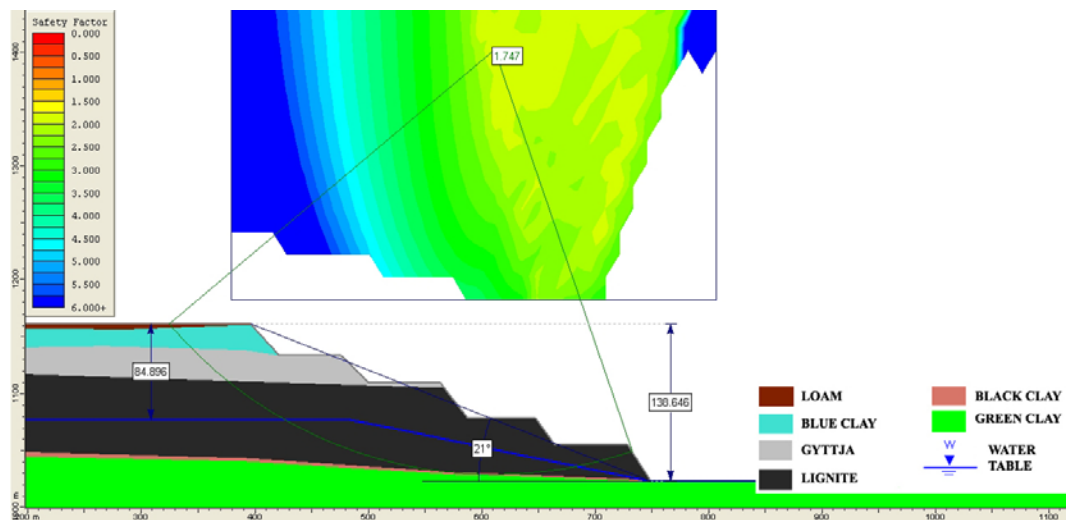


Figure B.1 Section#1

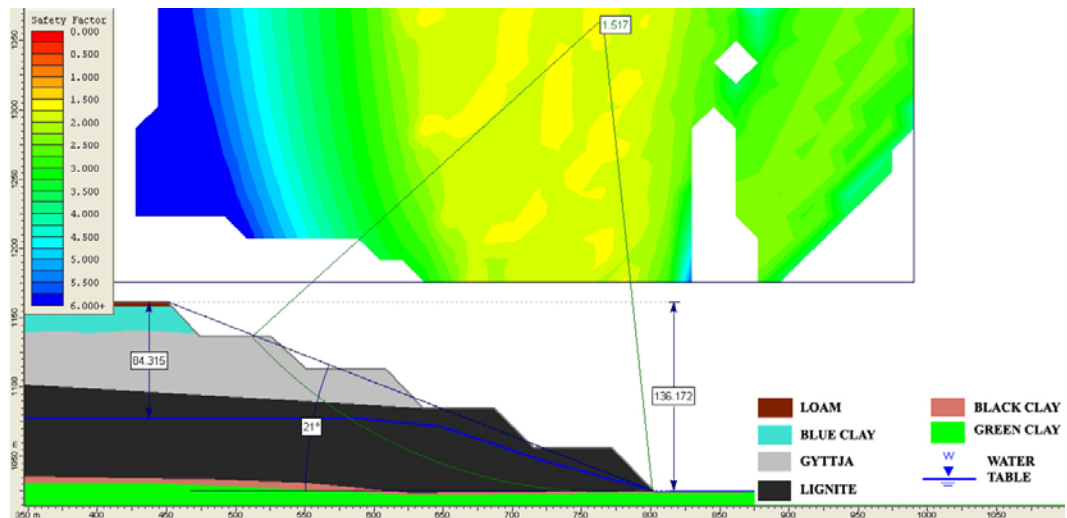


Figure B.2 Section#2

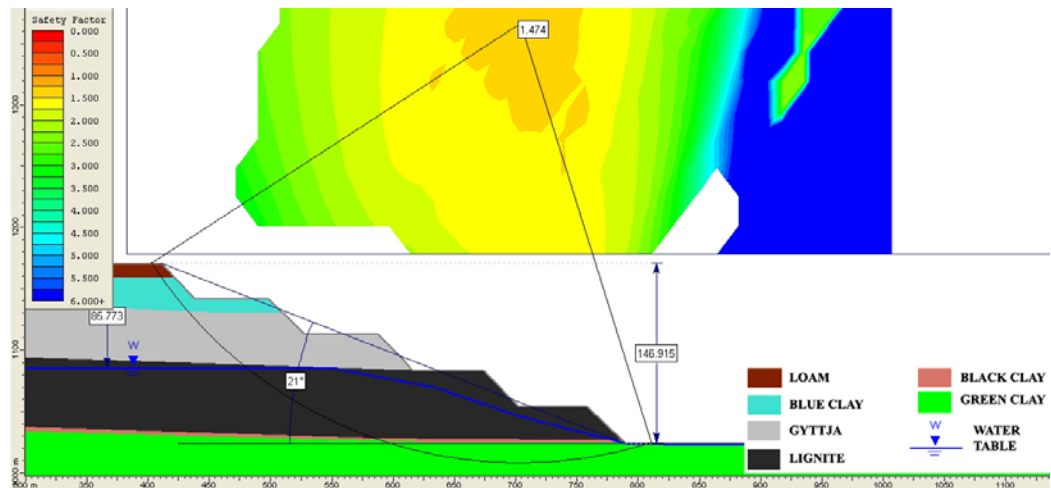


Figure B.3 Section#3

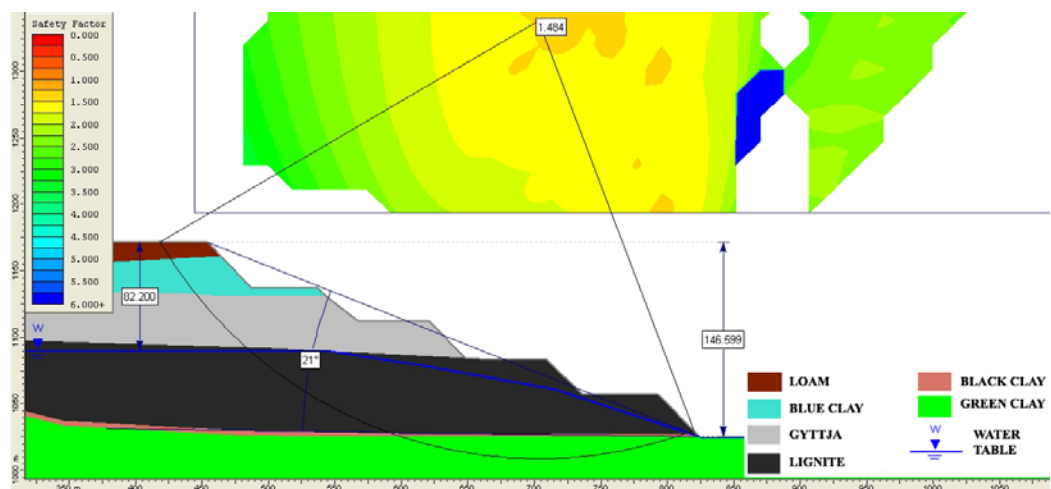


Figure B.4 Section#4

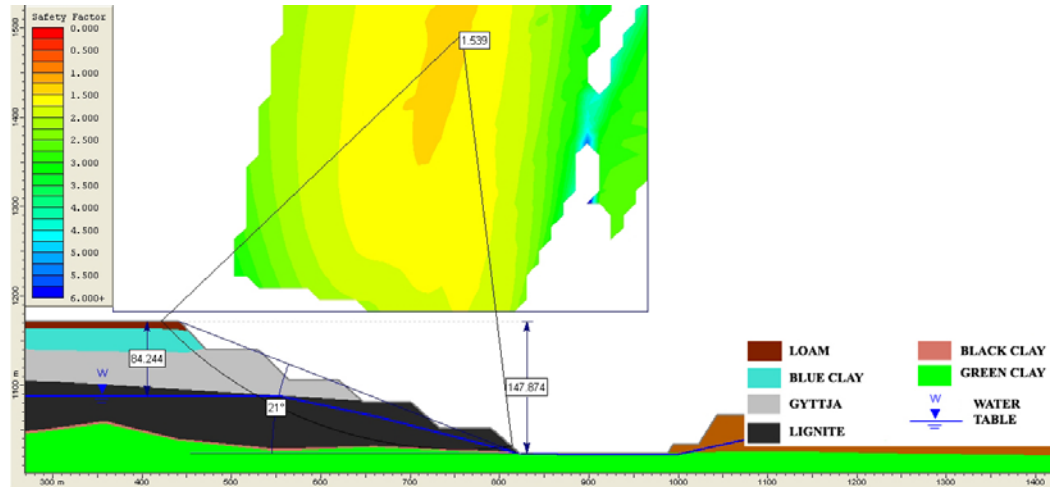


Figure B.5 Section#5

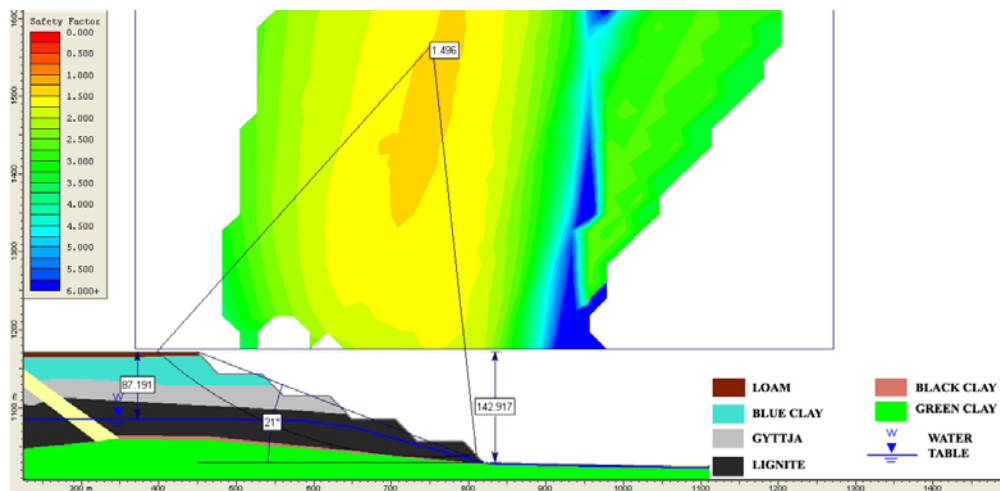


Figure B.6 Section#6

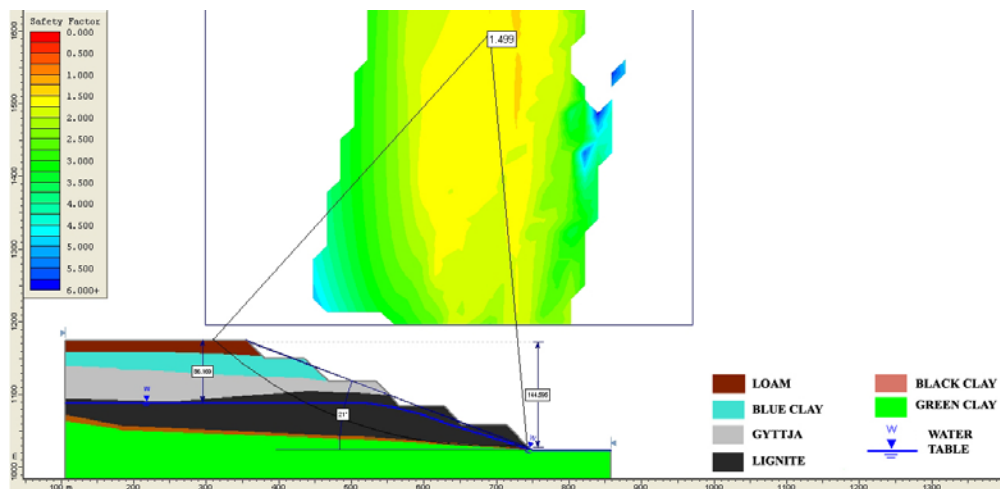


Figure B.7 Section#7

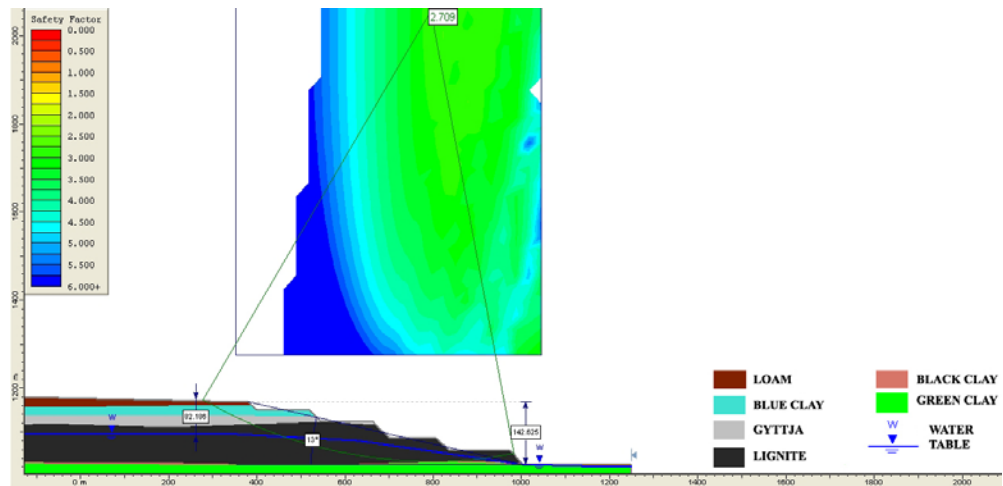


Figure B.8 Section#8

APPENDIX C

SLIDE SOFTWARE GRAPHICAL OUTPUTS FOR PERMANENT SLOPES HAVING GROUND WATER LEVEL 50 m BELOW THE SURFACE

Limit equilibrium analyses graphical outputs illustrating the slip circles and factor of safety values when the ground water level has a depth of 50 m from the slope crest.

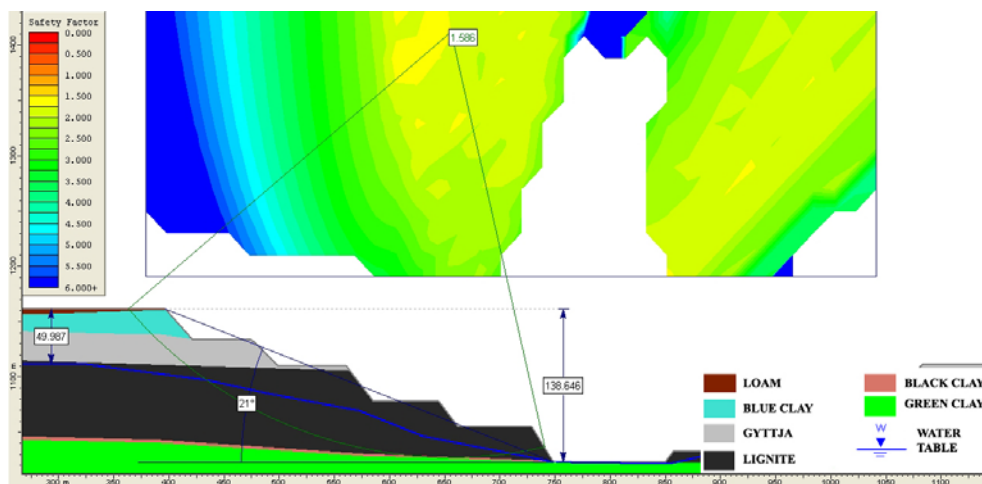


Figure C.1 Section#1

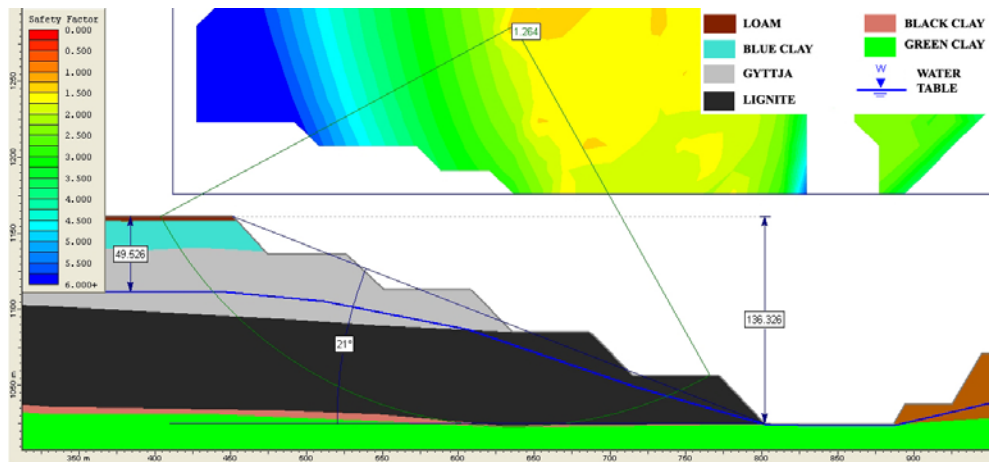


Figure C.2 Section#2

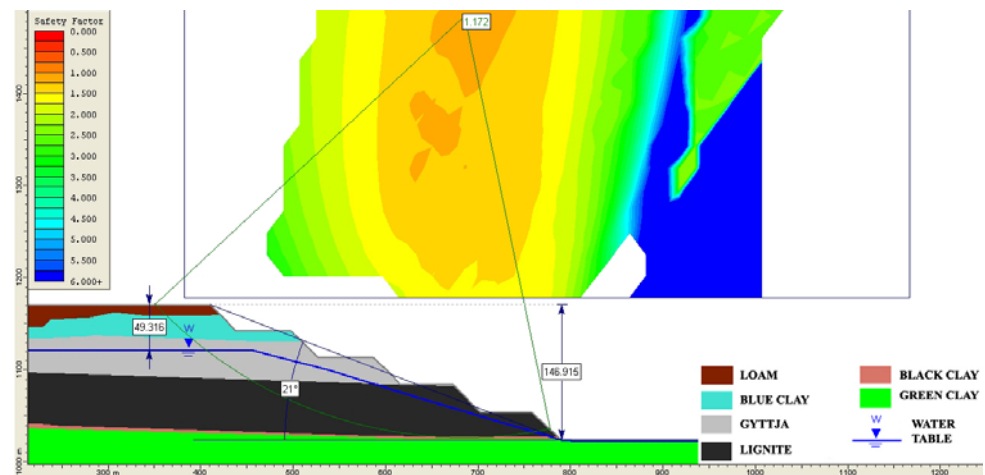


Figure C.3 Section#3

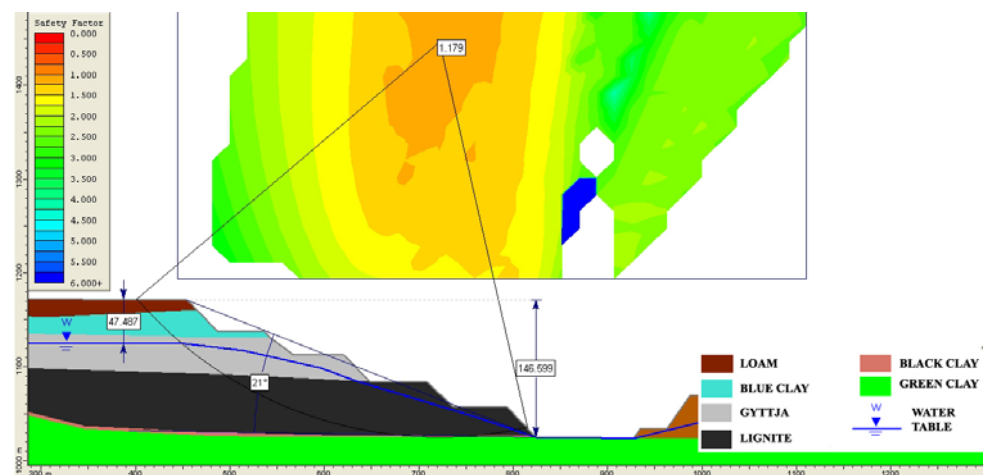


Figure C.4 Section#4

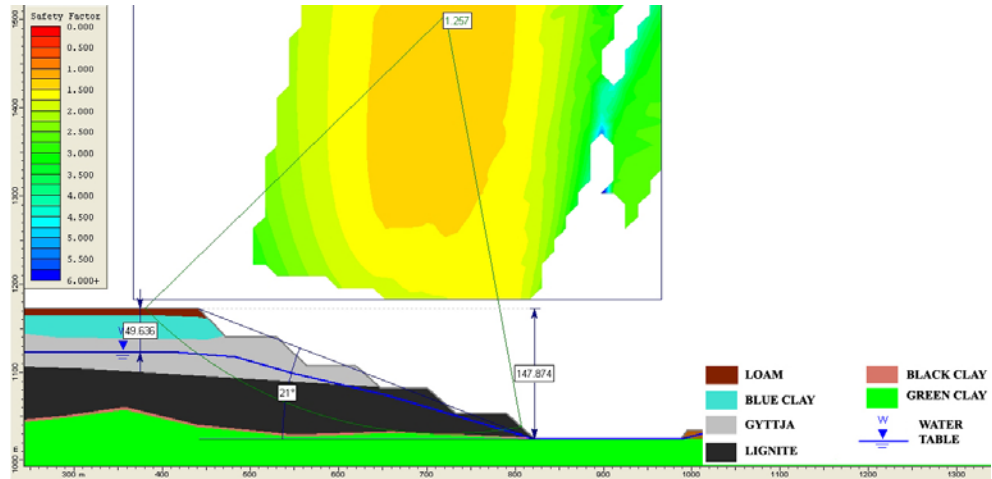


Figure C.5 Section#5

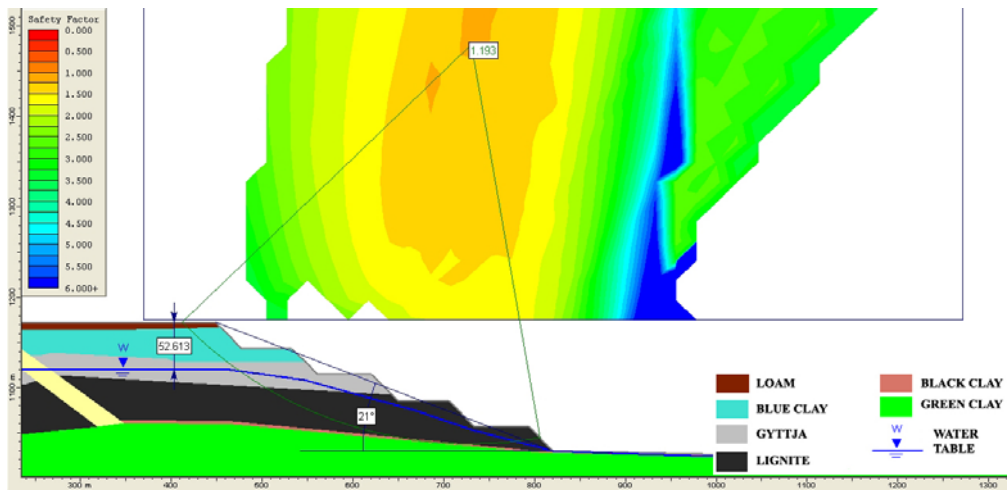


Figure C.6 Section#6

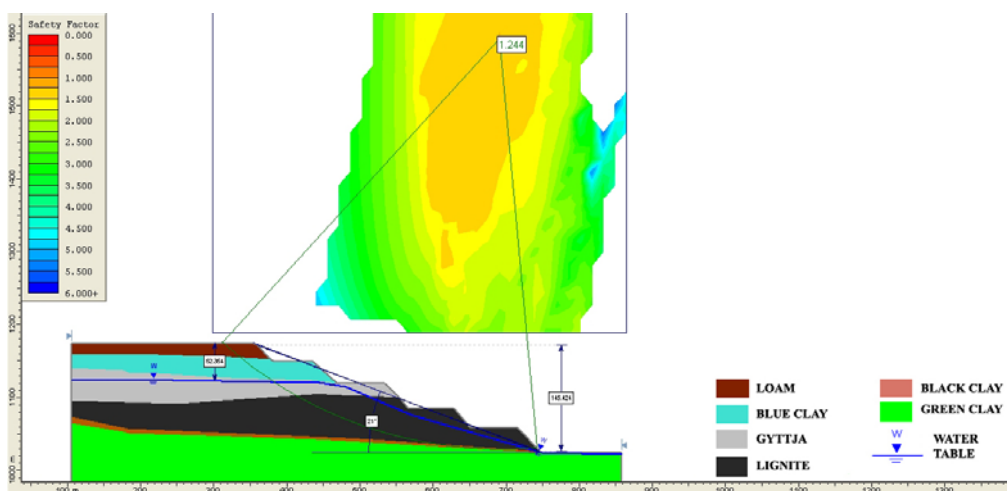


Figure C.7 Section#7

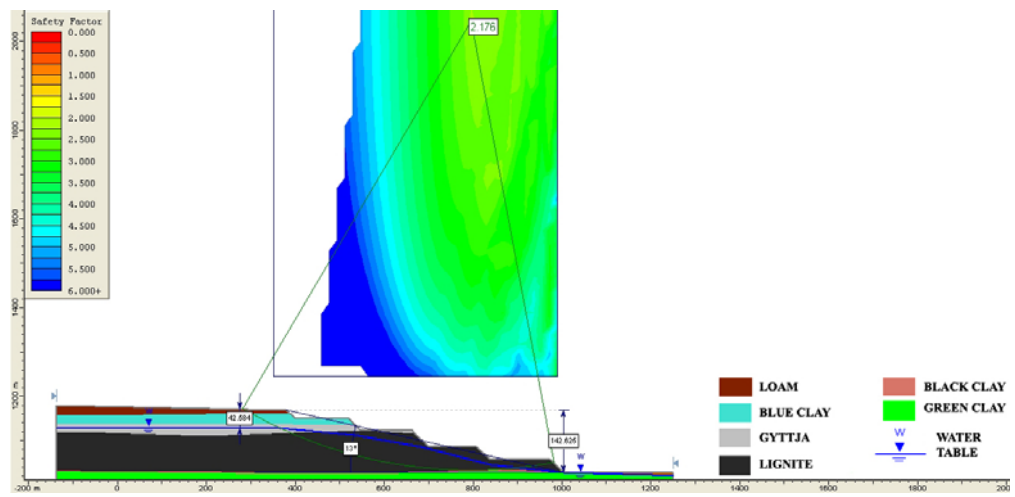


Figure C.8 Section#8

APPENDIX D

SLIDE SOFTWARE GRAPHICAL OUTPUTS FOR PERMANENT SLOPES HAVING GROUND WATER LEVEL AT THE SURFACE

Limit equilibrium analyses graphical outputs illustrating the slip circles and factor of safety values when the ground water level has a depth of 50 m from the slope crest.

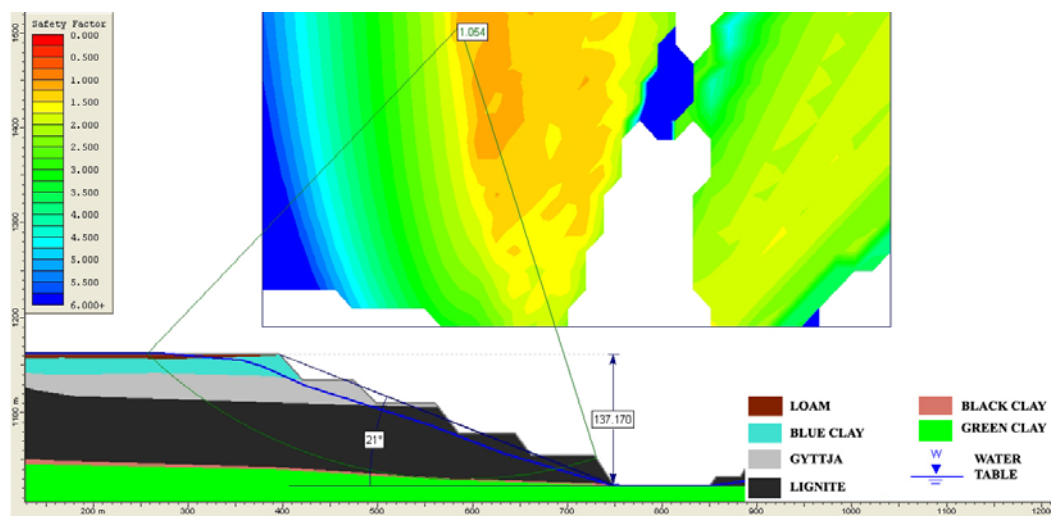


Figure D.1 Section#1

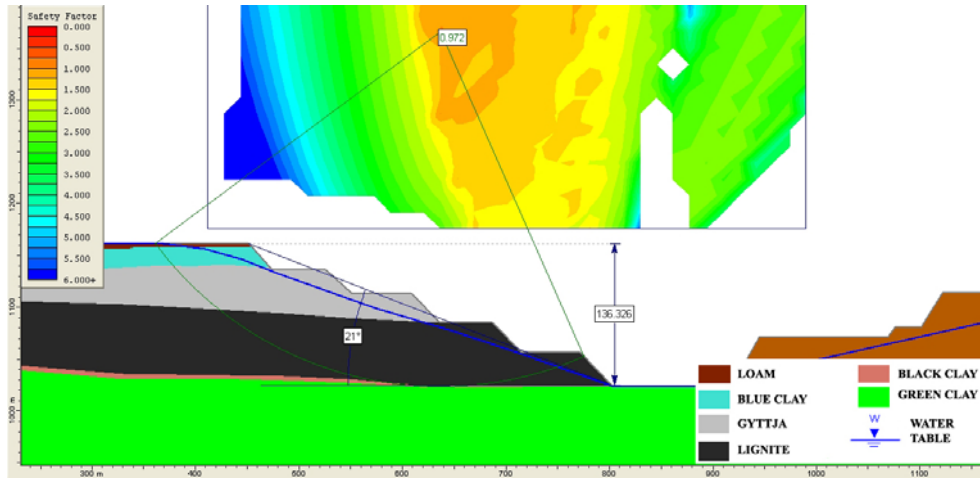


Figure D.2 Section#2

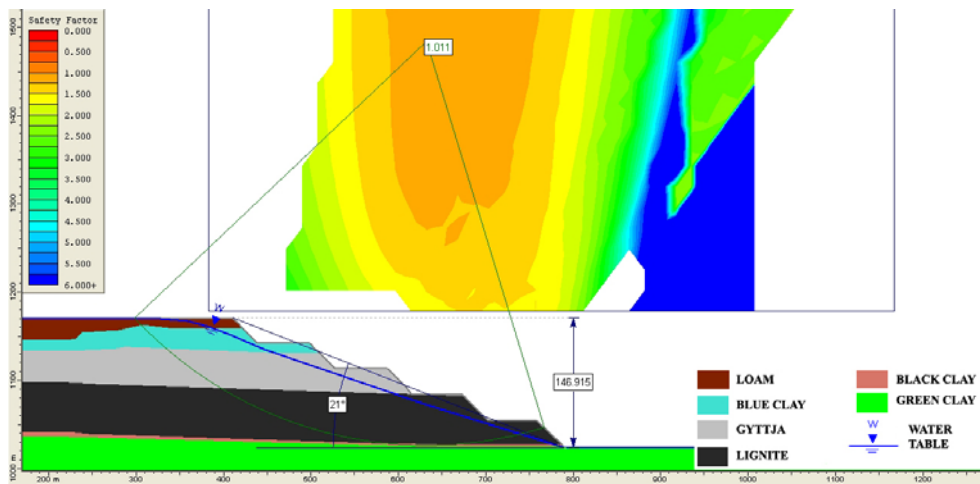


Figure D.3 Section#3

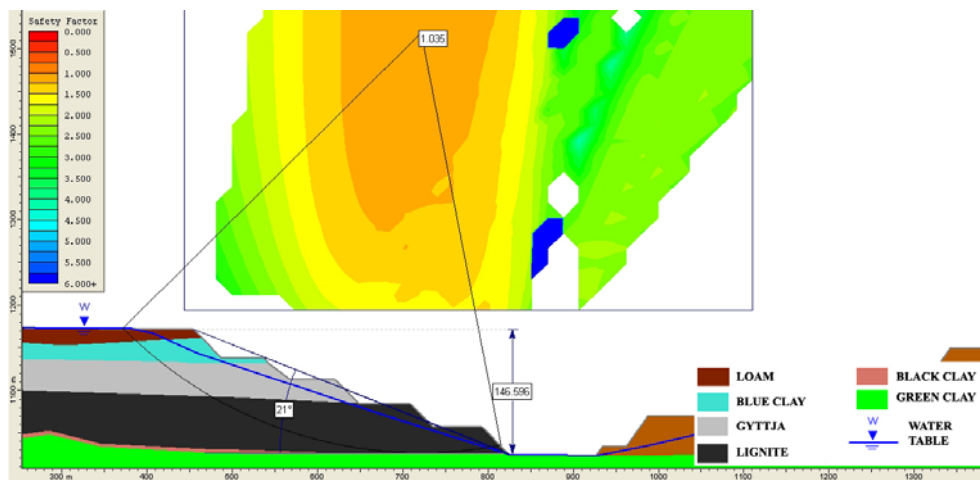


Figure D.4 Section#4

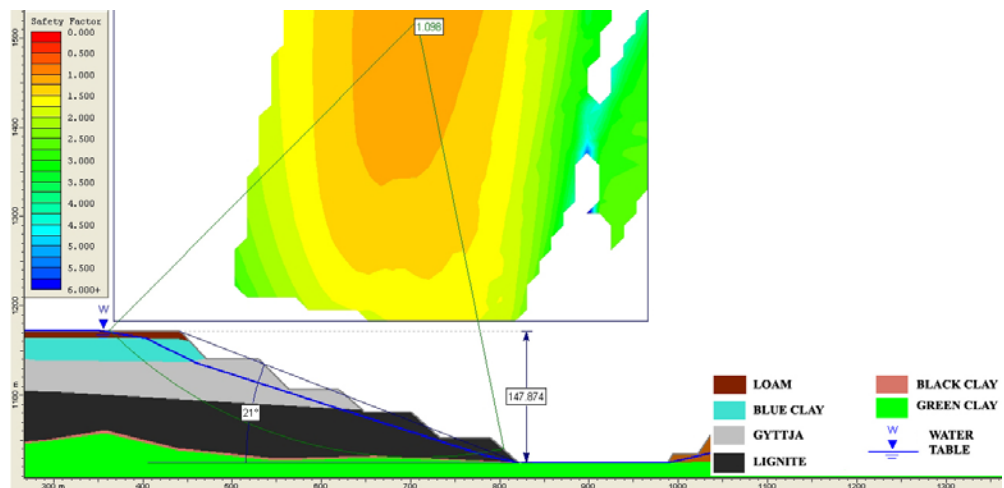


Figure D.5 Section#5

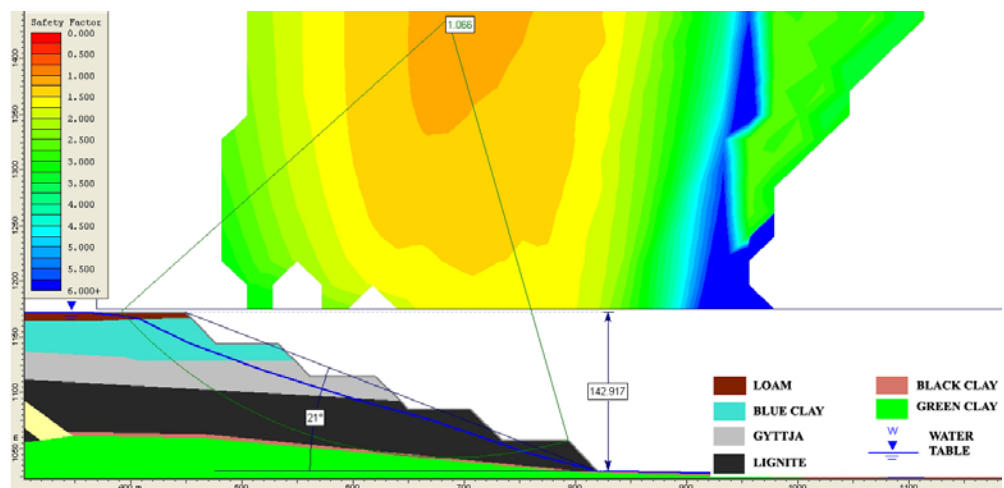


Figure D.6 Section#6

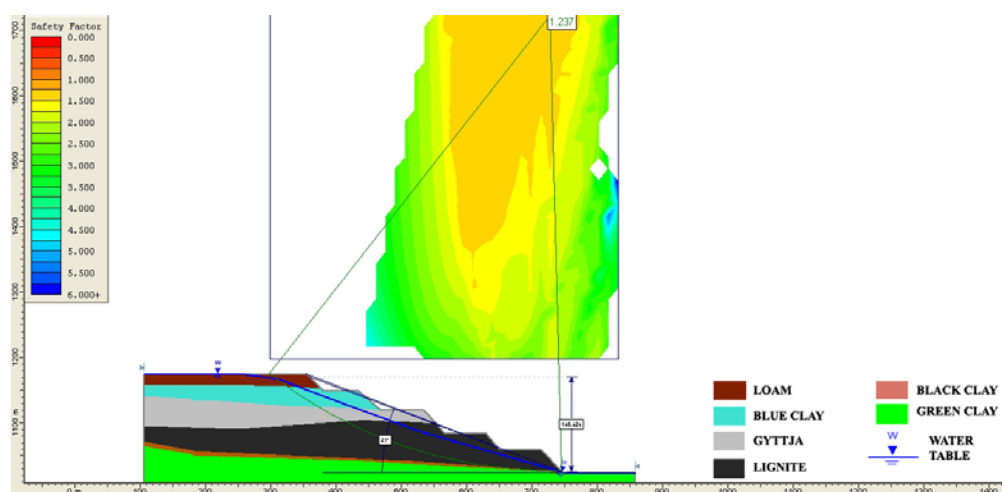


Figure D.7 Section#7

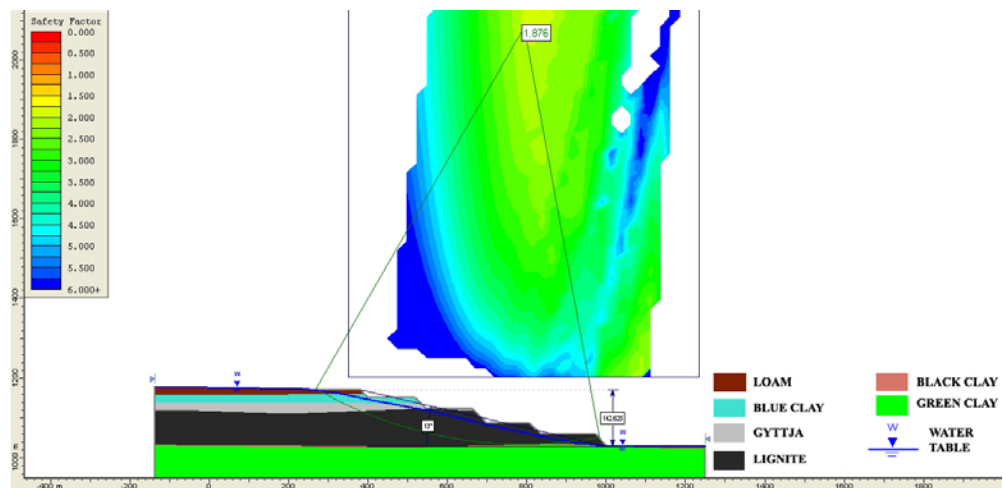


Figure D.8 Section#8

APPENDIX E

SLIDE SOFTWARE GRAPHICAL OUTPUTS FOR BUCKET WHEEL EXCAVATOR PANELS

Limit equilibrium analyses graphical outputs illustrating the slip circles and factor of safety values when the ground water level is on the surface at the slope crest.

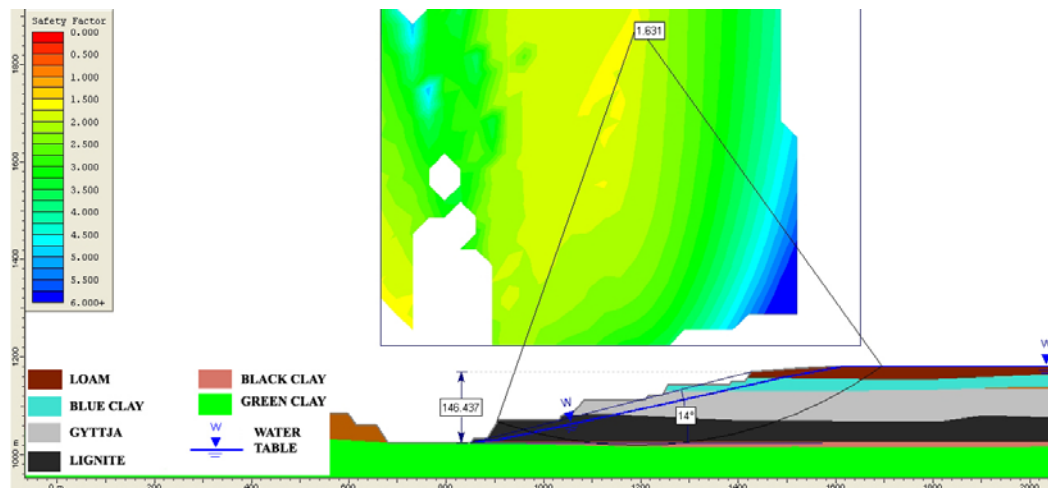


Figure E.1 Section#1

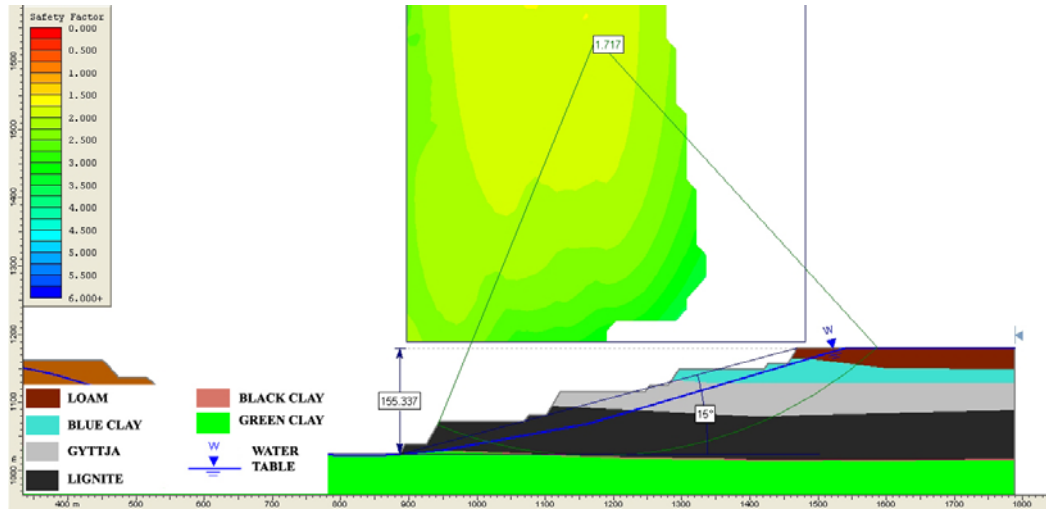


Figure E.2 Section#2

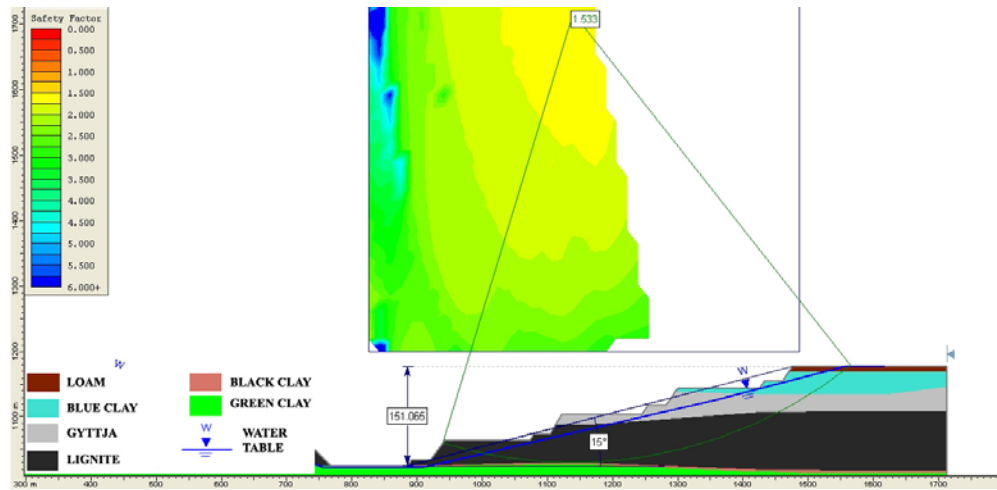


Figure E.3 Section#3

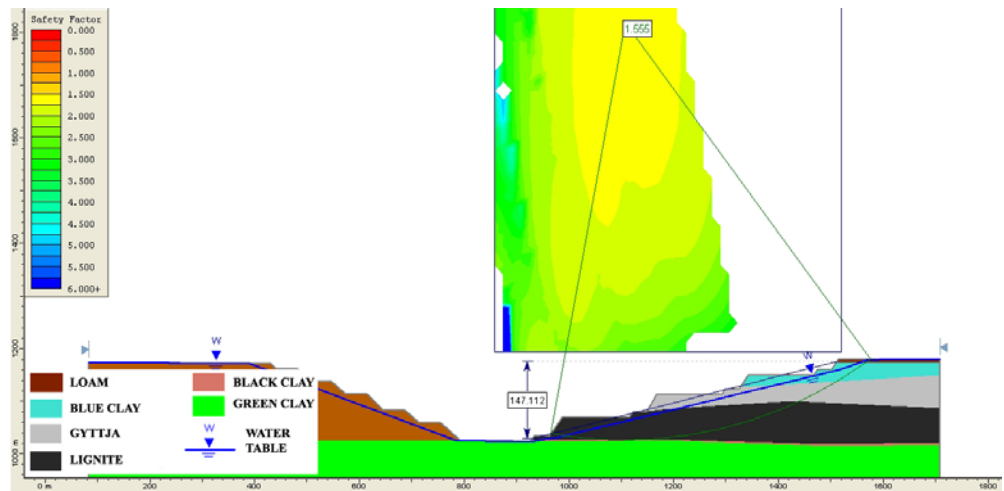


Figure E.4 Section#4

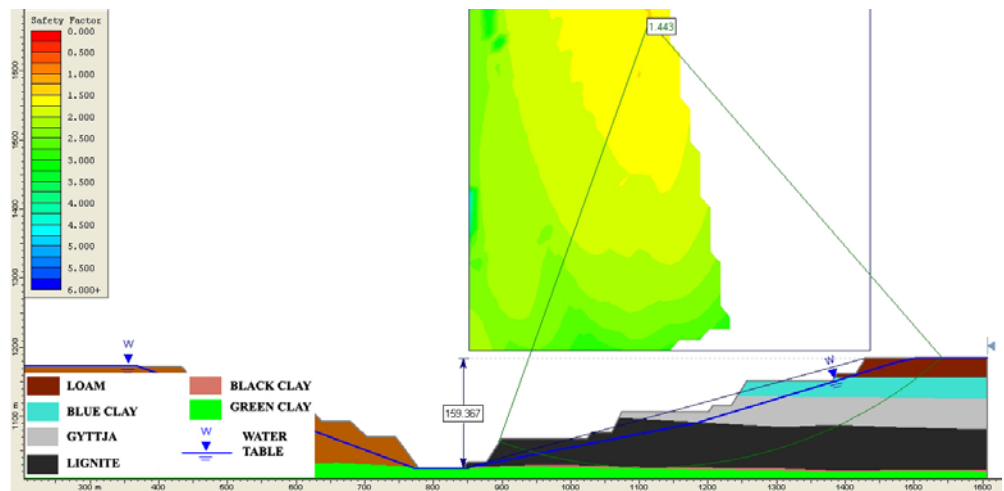


Figure E.5 Section#5

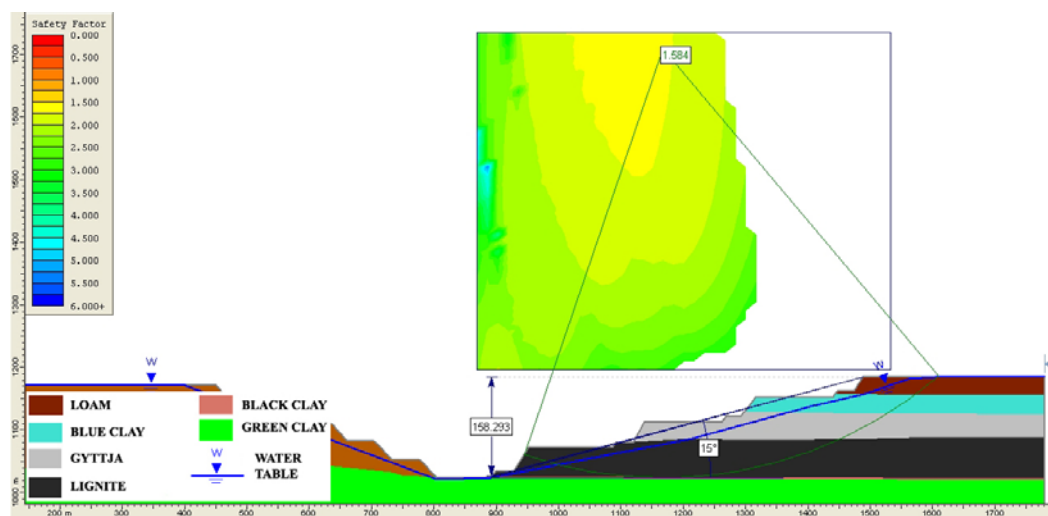


Figure E.6 Section#6